This dissertation has been 64–10,104
microfilmed exactly as received

CHAUDHARI, Ram Das, 1927–
SUPERCONDUCTIVITY IN THIN FILMS.

University of British Columbia, Ph.D., 1964
Physics, general

University Microfilms, Inc., Ann Arbor, Michigan

SUPERCONDUCTIVITY IN THIN FILMS

by

RAM DAS CHAUDHARI

B.Sc. University of Agra, 1949

M.Sc. University of Agra, 1953

A THESIS SUBMITTED IN PARTIAL FULFILMENT OF THE REQUIREMENTS FOR THE DEGREE OF DOCTOR OF PHILOSOPHY

in the Department

of

PHYSICS

We accept this thesis as conforming to the required standard

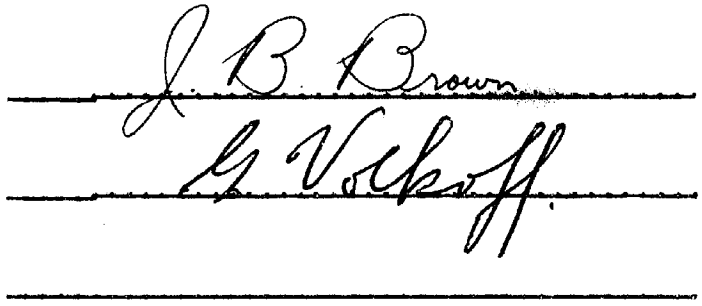

THE UNIVERSITY OF BRITISH COLUMBIA

December, 1963

TABLE OF CONTENTS

		Page
ABSTRACT		i
LIST OF ILLUSTRATIONS		iii
ACKNOWLEDGMENTS		v
CHAPTER		
I	Introduction and Phenomenological Theories	1
II	Microscopic Theories of Superconductivity	15
III	Superconductivity in Thin Films - a Review	30
IV	Specimen Preparation and Mounting	46
V	Experimental Set-up and Procedure	56
VI	Experimental Results and Their Discussion	68
VII	Summary and Conclusions	86
BIBLIOGRAPHY		89

ABSTRACT

This thesis describes experiments on destruction of superconductivity by electric currents and magnetic fields in thin films of indium and tin, of varying thickness. The indium films in the thickness range of 585 Å to 3540 Å were deposited on sapphire rods at liquid nitrogen temperature in vacuum better than 10^{-5} mm. of Hg. Only two tin films, 910 Å and 3250 Å in thickness deposited at room temperature on sapphire rods, were examined. All the measurements were made in the temperature region $0 \leqslant \Delta T \leqslant 0.4^{\circ}K$ where $\Delta T = T_c - T$.

The critical current measurements on a 585 Å thick indium film are the first measurements ever made by combining the use of a compensated geometry and fast rising current pulses. The current pulses used had a rise time of 7 nano seconds. The measurements were made by using Tektronix 661 sampling oscilloscope having a rise time of 0.35 nano seconds. The temperature dependence of the critical currents in the region $0 \leqslant \Delta T \leqslant 0.15^{\circ}K$ is in complete agreement with G - L theory. For a number of indium films, the critical currents were measured by using pulses having a rise time of 1.2 micro seconds. The critical currents have been found to vary linearly with the film thickness, in agreement with G - L theory.

Measurements with fast pulses seem to indicate the existence of a transition delay of 6 nano seconds, independent of current amplitudes. The transition from the superconducting to the normal state, immediately following the transition delay, appears to be extremely fast. Analysis of

the thermal rise in the resistance after the transition, seems to give a qualitative evidence for the existence of thermal propagation mechanism suggested by Bremer and Newhouse.

For the critical field data, the temperature dependence is in accordance with G - L theory in the range $0 \leqslant \Delta T \leqslant 0.3^{\circ}$ K for both indium and tin films. The effective penetration depth calculated in the manner of Ittner, and Douglass and Blumberg was found to be dependent on thickness and mean free path. The critical magnetic fields were found to be inversly proportional to the film thickness in agreement with G - L theory.

J. B. Brown.

J. B. Brown

ILLUSTRATIONS

Figure		Facing Page
	Photograph showing the cryostat and the magnetic field coil, compensating coils mounted on the portable aluminium frame	64
4.1	Vacuum system for the vaporisation chamber	46
4.2	Vaporisation chamber	47
4.3 a,b	Specimen holder	52
4.4 a,b	Electrical representation of specimen holder	53
5.1	Vacuum system for the cryostat	58
5.2	Circuit diagram of the thyratron pulser	61
5.3	Circuit diagram of the discharge line pulser	61
6.1	Graph showing variation of ρ as a function of d^{-1}	70
6.2	Plot of $(\rho d)^{-1}$ versus log d	70
6.3	Graph of δT_c versus d	72
6.4 (a,b,c)	Electron micrographs of the indium and tin films	73
6.5	Transition curve for a tin film	73
6.6	Plot of normalised I_c versus ΔT	74
6.7 a,b	Oscillographs of voltage pulses from the specimen	76
6.8	Plot of I_c versus ΔT for a 585 Å thick film	76

Figure		Facing Page
6.9	Plot of the Joule heat Q developed in the specimen versus the ratio of the observed to the calculated temperature rise	80
6.10	Plot of the critical currents versus thickness for various values of ΔT	82
6.11	A plot of normalised H_c versus ΔT for various films of indium	83
6.12	A plot of H_c versus d^{-1}	83
6.13	A plot of λ_ϵ versus y for the indium films	83
6.14	A plot of λ_ϵ versus y for the tin films	83
6.15	A plot of $H_c/(1-t)^{1/2}$ versus $(1-t)$ for tin films	84
6.16	A plot of $H_c/(1-t)^{1/2}$ versus $(1-t)$ for indium films	84

ACKNOWLEDGEMENTS

It gives me great pleasure to express my indebtedness to Dr. J.B. Brown, my supervisor, for his guidance, help, kindness and for arranging financial support. I am also indebted to Dr. D.V. Osborne, now at the University of St. Andrews, Scotland, for his valuable help and kindness during Dr. Brown's absence. Besides, I would like to express my appreciation and thankfulness to the following:

1. The Government of Madhya Pradesh, India, for granting me leave of absence.
2. Mr. R.W. Weissbach for making liquid helium available, helping in constructing the apparatus and doing the drawings.
3. Mr. J. Lees for making all the glass equipment.
4. Workshop staff for making many pieces of apparatus.
5. Prof. R.E. Burgess and Dr. J.B. Warren for lending many pieces of their equipment.
6. Dr. B.L. White and Mrs. A.E. Aldridge for weighings with the micro-balance.
7. Mr. W.R. Irvine for his help in taking pictures with the electron microscope.
8. Dr. G. Jones and Mr. John Turner for their advice on electronics problems.
9. Dr. P.W. Matthews, Mr. J.D. Jones, Mr. S.N. Sharma, Mr. A.R. Kshatriya and Mr. D.S. Sahri for their assistance in taking down the data.

10. Mr. J.R. Henderson for his help in programming the IBM 1620 computer.

11. Mrs. R.E. Bartley for typing the thesis.

CHAPTER I

INTRODUCTION

Superconductivity was discovered in 1911 by Kamerlingh Onnes while he was investigating the variation of the electrical resistance of mercury at the liquid helium temperatures, available for the first time as a consequence of his successful liquefaction of helium gas. He found that the resistance of mercury dropped abruptly to zero at about 4° K. This phenomenon of the disappearance the electrical resistance was called superconductivity. The infinite conductivity in the superconducting state was further demonstrated by Onnes and Tuyn (1924) by inducing 'persistent' currents in a superconducting metallic ring when subjected to a changing magnetic field. Today a large number of metals, compounds and alloys are known to be superconductors. An exhaustive list of these has been given by Matthias et al (1963).

The temperature at which a metal becomes superconducting is known as the transition temperature, T_c, and is characteristic of the metal. For pure, homogeneous and strain free bulk specimen, the transition is usually quite sharp.

Below T_c the superconductivity can be destroyed by either applying a magnetic field or passing an electric current through the superconductor, the value of the minimum magnetic field or electric current being a

function of the temperature for any bulk superconductor. To a good approximation, the critical magnetic field, which is the threshold field needed to destroy superconductivity in a wire placed with its axis parallel to the field is given by,

$$H = H_o \left[1 - \left(\frac{T}{T_c}\right)^2\right] \qquad 1.1$$

where H_o is the critical field at the absolute zero and T is the temperature of the metal. Similarly the minimum current needed to destroy the superconductivity is known as the critical current. According to what is known as Silsbee's hypothesis, the critical current is that which produces a magnetic field equal to the critical field at the surface of the specimen. This, however, is not true for all types of superconductors.

For a number of years following Onnes' discovery, it was believed that the superconducting state was fully characterised by infinite conductivity. However, this is not so as the following example will show. From Maxwell's equations we know that

$$\nabla \times \vec{E} = -\frac{\vec{dB}}{dt} \qquad 1.2$$

where $\vec{E}$ and $\vec{B}$ are the electric and the magnetic fields. If we make use of Ohm's law, $\vec{E} = \frac{\vec{J}}{\sigma}$ where $\vec{J}$ is the current density and σ is the electrical conductivity and put $\sigma = \infty$ for a superconductor, we find $\dot{\vec{B}} = 0$ or B is constant in time. However, the application of this result leads to the following paradox. Consider, firstly, cooling a sphere below T_c and then applying a magnetic field to it; secondly applying the magnetic field first and then cooling the sphere below T_c. These two processes should lead to two different situations: in the first case there should be no magnetic field inside the superconductor whereas in the second case, all

the magnetic field should be frozen in after the external magnetic field has been removed. Thus the magnetic behaviour of a superconductor should depend upon the past history of the superconductor, resulting in an infinity of states. Hence the state of the infinite conductivity does not lead to a state of thermal equilibrium because the two external co-ordinates do not lead to a unique internal state. Meissner and Ochsenfeld (1933) discovered experimentally that the correct state of a superconductor is not specified by the condition that B = constant but that B = 0. This discovery is known as Meissner - Ochsenfeld effect. Thus a superconductor is not only a perfect conductor but also a perfect diamagnet. In fact, the diamagnetic aspect of superconductivity is more basic than the existence of persistent currents arising due to infinite conductivity because the former state is a state of thermal equilibrium as opposed to latter which is only metastable.

LONDONS' THEORY

F. London and H. London (1935) proposed a phenomenological theory to account for the electromagnetic properties of a superconductor. Essentially, it was an attempt to blend the two characteristics of a superconductor - the infinite conductivity and the perfect diamagnetism, into a single theory. They assume that the supercurrent is always determined by the local magnetic field. For a superconductor, they replace Ohm's law by the following two equations:

$$\left.\begin{aligned} \operatorname{curl}(\Lambda \vec{J}_s) &= -\frac{\vec{H}}{C} \\ \frac{\partial}{\partial t}(\Lambda \vec{J}_s) &= \vec{E} \end{aligned}\right\} \qquad 1.3$$

where Λ is a constant characteristic of the superconductor, $\vec{J}_s$ is the supercurrent. If these equations are applied to solve the problem of a

superconductor in a magnetic field, it turns out that the field penetrates only a thin layer of a bulk superconductor. The penetration depth, λ, in a bulk superconductor is defined by the relation,

$$\lambda = \frac{1}{H(o)} \int_o^\infty H(x)\, dx \qquad 1.4$$

where $H(0)$ is the magnetic field at the surface of the superconductor. According to the London picture, the magnetic field will decay exponentially within a superconductor. In fact, the experiments generally give integrated flux in the interior of a superconductor and it is difficult to deduce how the field changes in the interior. The application of the Londons' equations to the problem of the current flow in a bulk superconductor leads to the similar conclusion that the supercurrent is confined to a thin layer on the surface.

The first direct experimental evidence of penetration effects was obtained by Shoenberg (1939). He measured the temperature variation of the magnetic susceptibility of mercury colloids of particle size between 10^{-6}cm and 10^{-5}cm. The penetration depth was found to vary with the temperature in accordance with the law,

$$\frac{\lambda(T)}{\lambda(0)} = \frac{1}{\left[1-\left(\frac{T}{T_c}\right)^4\right]^{1/2}} \qquad 1.5$$

Lock measured the temperature variation of λ by measuring the change in the magnetic susceptibility of thin films. A second method to study the temperature variation of λ is due to Casimir who measured the change in the mutual inductance of two coils containing closely fitting cylindrical specimens. This method was also successfully used by Desirant and Shoenberg in their measurement on tin and mercury. Shalnikov and Sharvin used a variation of Casimir's method. Instead of using oscillating currents in the primary, they oscillated the temperature. A third method

suggested and applied by Pippard is based on the measurement of surface impedance of a superconductor at microwave frequencies. The penetration depth λ, besides being temperature dependent is also found to vary with specimen thickness in the case of thin superconductors. This variation will be discussed later.

THERMODYNAMICS

The superconductive transition, in the absence of the magnetic field is a transition of second order. Keesom and Kok were the first to show a jump in the specific heat. In 1934, they also showed that there was no latent heat in the absence of a magnetic field. In the initial stages the thermodynamics of the transition was developed by Keesom, Rutger and Gorter. Gorter's analysis is based on the assumption that the transition is a reversible one. That this is so was vindicated by the discovery of Meissner effect.

If we assume the normal state to be non-magnetic and the superconducting state to be diamagnetic and further, neglect the surface effects and penetration effects, then by the usual procedure of equating the Gibb's energies in the two phases, we readily arrive at the following expressions.

$$\Delta C = C_s - C_n = \frac{VT}{4\pi}\left[H_c \frac{d^2H_c}{dT^2} + \left(\frac{dH_c}{dT}\right)^2\right]$$

$$S_n - S_s = -\frac{VH_c}{4\pi}\frac{dH_c}{dT}$$

$$Q = -\frac{VTH_c}{4\pi}\frac{dH_c}{dT}$$

Here C_s, C_n; S_s, S_n are the specific heats and entropies respectively in the superconductive and normal states and V is the atomic volume of the

material. These equations have been experimentally verified.

Gorter's two fluid model was the most successful one to account for the thermal properties of a superconductor. In the two fluid models, the superconductive state is supposed to be formed as a result of the condensation of the metal electrons, the degree of condensation, ω, being a variable parameter, $0 \leqslant \omega \leqslant 1$. The free energy may be written as

$$F(T, \omega) = U_0 - \beta \omega - \tfrac{1}{2} \gamma T^2 K(\omega, T) + F_L(T)$$

where the kernel $K(\omega, T) \geqslant 0$; $K(0, T) = 1$, β = constant, U_0 is zero point free energy, γ is Sommerfeld constant and $F_L(T)$ is the lattice free energy. In thermal equilibrium, ω adjusts its value so as to minimise the free energy. The various two fluid models may be obtained by assuming different expressions for the kernel $K(\omega)$. Schafroth 1960 has summarised the various models proposed.

SURFACE ENERGY AND INTERMEDIATE STATE

As remarked earlier, the above description does not take into account the surface and the penetration effects. The existence of a surface energy must be postulated for the following three reasons.

(i) Consider an oblong superconductor to be placed in a longitudinal magnetic field $H > H_c$ and let the field be reduced below H_c. It can be shown that the free energy will be lower for the case when the superconductor breaks into a domain structure of alternating superconducting and normal layers oriented such that the magnetic field passes through normal layers. Thus it will not be necessary for the specimen to exclude the magnetic flux and thus there will be no Meissner effect. This is inconsistent not only with the experimental findings but the very concepts

of Gorter - Casimir theory. However if we assume the existence of a surface energy necessary for the creation of a superconducting - normal boundary, this will inhibit the breaking of the specimen into normal and superconducting regions and the flux will have to be excluded, giving rise to Meissner effect. Obviously this energy will have to be positive, its magnitude can be shown to be such that the surface energy $\alpha_{ns} > \frac{\lambda H_c^2}{8\pi}$

(ii) Existence of a negative surface energy is necessary for explaining the unusually high critical magnetic fields for the hard superconducting metals and alloys. Similarly even in the soft superconductors some regions having strains or defects must be postulated to be a seat of negative surface energy which is necessary for the growth of superconducting nuclei and their consequent growth throughout the body. Faber (1952) has proposed a mechanism for the propagation of the superconducting phase on the basis of the existence of a negative surface energy. The observed velocities of propagation are found to be in agreement with his model. Abrikosov (1957) and Goodman (1962) have found it necessary to assume existence of a negative surface energy to explain the magnetic behaviour of alloys.

(iii) Consider a superconducting body of non-zero demagnetising coefficient e.g. a sphere to be placed in a homogeneous magnetic field. The sphere, in order to keep the magnetic field away from the interior, makes the field inhomogeneous as a result of which the sphere breaks up into a mixture of normal and superconducting domains as the magnetic field is increased from a value $\frac{2}{3} H_c$ to H_c. In order that these domains be of finite size, a positive surface energy at the interface of the normal and superconducting boundary must be postulated.

The mixed state into which a superconductor of non-zero demagnetising coefficient breaks in a magnetic field close to H_c, is known as the intermediate state. The first experimental evidence for the existence of the intermediate state was obtained by Shalnikov (1945) by mapping the magnetic field inside a sphere using a bismuth wire probe. The magnetostatics of the intermediate state has been discussed by Shoenberg (1952) and London (1950).

THE PIPPARD THEORY

Pippard (1953) suggested a modification of London equations by introducing the concept of coherence length ξ. According to him, the current density in a superconductor does not merely depend upon the vector potential at a given point but on the vector potential in a region surrounding the point. He replaced London equation $\Lambda c \vec{J}_s = \vec{A}$ by the relation,

$$\vec{J}_s(\vec{r}) = -\frac{3}{4\pi c \Lambda \xi_0} \int \frac{\vec{R}\,[\vec{R}.\vec{A}(r')]\exp(-R_0/\xi_0)\exp(-R/l)\,d\tau'}{R^4} \qquad 1.6$$

where $\vec{R} = \vec{r}-\vec{r}'$, l is the mean free path of the electrons and ξ_0 is a characteristic length dependent upon the metal and independent of impurity content. The coherence length ξ is related to ξ_0 by the equation,

$$\frac{1}{\xi} = \frac{1}{\xi_0} + \frac{1}{al} \qquad 1.7$$

where a is a constant of the order of unity and l is the mean free path. ξ depends upon impurity content, for pure metals $\xi = \xi_0 = 10^{-4}$ cm. Pippard cited a number of properties in favour of his concept of the coherence length. These are:

(1) The sharpness of the phase transitions in zero field.

(2) The variation of the penetration depth λ with mean free path.

(3) The existence and the size of the surface energy.

(4) Small change in the penetration depth with magnetic field.

ξ_0 can be interpreted as a measure of the size of the wave packets of the superconducting electrons. On the basis of the uncertainty principle, Faber and Pippard (1955) calculate ξ_0 and find it to be given by,

$$\xi_0 = a \frac{\hbar v}{k T_c} \qquad 1.8$$

where a is an adjustible parameter, v is the Fermi velocity and k is the Boltzmann constant.

According to the Pippard theory, the penetration of the magnetic field inside a superconductor is not exponential but has a much more complicated form and actually reverses sign at large depths. Sommerhalder (1961) has experimentally verified the direction reversal of the magnetic field.

The Bardeen - Cooper - Schrieffer theory, (B C S) to be described in the following chapter, gives a relation between J and A similar to Pippard's.

GINZBURG - LANDAU THEORY

The phenomenological theory proposed by Ginzburg and Landau (1950) can be considered to be an extension of the general theory of the second order phase transitions given by Landau and Lifshitz (1958). The superconducting state in G-L theory is characterised by an order parameter ψ such that at $T = T_c$, $\psi = 0$; $T < T_c$, $\psi > 0$ and $|\psi|^2 = n_s$ where n_s is the

density of superconducting electrons. ψ is treated as a kind of wave function of the superconducting electrons.

In the absence of a magnetic field and near T_c, the free energy in the superconducting state, F_{so}, is written as,

$$F_{so} = F_{no} + \alpha |\psi|^2 + \beta |\psi|^4 \qquad 1.9$$

where F_{no} is the free energy in the normal state and α and β are temperature dependent coefficients. Near T_c, α and β are assumed to have the form,

$$\left.\begin{aligned} \alpha(T) &= (T_c - T)\left(\frac{\partial \alpha}{\partial T}\right)_{T=T_c} \\ \beta(T) &= \beta(T_c) = \beta_c \end{aligned}\right] \qquad 1.10$$

Remembering that, $F_{so} - F_{no} = \frac{H_{cb}^2}{8\pi}$

it is easy to show that

$$H_{cb}^2 = \frac{4\pi (T_c - T)^2}{\beta_c}\left(\frac{\partial \alpha}{\partial T}\right)^2_{T=T_c} \qquad 1.11$$

This equation has been verified experimentally thereby lending justification for the above form for α and β. Bardeen (1954) and Ginzburg (1956) employ different forms for α and β to extend the application of the theory to lower temperatures.

Consider now the superconductor to be placed in a time-independent magnetic field H. The expression for free energy can now be written as,

$$F_{sH} = F_{so} + \frac{H^2}{8\pi} + \frac{1}{2m}\left|-i\hbar\nabla\vec{\psi} - \frac{e}{c}\vec{A}\psi\right|^2 \qquad 1.12$$

The second term in the above expression is the usual volume term and the third term is the gauge - invariant contribution to the energy originating as a result of gradual extended variation of the order parameter . This variation in ψ is similar in nature to the Pippard's idea of coherence

length. The outstanding feature of the G - L theory is its ability to treat a superconductor in fields quite near H_c. The order parameter $\psi(r)$ introduced above is not the true wave function of the superconducting electrons but is a certain average quantity related to the true wave function $\psi(r, r_i')$ in the following manner,

$$\psi^*(r)\,\psi(r') = \int \psi(r, r_i')\,\psi(r', r_i')\,dr_i'$$
$$= \rho(r, r')$$

where $\rho(r, r')$ is the density matrix. In order to obtain an equation for ψ, we minimise the total free energy $\int F_{sH}\,dV$.

The variation with respect to ψ^* yields,

$$\frac{1}{2m}\left(-i\hbar\nabla - \frac{e}{c}\vec{A}\right)^2\psi + \frac{\partial F_{so}}{\partial \psi^*} = 0 \qquad \text{1.13a}$$

Besides, since the variation $\delta\psi^*$ is arbitrary, the following condition must hold.

$$\vec{n}\cdot\left[-i\hbar\nabla\psi - \frac{e}{c}\vec{A}\psi\right] = 0$$

where $\vec{n}$ is the unit vector normal to the boundary. Similarly if we vary A and assume div $\vec{A}$ = 0, we obtain,

$$\nabla^2 A = \frac{4\pi}{c}\vec{J} = \frac{2\pi i e\hbar}{mc}\left(\psi^*\nabla\psi - \psi\nabla\psi^*\right) + \frac{4\pi e^2}{mc^2}|\psi^2|\vec{A} \qquad \text{1.13b}$$

where $\vec{J} = -\frac{ie\hbar}{2m}\left(\psi^*\nabla\psi - \psi\nabla\psi^*\right) - \frac{e^2}{mc}\psi^*\psi$

Once again if we assume that the variation in ψ does not contribute to the energy, the expression for $\vec{J}$ reduces to London s expression. The equations 1.12 form a set of coupled non-linear equations which have been solved for one dimensional case.

Consider a superconducting - normal boundary and choose X axis normal to the boundary such that for the superconducting phase $X > 0$. Let the magnetic field H be directed along the Z axis and the current $\vec{J}$ and vector potential $\vec{A}$ along Y axis. It is clear that $\psi = \psi(X)$, $\vec{J} \cdot \vec{n} = 0$, $\text{div } \vec{J} = \frac{dJx}{dx} = 0$ and ψ is real. Making use of the above equations we find that the equations 1.13 after some work reduce to the following,

$$\frac{d^2\psi}{dx^2} + \frac{2m}{\hbar^2}|\alpha|\left[1 - \frac{e^2}{2mc^2}\frac{A^2}{|\alpha|}\right]\psi - \frac{2m}{\hbar^2}\beta\psi^3 = 0 \qquad 1.14$$

$$\frac{d^2\vec{A}}{dx^2} - \frac{4\pi e^2}{mc^2}\psi^2\vec{A} = 0 \qquad 1.15$$

Now we make the following substitutions,

$$x = \frac{x}{\lambda_0}, \quad \lambda_0^2 = \frac{mc^2}{4\pi e^2 \psi_\infty^2}, \quad \psi_0^2 = \frac{\psi^2}{\psi_\infty^2}, \quad a = \frac{A}{\sqrt{2}H_{cb}}\lambda_0$$

$$\kappa = \frac{\sqrt{2}\,e}{\hbar c} H_{cb}\lambda_0^2, \quad \vec{H} = \text{curl } \vec{A}, \quad \vec{h} = \frac{\vec{H}}{\sqrt{2}\,H_{cb}} \qquad 1.16$$

where λ_0, k and H_{cb} are the three parameters determined experimentally, ψ_∞ is the value of ψ in zero field. The parameters H_{cb} and λ_0 are bulk critical field and weak-field penetration depth respectively. The various field and size effects can be expressed in terms of these parameters. The equations now in terms of the new variables become,

$$\frac{d^2\psi}{dx^2} = \kappa^2\left\{\psi_0^3 - \psi_0 + a^2\psi_0\right\} \qquad 1.17$$

$$\frac{d^2a}{dx^2} = \psi_0^2 a \qquad 1.18$$

Ginzburg (1958) calculated the critical current and the critical magnetic field for a film deposited on a cylindrical rod. Consider a film of thickness $d \sim 10^{-5}$ cm. or less deposited on a rod of such diameter that the film could be regarded as planar. Let a current I be passed through the film and a magnetic field H be applied along the axis.

Ginzburg solved equations 1.17 and 1.18 by applying appropriate boundary conditions in addition to putting $\frac{dH_{IC}}{d\psi_0} = 0$ where H_{IC} is the magnetic field due to the current I_c. His solutions for the following two cases are,

(i) $\frac{\psi_{0K} d}{\lambda_0} \ll 1$,

$$\frac{H_{Ic}}{H_{cb}} = \frac{2\sqrt{2}}{3\sqrt{3}} \frac{d}{\lambda_0} \left[1 - \left(\frac{H}{H_{cb}}\right)^2 \frac{d^2}{24\lambda_0^2}\right]^{3/2} \quad \text{---1.19}$$

$$\psi_{0K} = \frac{\sqrt{2}}{\sqrt{3}} \left[1 - \left(\frac{H_0}{H_{cb}}\right)^2 \frac{d^2}{24\lambda_0^2}\right]^{1/2} \quad \text{---1.20}$$

(ii) $\frac{\psi_{0K} d}{\lambda_0} \gg 1$,

$$\frac{H_{cI}}{H_{cb}} = \left[\frac{8}{5}\sqrt{\left(\frac{3}{5}\right)^3} \frac{d}{\lambda_0} - 2\left(\frac{H}{H_{cb}}\right)^2\right]^{1/4} \quad \text{---1.21}$$

$$\psi_{0K} = \sqrt{\frac{3}{5}} \quad \text{---------- 1.22}$$

where ψ_{0K} is the value of ψ_0 when $H_I = H_{IC}$

When I = 0, equation 1.19 reduces to

$$\frac{H_c}{H_{cb}} = \frac{\sqrt{24}\,\lambda_0}{d} \qquad 1.23$$

When H = 0, equation 1.19 reduces to

$$\frac{H_{cI}}{H_{cb}} = \frac{2\sqrt{2}}{3\sqrt{3}} \frac{d}{\lambda_0} \qquad 1.24$$

From equations 1.23 and 1.24 we obtain,

$$H_{Ic}\, H_c = \frac{8}{5} H_{cb}^2 \qquad 1.25$$

The temperature dependence of H_{cb} and λ_0 is known to be,

$$H_{cb} = H_0 \left[1 - \left(\frac{T}{T_c}\right)^2\right] \qquad 1.26$$

$$\lambda_0 = \lambda_{00} \left[1 - \left(\frac{T}{T_c}\right)^4\right]^{-1/2} \qquad 1.27 \text{ where}$$

λ_{00} is the weak-field penetration depth at 0° K.

Near T_c,

$$H_{cb} = \left|\frac{dH_{cb}}{dT}\right| \Delta T \quad , \quad \lambda_o = \frac{\lambda_{oo}\sqrt{T_c}}{2(\Delta T)^{1/2}}$$

and

$$\left|\frac{dH_{cb}}{dT}\right|_{T_c} = \frac{2H_0}{T} \quad \text{where} \quad \Delta T = T_c - T \ll T$$

Making above substitutions, the equations 1.23 and 1.24 become

$$H_c = \frac{\sqrt{6}\,\lambda_{oo}\sqrt{T_c}}{d} \left|\frac{dH_{cb}}{dT}\right| (\Delta T)^{1/2} \qquad 1.28$$

$$H_{cI} = \frac{4\sqrt{2}\,d}{3\sqrt{3}\,\lambda_{oo}\sqrt{T_c}} \left|\frac{dH_{cb}}{dT}\right| (\Delta T)^{3/2} \qquad 1.29$$

For the case, however, when $\frac{\psi_{ok}\,d}{\lambda_o} \gg$ from equation 1.21, it easily follows that near T_c, H_{cI} is given by,

$$H_{cI} = \left[\frac{0.64\,d}{\lambda_{oo}\sqrt{T_c}}\right]^{1/4} \left|\frac{dH_{cb}}{dT}\right| (\Delta T)^{1.12} \qquad 1.30$$

Gorkov (1959) has derived G - L equations 1.14 and 1.15 from the B C S theory by using Green function technique.

CHAPTER II

THE MICROSCOPIC THEORIES OF SUPERCONDUCTIVITY

The phenomenological theories summarised in the last chapter, though adequate for the description of many superconducting properties, do not give the basic understanding of the superconducting phase from the atomistic point of view; however, they point out the properties which a microscopic theory ought to derive. The fact that the superconductivity occurs in metals and alloys of diverse structures, points out that the detailed knowledge of the metallic structure should not be necessary for at least a qualitative understanding of the superconducting properties from an atomic point of view. This observation seems to simplify the solution of the problem. However, the greatest difficulty in constructing microscopic theories lies in the fact that the energy of condensation, the energy required to bring the superconductor back to the normal state, is of the order of 10^{-8} e.v. per atom. This is extremely small when one compares this with the Fermi energy of the conduction electrons which is of the order of 10-20 e.v., or the correlation energy of the conduction electrons due to the Coulomb interaction which is of the order of 1 e.v.; in fact the latter is neglected in the Bloch - Sommerfeld theory, successful in explaining the normal state conductivity of the metals. The absence of statistical fluctuations, as revealed by the sharpness of the phase transition, indicates that the superconducting phase is highly correlated. Thus the basic problem is to find the interaction which correlates a large

number of electrons in such a manner as to lower the energy of the system by a very small amount.

The problem of developing a satisfactory microscopic theory could be divided into two parts, the first is to isolate the right interacting mechanism for the phase transition and the second is to develop the mathematical technique for handling the interaction. The earlier attempts at deriving a suitable microscopic theory made by Ginzburg, Heisenberg and Koppe, Born and Cheng, Tisza, and Bardeen (see Schafroth 1960) proved fruitless due to their failure to recognise the right type of interaction.

The normal state conductivity of the metals finds adequate explanation in terms of the single electron wave functions of Bloch theory. In this theory the field acting on a given electron arises from the smeared out field of the other electrons in the uniform background of the positive charge, the resulting potential being periodic having periodicity of the lattice. The Schroedinger's equation for the entire system separates out into single particle Schroedinger's equations, the solutions being single particle wave functions. Any departure in the periodicity of the lattice results in the scattering of the electrons. The lattice deviations fall into two categories, dynamic and static. The dynamic deviations are caused by the lattice vibrations which give rise to temperature dependent resistivity, the static ones are due to impurities and defects which contribute to the residual resistivity which is temperature independent. If we consider only the dynamic deviations, then to obtain a more quantitative picture, the lattice vibrations may be considered in terms of the quantised modes i.e. phonons. The resulting interaction between electrons and phonons is known as electron phonon interaction. In order to make transition from one state to another the electron may emit or absorb a

phonon, in doing so the energy must be conserved, i.e.

$$\epsilon(\vec{k}) \pm \hbar q s = \epsilon(\vec{k} \pm \vec{q}) \qquad 2.1$$

where $\epsilon(k)$ is the electronic energy $\frac{\hbar^2 k^2}{2m^*}$, m^* being the effective mass of the electron, $\hbar q s$ is the phonon energy, s being the velocity of sound $\vec{k}$ and $\vec{q}$ are the wave vectors of the electron and phonon respectively. The resulting state K' is given by $\vec{K}' = \vec{K} \pm \vec{q}$ The lowest energy of the system is obtained when the lowest states are filled, this can be regarded in momentum space as filling of a Fermi sphere.

When the Bloch - Sommerfeld theory outlined above failed to give even a qualitative description of the superconducting state, it was felt that the free electron model does not give correct interaction between the electrons. In view of the experimentally established fact that in transition from normal to superconducting state the lattice does not undergo a change and also that the ions in the lattice are much more massive than the electrons, it was considered unlikely that the lattice would play an important role in the establishment of the superconductive state. However, in such a situation Fröhlich (1950) introduced a new idea that the electron phonon interaction was responsible for superconductivity. Fröhlich et al (1950) were the first to introduce field theory into solid state physics. By making use of the field-theoretic approach, Fröhlich was able to show that the electron phonon interaction contributes a small term to the energy of the system. His Hamiltonian for a system of N free electrons contained in a volume V, which interact with phonons, treated in Debye approximation can be written as,

$$H = H_0 + H' \qquad 2.2$$

$$H_0 = H_e + H_{ph} \qquad \text{2.3}$$

where

$$H_e = \sum_{i=1}^{N} \frac{p_i^2}{2m} = \sum_{i=1}^{N} \frac{\hbar^2}{2m} k_i^2 \qquad \text{2.4}$$

$$H_{ph} = \sum \hbar \omega_q n_q \qquad \text{2.5}$$

Here He refers to the electrons, H_{ph} to the phonons and H' to the interaction between electrons and phonons and $n_q = 0, 1, 2 \ldots$ is the occupation number of a phonon having wave number q, the corresponding frequency $\omega_q = |q|S$. The interaction H' is assumed to be,

$$H' = \frac{g}{V^{1/2}} \sum_q \sum_{i=1}^{N} \left(\frac{\hbar \omega_q}{2}\right)^{1/2} \left[b_q e^{i\vec{q}\cdot\vec{x}_i} + b_q^\dagger e^{-i\vec{q}\cdot x_i} \right] \qquad \text{2.6}$$

where x_i is the position operator of the i^{th} electron, g is a coupling constant and b_q and $b_q^\dagger$ are absorption and emission operators for a phonon, obeying the commutation relations,

$$\left.\begin{aligned} [b_q, b_{q'}^\dagger] &= \delta_{qq'} \\ [b_q, b_{q'}] = [b_q^\dagger, b_{q'}^\dagger] &= 0 \ , \ b_q^\dagger b_q = n_q \end{aligned}\right] \qquad \text{2.7}$$

Treating the Hamiltonian by second order perturbation theory leads to two consequences.

(i) Electron Self Energy

The shift in the energy eigenstate of He which is analogous to the appearance of the self energy of the electron in quantum field theory. This shift is taken care of by renormalisation procedure and Ho is considered to describe a 'clothed' electron which is accompanied by a phonon cloud.

(ii) Electron - Electron Interaction

The interaction energy $\epsilon(K_1\ K_2)$ between two electrons in states K_1 and K_2 is found to be

$$\epsilon(k_1, k_2) = -\frac{g^2}{2V} \sigma_0^{-2} \frac{|k_1 - k_2|^2}{(k_1^2 - k_2^2)^2 - \sigma_0^2 |k_1 - k_2|^2} \qquad \text{2.8}$$

where $$\sigma_0 = \frac{2ms}{\hbar} \qquad 2.9$$

This energy is found to represent a true dynamical effect and was regarded by Fröhlich to be the cause of superconductivity. Considering that σ_0 is small compared to K_0, the wave number at the Fermi surface, this interaction can be considered to be a short range attraction in K space. Fröhlich's theory predicted isotope effect, $T_c\sqrt{M}$ = constant where M is the isotopic mass of the ion. In fact the isotope effect was experimentally discovered by Maxwell (1950) and Reynolds et al (1950). The mathematical technique used by Fröhlich is questionable and many of the predictions made by the theory are found to be wrong. The importance of the theory however lies in the isolation of the right interaction. The Frohlich Hamiltonian, however seems to be a lasting contribution to the theories of superconductivity as it forms the starting point of the Bogoliubov theory.

The mathematical problem of handling the electron-phonon interaction proved to be quite difficult. If one bears in mind the great qualitative difference in the two phases, it is not surprising that the perturbation expansion from the normal state was found to be inadequate. In fact the development of the first successful microscopic theory, namely B C S theory, had to await two main developments; one was the treatment of electron phonon interaction by Bardeen and Pines (1955) which was based on the collective mode description formulated by Bohm and Pines (1953) and the other was the role of pair correlations giving rise to attractive interaction between the electrons, given by Cooper (1956). The collective mode treatment of the electron interaction is based on the model of the elementary excitations in the solids. There are three principal excitations in the solids, phonons, plasmons and quasi-particles. An excitation is considered to be well-defined if its life time τ is large enough to make

the uncertainty in the energy $\frac{\hbar}{\tau}$ small in comparison with the excitation energy. All the excitations are designated by an appropriate wave vector $\vec{K}$. The phonon energies do not change much by the transitions and can be taken care of by renormalisation procedure. The plasmons, the quanta of the plasma oscillations of the electron gas, have too high an energy to be excited at low temperatures and thus the quasi-particles are important for the problem of superconductivity. In the normal state at $T = 0^{\circ}$ K, all states below Fermi level are occupied and all above are empty. An electron may be excited above Fermi level thereby leaving a hole below the Fermi level. The excited particles above and the holes below the Fermi surface are to be regarded as the elementary quasi-particle excitations, their energies $\epsilon(\vec{K})$ being measured relative to the Fermi energy E_F. In the normal state $\epsilon(\vec{K})$ is a continuous function of $\vec{K}$, vanishing at the Fermi surface. The various excited configurations can be described in terms of occupation numbers in K space. In a superconductor, the excitation spectrum differs in that a finite energy equal to the energy gap is required to excite a particle from the superconducting ground state. In a superconductor the energy of a quasi-particle may be written as

$$E_k = \sqrt{\epsilon(k)^2 + \Delta_k^2} \qquad 2.10$$

where $\epsilon(K)$ is the Bloch energy in the normal state and Δ_K is the energy gap parameter.

A quasi-particle is to be treated as being 'clothed' by interactions with phonons, plasmons and other excitations. While discussing the dynamics of quasi-particles, it is essential to include the screening action and the backflow of electrons, former arising out of high mobility of the electrons and latter being necessary in order that quasi-particles obey

the equation of continuity.

The application of field theory to the interaction between electrons and phonons admits of the possibility of the emission and absorption of virtual phonons analogous to the exchange of virtual photons giving rise to Coulomb potential. In fact, in view of the small phase space available for the excitations, a consequence of the extreme smallness of condensation energy, the effective interaction between the electrons, giving rise to superconductivity may be pictured as follows. A particle near the Fermi surface in a state $\vec{K}_1$ emits a virtual phonon of wave vector $\vec{q}$ and is scattered to a state $\vec{K}_1' = \vec{K}_1 - \vec{q}$, the virtual emission being possible because of the uncertainty relation $\Delta E\, \Delta t \approx \hbar$. A second electron in the state K_2 absorbs the phonon, thereby going to a state $\vec{K}_2' = \vec{K}_2 + \vec{q}$. The net effect is to scatter electrons from their original states $\vec{K}_1$, $\vec{K}_2$ to K_1', K_2' with the conservation of the wave vector,

$$\vec{K}_1 + \vec{K}_2 = \vec{K}_1 + \vec{K}_2. \qquad 2.11$$

This interaction between the pair of the particles comes out to be attractive if the energy difference between the initial and the final states is less than the energy of the virtual phonons, $\hbar\omega_{ph}$. Superconductivity results if this attractive interaction dominates the repulsive screened Coulomb interaction.

Cooper (1956) showed that even a very small net attractive interaction was sufficient that two quasi-particles may form a bound state. He also showed that for attractive interactions, the Fermi sea is unstable against the formation of such bound pairs. This bound state is depressed in energy below the normal continuum of levels, thereby leading to a gap in the energy spectrum. Existence of such a gap was conceived earlier

by many workers to account for various superconductive properties. Thus Cooper's discovery supplied the final missing link for the successful solution of the problem. The existence of the Cooper's pairs has been vindicated by the experiments on flux quantisation in the superconductors. The physical consequence of the pairing is to produce a long range correlation between particles of opposite spin extending over distances of the order 10^{-4} cm, in agreement with Pippard's concept of the coherence length.

The coherence effects associated with the paired wave functions introduce a difference between the scattering in the normal and the superconductive states. In the normal state, the scattering from $\vec{K}, \vec{\sigma}$, where $\vec{\sigma}$ is the spin wave vector, to $\vec{K}', \vec{\sigma}'$ is entirely independent of the scattering from $-\vec{K}, -\vec{\sigma}$ to $-\vec{K}', -\vec{\sigma}'$, the probability of the former is proportional to $|B_{k\sigma, k'\sigma'}|^2$ and the latter $|B_{-k'-\sigma', -k-\sigma}|^2$. In superconducting state, one must add the matrix elements first and then square, due to reasons of coherence of the paired wave functions.

THE B C S THEORY

B C S write the Hamiltonian for a fermion system as:

$$H = \sum_{k>k_F} \epsilon_k n_{k\sigma} + \sum_{k<k_F} |\epsilon_k| (1 - n_{k\sigma}) + H_{coulomb}$$
$$+ \tfrac{1}{2} \sum_{kk'\sigma\sigma'k_0} \frac{2\hbar\omega_k |M_k|^2 c^\dagger(k'-k,\sigma) c(k',\sigma') c^\dagger(k+k,\sigma) c(k,\sigma)}{(\epsilon_k - \epsilon_{k+k})^2 - (\hbar\omega_k)^2} \qquad 2.12$$

Here c's are the creation and annihilation operators obeying the Fermi commutation relations,

$$\left.\begin{aligned} [c_{k\sigma}, c^\dagger_{k'\sigma'}]_+ &= \delta_{kk'}\,\delta_{\sigma\sigma'} \\ [c_{k\sigma}, c_{k'\sigma'}]_+ &= 0 \end{aligned}\right] \qquad 2.13$$

Single particle number operator $n_{k\sigma} = c^\dagger_{k\sigma} c_{k\sigma}$, ϵ_k is the Bloch energy measured relative to the Fermi surface, M_k is the matrix element for electron

phonon interaction, ω_κ is the frequency of a phonon with wave number K, σ is the spin wave number, the primes referring to the excited states. According to the calculations of Bardeen and Pines (1955), M_k calculated for the zero point amplitude of the lattice vibrations is given by

$$|M_k|^2 = |v_k|^2 \frac{\hbar}{2\omega_K} \qquad 2.14$$

where v_k are the effective matrix elements for electron lattice interaction. Since M_k^2 varies with isotopic mass in a way similar to ω_k, the ratio $\frac{M_k^2}{\hbar\omega_k}$ is independent of the isotopic mass.

For the excitation energies $|\epsilon_K - \epsilon_{K+k}| < \hbar\omega_\kappa$ the phonon interaction is negative (attractive). This is opposed by the repulsive Coulomb interaction which for free electrons in a unit volume is $\frac{4\pi e^2}{k^2}$ If one takes screening into account, k^2 should be replaced by $k^2 + k_s^2$, k_s depending upon the electron density. The criterion for the appearance of the superconductivity then is, that the attractive phonon interaction should exceed the Coulomb interaction:

$$\left\langle -\frac{2|M_k|^2}{\hbar\omega_K} + \frac{4\pi e^2}{K^2 + k_s^2} \right\rangle < 0 \qquad 2.15$$

A detailed discussion by Pines (1958) shows that this criterion is in reasonable agreement with the one empirically established by Matthias (1957) for the appearance of superconductors in the periodic system.

The next step is to introduce pair correlations by including only those configurations in which the states are occupied in pairs, the pairs having vanishing total momentum and spins. Introduction of the pair correlations at this stage amounts to the introduction of selected sub-sets in the matrix elements so as to give a coherent low state. A pair is designated by a wave vector K independent of the spin. To treat the pair

correlations new creation and annihilation operators are introduced as defined below:

$$\left.\begin{aligned} b_k &= c_{-k\downarrow} c_{k\uparrow} \\ b_k^\dagger &= c_{k\uparrow}^\dagger c_{-k\downarrow}^\dagger \end{aligned}\right] \qquad 2.16$$

These operators satisfy the commutation relations,

$$\left.\begin{aligned} [b_k, b_{k'}^\dagger]_- &= (1 - n_k - n_{-k})\,\delta_{kk'}, \quad [b_k, b_{k'}] = 0 \\ [b_k, b_{k'}]_+ &= 2 b_k b_{k'} (1 - \delta_{kk'}) \end{aligned}\right] \qquad 2.17$$

In terms of these the Hamiltonian 2.12 may be written as

$$H_{red} = 2\sum_{k>k_F} \epsilon_k b_k^\dagger b_k + 2\sum_{k<k_F} |\epsilon_k| b_k b_k^\dagger - \sum_{kk'} V_{kk'} b_k^{*\prime} b_k \qquad 2.18$$

Since the interaction term is negative in sign, V_{KK1} will be positive for a superconductor. If ω is the average phonon frequency, the important matrix elements lie in the region,

$$-\hbar\omega < (\epsilon_k, \epsilon_{k'}) < +\hbar\omega \qquad 2.19$$

Hence $V_{KK'}$ is replaced by,

$$\left.\begin{aligned} V_{kk'} &= V \qquad \text{for } -\hbar\omega < (\epsilon_k, \epsilon_{k'}) < +\hbar\omega \\ V &= 0, \text{ otherwise,} \end{aligned}\right] \qquad 2.20$$

assuming that $V_{KK'}$ is isotropic and constant over a thin shell. Thus the Hamiltonian 2.18 becomes

$$H_{red} = 2\sum_{k>k_F} \epsilon\, b_k^\dagger b_k + 2\sum_{k<k_F} |\epsilon_k| b_k^\dagger b_k - V \sum_{kk'}{}' b_{k'}^\dagger b_k \qquad 2.21$$

where $\sum'$ extends only in the region defined by 2.19.

B C S employ a self consistent method to obtain wave function for the Hamiltonian 2.18 and the best of these wave functions is chosen

by a variation principle. A wave function for N independent pairs is written as

$$\psi_{oN} = \mathcal{P}_N \prod_k \left[\sqrt{(1-h_k)} + \sqrt{h_k}\, b_k^{*} \right] \phi_0 \qquad 2.22$$

where $\mathcal{P}_N$ is the projection operator selecting states having exactly N pairs, ϕ_0 is the vacuum operator and the quantities h_k,

$$0 \leq h_k \leq 1 \qquad 2.23$$

are the parameters to be so determined as to minimise the expectation value of the energy W(o) given by,

$$W(o) = (\psi_0, H_{red}\, \psi_0) \qquad 2.24$$

W(o) is found to be,

$$W(o) = \sum_k 2\epsilon_k h_k - V \sum_{kk'} \left\{ h_k (1-h_{k'})\, h_{k'} (1-h_k) \right\}^{1/2} \qquad 2.25$$

The first term is the difference in the kinetic energy of the two phases, the factor 2 is due to pairing. The first term can be positive or negative. The second term gives the correlation energy for transition from the state $(\vec{K}, -\vec{K})$ to $(\vec{K}', -\vec{K}')$. The parameter h_k can be interpreted to be the probability that the state $(\vec{K}, -\vec{K})$ is occupied.

Minimising W(o) with respect to h_k results:

$$h_k = \frac{1}{2}\left(1 - \frac{\epsilon_k}{E_k}\right) \qquad 2.26$$

$$\epsilon(o) = \frac{V}{2} \sum_k \frac{\epsilon(o)}{\left[\epsilon_k^2 + \epsilon^2(o)\right]^{1/2}} \qquad 2.27$$

where

$$\epsilon(o) = V \sum_{k'} \left[h_{k'} (1-h_{k'}) \right]^{1/2} \qquad 2.28$$

and

$$E_k = \left[\epsilon_k^2 + \epsilon^2(o)\right]^{1/2} \qquad 2.29$$

~~Substituting 2.26 into 2.28,~~ we obtain,

$$\frac{1}{V} = \sum_k \frac{1}{2(\epsilon_k^2 + \epsilon_o^2)^{1/2}} \qquad 2.30$$

If we replace the summation by integration and remembering that for the states within the range $|\epsilon_k| < \hbar\omega$, $V = 0$, we have,

$$\frac{1}{N(0)V} = \int_0^{\hbar\omega} \frac{d\epsilon}{2(\epsilon_k^2 + \epsilon_0^2)} \qquad 2.31$$

where N(o) = density of states at the Fermi surface. From 2.31 we have,

$$\epsilon_0 = \frac{\hbar\omega}{\sinh\left[1/N(0)V\right]} \qquad 2.32$$

Making use of 2.29, 2.28, 2.24 and 2.32, the expression for W(o) the energy in the ground state is found to be,

$$W(0) = \frac{-2N(0)(\hbar\omega)^2}{\left(e^{2/N(0)V} - 1\right)} \qquad 2.33$$

B C S also calculate the magnitude of the energy gap which is equal to the energy to break up a pair. At $0^\circ K$, this is found to be $2\epsilon_0$ As $\frac{1}{N(0)V} \approx 3 - 4$, from equation 2.29,

$$2\epsilon(0) = 4\hbar\omega \exp\left[-1/N(0)V\right] \qquad 2.34$$

B C S extended the above treatment to expressions for energy gap at temperatures above 0° K and also derived an expression for T_c. For temperature T, $0 < T < T_c$, increasing number of electrons are excited into quasi-particle single electron states, at the same time there exist the Cooper pairs. Essentially this is a two fluid picture. At the temperature T, the ground state energy W(T) contains a kinetic energy term and correlation energy term, both being modified to take into account the presence of the normal electrons. If we denote the probability of the occupation of K or of -K by a single normal electron by f_k, the two terms can be written as:

$$\left[W(T)\right]_{K.E} = 2\sum_k |\epsilon_k| \left[f_k + (1 - 2f_k)h_k\right] \qquad 2.35$$

and

$$[W(T)]_{corr.} = -V \sum_{kk'} \left\{ h_k (1-h_{k'}) h_{k'} (1-h_k) \right\}^{1/2} \times (1-2f_k)(1-2f_{k'}) \qquad 2.36$$

As before, by minimising free energy with respect to h_k and f_k, one obtains the following expressions:

$$h_k = \left[1 - \frac{\epsilon_k}{E_k} \right] \qquad 2.37$$

where

$$E_k = \left[\epsilon_k^2 + \epsilon^2(T) \right]^{1/2} \qquad 2.38$$

$$f_k = \left[\exp\{(E_k/k_B T) + 1\} \right]^{-1} \qquad 2.39$$

$$\frac{1}{N(0)V} = \int_0^{\hbar\omega} \frac{d\epsilon}{\left[\epsilon^2 + \epsilon^2(T)\right]^{1/2}} \tanh \left\{ \frac{\left[\epsilon^2 + \epsilon^2(T)\right]^{1/2}}{2 k_B T} \right\} \qquad 2.40$$

$$T_c = (1/k_B)\, 1.14\, \hbar\omega \exp\left[-1/N(0)V\right] \qquad 2.41$$

where K_B is the Boltzmann's constant, and for T_c, $\epsilon(T_c) = 0$

Equations 2.41 and 2.34, yield

$$2\epsilon(0) = 3.52\, k_B T_c \qquad 2.42$$

The B C S theory successfully establishes the following:

1. A criterion for the appearance of superconductivity. Pines (1958) has discussed the appearance of superconductivity in the periodic system and finds that the theory qualitatively explains the variation of T_c from one metal to another.
2. Existence of an energy gap. Biondi et al (1958) give a review of experimental work done for the measurement of the energy gap. The temperature dependence of the energy gap predicted by the theory has also been verified.
3. Isotope effect. Although it may be noted that Geballe et al (1961) found that ruthenium does not exhibit any isotope effect.

4. Coherence properties. The measurement of ultrasonic attenuation on single crystals by many workers e.g. Morse et al (1959) are in good agreement with the theory.

The theory also accounts satisfactorily for:

(1) The temperature variation of the specific heat in the superconducting state,

(2) The second order phase transition.

B C S theory does not yet provide an acceptable explanation of the Meissner effect and persistence of currents. The theory is also unable to account for the Knight shift. Bardeen (1962a). Another failing of the theory is the discovery of the existence of superconductors amongst the ferromagnetic materials. (Bardeen (1962a.)

THE BOGOLIUBOV THEORY

Bogoliubov (1958) developed a new approach for treating superconductivity. As a starting point he assumes the Fröhlich Hamiltonian for an electron gas interacting with phonons. In view of the fact that only the electrons in a thin shell near the Fermi surface are important, one can think of a description of the electronic state in terms of excitations over an appropriate ground state. Out of many ways of defining such excitations and the ground state, Bogoliubov considers the ones involving the pairs of electrons with opposite spins and momenta, with a coefficient which is undetermined to start with. The coefficients must be such as not to produce non-integrable divergencies in the perturbation theory. This condition determines the coefficients. For an attractive interaction one finds a

new ground state lower than the Fermi state. Bogoliubov interprets this to be the superconducting ground state.

Bogoliubov theory is supposed to be based on better mathematical foundations than B C S theory. Yosida (1958) has demonstrated the equivalence of the two methods in so far as the energy spectrum at the absolute zero is concerned. The Bogoliubov theory successfully explains all the superconducting properties explained by B C S theory.

The methods developed by B C S and Bogoliubov are finding increasing use in the theory of elementary particles. Nambu and Jona - Lasimo (1961) have constructed a dynamical model of the elementary particles analogous to superconductivity model. They suggest that the nucleon mass arises largely through the same mechanism as the appearance of the energy gap in the theory of superconductivity. The microscopic theories of superconductivity, besides securing a better physical understanding of the phenomenon, have given rise to a great spurt in the experimental work.

CHAPTER III

SUPERCONDUCTIVITY IN THIN FILMS - A REVIEW

There are a large number of factors which govern the structure and the properties of evaporated films. Some of these are: vacuum conditions, rate of deposition, presence of the residual gases, the nature and the geometry of the substrate, stresses in the film and angle of the incidence of the vapour beam.

In order that the films with reproducible characteristics may be obtained, a good vacuum is essential. Vacuums of the order of 10^{-6} mm of Hg or better are desirable. A good vacuum has two important effects: firstly it prevents the oxidation of the film and secondly it reduces the amount of absorbed gases in the films, thereby ensuring a smoother structure. The above are also helped by high rates of deposition. Levinstein (1949) found that the tendency for agglomeration formation decreased as the rate of deposition increased. Presumably, with higher rates, more nuclei are formed initially and these act as nucleation centres to ensure a fine grain size resulting in a smooth structure. Behrndt et al (1960) found that the films deposited at the liquid nitrogen temperature possessed smoother surface than the ones deposited at the room temperature. In practice, the rates of deposition are limited by the amount of power the heater can handle and also by the consideration of the homogeneity of the film. Kahan et al (1960) found that the high rate of deposition results in the

film having low residual resistivities at low temperatures but the grains are found to be coarse, the average grain diameter varying between 5 and 25 microns. On the other hand the films of higher residual resistivity, deposited with the substrate at room temperature and lower deposition rate showed fine grain structure, almost near the limit of optical resolution. This seems to be in disagreement with the findings of Levinstein stated above. Perhaps in Kahan's films the higher evaporation rates resulted in the temperature rise of the substrate, thereby making the nuclei more mobile which resulted in the formation of bigger grain size.

Presence of gases excercises considerable influence on the structure and properties of thin films. Of all the gases present, oxygen is most undesirable, its presence results in the oxidation of the film. This can be minimised by having good vacuum and employing some getters to get rid of oxygen. Some metals notably tantalum and tungsten have a great affinity for oxygen resulting in the formation of volatile oxides which could be collected on a shield before commencing deposit on the substrate. High deposition rates also are helpful in diminishing the oxidation of the film because of the reduced transit time and the condensation time - the periods when the atoms seem to be in an active state of being oxidised. Water vapour, another common impurity in the vacuum system, can be substantially removed by a suitable liquid nitrogen trap.

The nature of the substrate is an important factor governing the film quality. The substrate must be cleaned thoroughly. Various methods have been used for cleaning, ranging from use of detergents, acids, followed by degreasing baths to ultra-sonic cleaning. In order to free the substrate from the occluded gases, the substrates have been baked in vacuum.

The thermal conductivity of the substrate and the coefficient of expansion relative to the condensate are important factors governing the grain size and the stresses in the film. The crystalline state of the substrate is a factor which affects the directional growth of the nuclei. Evans and Wilman (1952), on the basis of the electron diffraction studies show that the amorphous or inactive crystalline substrates have tendency to cause the films to grow in the preferred directions. The temperature of the substrate, which is an important factor governing the mobility of the condensate nuclei, may influence this process. Rhodin (1949) found with different substrate materials that there was a characteristic base temperature leading to maximum orientation. On this basis, he concludes that the condensed atoms must possess a certain minimum kinetic energy to enable them to move into preferred positions. In the single crystal substrates, the deposit crystals are often found oriented with respect to the substrates. This phenomenon is known 'epitaxy'. No satisfactory theory of epitaxy exists, the model which has received more support is that of Franck and Van der Merwe (1949). According to them, the first step in the growth of the oriented layer is the formation of a monolayer of the deposit which has the same spacing as the substrate. This monolayer is in a state of constraint and if the constraint exceeds a certain critical value, dislocation will occur which will hinder the growth of the nuclei in the initial orientation. The creation of a dislocation needs some activation energy, hence the deposition at the low temperatures will tend to reduce and prevent the formation of dislocation. However, the deposition at very low temperatures, such as liquid helium temperatures, may lead to many faults or defects being frozen in. The condensation in such situations corresponds to quenching.

ELECTRICAL CONDUCTION IN THIN FILMS

The electrical resistivity ρ of the metals can be written as:

$$\rho_{total} = \rho_{lattice} + \rho_{residual} + \rho_{thickness}$$

The third component arises from the boundary scattering of the electrons, the first two are the same as for the bulk metal. The resistivity of thin films depends upon thickness. For a first few angstrom thick layers, resistivity may be infinite. For a detailed examination of the dependence of resistivity on film thickness, the film may be divided into four domains in thickness:

(1) When film thickness is too small for the conduction to begin. The thickness of this domain will depend upon a large number of factors such as the deposit material, substrate and conditions of condensation.

(2) The conduction just sets in, the electrical resistivity is still very high.

(3) Extending from about 200 Å up to a certain value till the resistivity continues to decrease with thickness.

(4) The resistivity becomes independent of thickness or decreases very slowly with thickness.

The theory of the mean free path effects (see Sondheimer 1952 for a review) is applicable to the film thickness in the third and the fourth domains. The resistivity of the film is given by:

$$\frac{\rho}{\rho_b} = \frac{4 l^b}{3 d \left(\ln \frac{l^b}{d} + 0.4228 \right)} \qquad \text{for } d \ll l^b \qquad 3.1$$

$$\frac{\rho}{\rho_b} = 1 + \frac{3}{8} \frac{l^b}{d} \qquad \text{for } d \gg l^b \qquad 3.2$$

where d is the film thickness, l is the mean free path and ρ_b is the bulk resistivity.

SUPERCONDUCTING TRANSITION WITH ZERO FIELD AND CURRENT

Unlike the transition in single crystal and strain-free superconductors, the superconducting transition in thin films is rather broad. The transition temperature when measured by resistance measurements is defined to be the temperature at which the resistance becomes half of its value in the normal state. Similarly if the transition is observed by measuring the magnetic induction, T_c is defined to be the temperature when the induction has half the value in the normal state. Likewise for sub-critical temperatures, the critical currents and fields are defined to be the ones required to restore the resistance to half the values in the normal state.

De Haas and Voogd (1931) showed that the resistance of a single crystal of tin vanishes discontinuously at T_c. At T_c, the transition is of the second order. The discontinuous drop in the resistance to zero value is cited by Pippard as an evidence for the existence of a coherence length in the superconductors.

The presence of physical or chemical impurity is known to lead to broader transitions. Aziz and Baird (1959) investigated the effect of grain size on the width of the transitions. They find, in agreement with the original findings of de Haas and Voogd, that the existence of grain boundaries broadens the transition in the direction of increasing temperature. Their experiments with samples of differing grain size showed that smaller grain size leads to wider transitions and that any crystal mis-orientation will also result in wider transitions. According to Faber (1957) any misoriented inclusion imbedded in a single crystal will lead to the estab-

lishment of strains resulting in the appearance of certain parts of the crystal having T_c greater than that for an ideal crystal.

Thin films are far from a thin slice of an ideal superconductor, which they are supposed to be for most theoretical treatments. The transitions in films are broad and this is a consequence of strains, inhomogeneity, edges and weak spots associated with the films. The transition temperature for films is often different from its value in bulk. Lock (1951) was first to point out the connection between the shift in T_c and the strains in the film resulting from the differential contraction between the film and the substrate. He could show experimentally that the transition temperature for the films could be above or below the bulk value depending upon whether the substrate contracted less or more than the film. By matching the thermal expansions, it was possible to make films having their transition temperature the same as that in the bulk. Toxen (1961) and Jennings and Swenson (1958) discussed quantitatively the effect of stresses on T_c and found that the change in T_c can be represented by the equation,

$$\delta T_c = \frac{52}{d} - \frac{750}{d^2} \qquad 3.3$$

where d is film thickness of their films.

The bulk of the work done on thin films has been done on films deposited on plane surfaces. Presence of the edges is an important cause of broad transitions. Kahan et al (1960) find that the transitions can be made much sharper by removing the edges. Annealing and etching also improves the sharpness of the transitions. De Lano, Jr. (1960) also discussed the edge effects and their removal by annealing, etching and trimming.

CURRENT TRANSITIONS IN FILMS

The critical currents in the bulk specimen are governed by Silsbee's hypothesis. In thin films the situation is different. Here, especially in the neighbourhood of T_c, the magnetic field penetrates the whole thickness. The following consideration based on London theory shows that I_c should vary as $(T_c - T)^{3/2}$. In case of current flow of current density J_s, the increase in the free energy is given by,

$$\Delta F = \frac{1}{2} \Lambda(T) J_s^2 \qquad 3.4$$

where $\Lambda(T)$ is assumed to be independent of J_s, which may not be valid for large currents. To obtain the critical current we equate the increase in the free energy to the difference of energy between normal and superconducting phases which is $H_c^2/8\pi$.

Thus we have,

$$1/2\ \Lambda(T)\ J_{sc}^2 = \frac{H_c^2}{8\pi} \qquad 3.5$$

Near T_c, both H_c and $[\Lambda(T)]^{-1}$ vary as $(T_c - T)$, leaving J_{sc} varying as $(T_c - T)^{3/2}$.

Rogers (1960) calculates the critical currents on the basis of microscopic theory by taking into account the change in the distribution of quasi-particles and energy gap with current. His values are found to be 25% lower than the ones calculated on semi-phenominological theories. However, the temperature dependence is found to remain unchanged.

Experimentally the situation is complicated by the fact that the appearance of the first trace of resistance results in the production of Joule heating which raises the temperature of the film, thereby lowering the ambient critical current. As stated earlier, in the films, the

transition in the absence of Joule heating, is broad, occupying several milli-degrees, a consequence of inhomogeneity and presence of weak spots in the film. Quite misleading results may be obtained if proper precautions are not taken to eliminate or account for the Joule heating. It is well known that the critical currents are found to be considerably lower when continuous currents are used instead of pulses. Most of the work has been done on flat films. The presence of sloping edges may be another factor for lower critical currents as superconductivity at thin edges would be destroyed first resulting in the heating of the film before the currents critical to the bulk portion of the film have been reached. Heating of the film will depend upon the current being passed through the film, the resistance of the film and also the thermal conductivity and capacity of the substrate. These factors will be important for the thermal hysterisis observed in the films.

No satisfactory model to account for heating effects in thin films exists. Bremer and Newhouse (1958) were the first to show experimentally the thermal propagation effects in the films. In their experiments, they passed a maintaining current I_M through the film, I_M being less than the critical current. A current pulse known as the nucleating current was passed through a wire held very close to the film and perpendicular to it. The magnetic field associated with the pulse together with that created by I_M was sufficient to restore resistance just below the nucleating wire; this resulted in the production of joule heating due to current I_M. The normal region was found to propagate along the film resulting in the restoration of normal state throughout the film. The velocities of propagation of these thermal wave fronts were found to be low, of the order of 20 cm per second. Evidence for the existence of this mechanism of thermal

propagation has been found by Broom and Rhoderick (1959, 1960) Cherry and Gittleman (1960) and Kolchin et al. (1961). Broom and Rhoderick find that the velocities of thermal propagation in their experiment were many times larger than observed by Bremer and Newhouse. This difference they attribute to larger currents and thinner films used in their experiment. Indeed these authors (1960) also report the successful construction of a new type of bistable element capable of being switched from one state to another in an interval of 10 μs. The bistable element works on the principle that at a given temperature below T_c for any film there exists a unique current which maintains the interphase boundary stationary. If the current is increased, the normal region spreads and if it is decreased, the superconducting region grows. Thus a current pulse in either direction riding over the biasing current will switch the element into the superconducting or the normal state. This device can be taken to be an evidence for the existence of the movement of the interphase boundary due to the thermal effects.

Cherry and Gittleman also found an evidence for thermal propagation of the interphase boundary on their experiment on a tin film of 1 micron thickness and 0.5 mm. width. They postulate an early formation of a normal region which could have been brought about due to a variety of causes e.g. local heating, local magnetic field, any metallurgical inhomogeneity, or by eddy current heating during the rise time of a fast current pulse (Pippard process). The velocities of the thermal propagation observed by them ranged from 10 to 10,000 cm. per second depending upon the current magnitudes and the bath temperature. Kolchin et al. also assume two different mechanisms for the thermal propagation, for slow rates of rise Joule heating is predominant, for a fast rate, eddy current heating becomes quite

effective.

The first attempt to measure the critical currents in evaporated thin films was made by Shalnikov (1940) by using continuous currents. The observed values were found to be considerably lower than those expected on the basis of the Silsbee's hypothesis.

Alekseevskii and Mikheeva (1957) used a compensated geometry to avoid any edge effects. Their films were deposited on a substrate in the form of a disc, the current being introduced through a lead perpendicular to the plane of the disc and taken out from the periphery. The films were prepared by sputtering tin on a substrate held at the liquid nitrogen temperature. The films were kept under vacuum until they were immersed in liquid helium. The critical currents were measured by using pulses of 0.1 sec duration and the temperature region over which the measurements were made was 0.5° below T_c. The H_{cI} was found to be proportional to $(\Delta T)^n$ where $n = 0.6$. In their later measurements (1960) these authors investigated the effect of rise time of the current pulse on the value of the critical current and found that the critical current continued to increase with the decrease in the rise time after which it did not show any change. By extrapolating the I_c this way they find $I_c \propto \Delta T$. However, in case of the films deposited at room temperature, near T_c, the dependence was found to be in agreement with the prediction of Ginzburg - Landau theory.

Glover III (1957) measured the critical currents in films of tin and lead to quite low temperatures by using continuous currents. His films were 50 Å in thickness. The critical current was found to vary as $\left[1 - \left(\frac{T}{T_c}\right)^2\right]^{-1/2}$ over entire temperature range but near T_c B C S function for critical currents was found to be a better fit.

Schmidlin and Crittenden (1958) with indium films find $I_c \propto \Delta T$ close to T_c. However, in some films they find that the proportionality departs from linearity thereby causing $I_c - \Delta T$ curve bending towards the ΔT axis. Crittenden, Cooper and Schmidlin (1960) determine critical current as a function of temperature for a tin film .06 μ thick, 5 mm long and 60 μ wide deposited on optically polished glass. The critical currents were measured by employing a circuit which increased the current slowly until the specimen switches when the current is cut off to zero within a micro second. The D.C. critical current below λ point is approximately fitted to the function $\frac{I_c}{I_{co}} = 1 - (\frac{T}{T_c})^4$, where I_{co} is the extrapolated critical current at the absolute zero. They observe a discontinuous jump in the critical current at the λ point. This could be attributed to the fact that the transitions observed were not free from heating effects. Near the transition temperature, the threshold critical currents (I_t) were found to be lower than I_c but the two became one at lower temperatures. These workers also find evidence for the thermal propagation of the interphase boundary similar to one observed by Bremer and Newhouse (1958).

Smallman et al. (1960) determine critical currents for tin films of various width and thickness by using pulses of rise time 60 μs. and decay time 40 μs. The substrates used by them were quartz and glass plates. The films of the same thickness on quartz showed greater critical current than the ones on glass, both on D.C. as well as on pulse tests. This difference arises due to better thermal conductivity of quartz and has been observed by several other workers. The film on glass under D.C. test showed a convex curvature with respect to temperature axis. They also noted thermal hysterisis and estimated the temperature rise of approximately 0.20°K.

Bremer and Newhouse (1959) on their tin films deposited on single crystal sapphire and glass substrates seem to verify Ginzburg - Landau theory for the temperature region close to T_c (within 30 milli-degrees). Their measurements were made in the temperature region $\Delta T \leqslant 0.3^{o}K$, in this range the calculated penetration depth for the bulk tin being $\geqslant$ 0.1 micron which was comparable to their film thickness of 0.30 microns. They also find that the critical current varies linearly with the film width, interpreting this to mean that the current was uniformly distributed over the film width, for the films whose thickness was comparable with λ . They also find I_c for the films on sapphire to be greater than the ones on glass.

Until now with the exception of the films of Alekseevskii and Mikheeva, most of the films used were deposited on flat substrates, using uncompensated geometry. The data on such films is hard to interpret because of the extreme distortion of the magnetic field of the current at the edges of the films. The first experiment on films evaporated on cylindrical substrates was done by Ginzburg and Shalnikov (1960). Their measurements were limited to the temperature region close to T_c. The tin films used by them ranged in thickness from 3.3×10^{-5} cm to 6.5×10^{-6} cm. The films were deposited at room temperature in a vacuum of the order of 10^{-6} mm. of Hg. For observing transitions they used d.c. The temperature and size dependence of their critical currents and critical magnetic fields is in agreement with the Ginzburg - Landau theory.

The transition from the superconducting to the normal state is an extremely fast one occuring in times of the order of a few nano-seconds. Kolchin et al.(1961) find that for sufficiently large currents the transition takes place in about 5 nano-seconds, the transition time depending upon the current amplitude. Schmidlin et al (1960) find the transition

times dependent upon the current amplitude and the film thickness and could vary within wide limits.

DESTRUCTION OF SUPERCONDUCTIVITY BY MAGNETIC FIELD

The measurement of the critical fields provide a test for the validity of the various theories of superconductivity. London theory is unable to account for the high critical magnetic fields observed for thin films. The failure arises due to two reasons, firstly London theory does not properly take into account the surface energy between superconducting and normal regions and secondly it is a weak field theory and its applicability is limited to the magnetic fields $\ll H_c$. Ginzburg - Landau theory is free from above shortcomings but like London theory it is a local theory. For the explanation of the critical field data, it has been found essential to incorporate the non-local aspects in the G.L. theory. The critical fields are calculated mainly for two limiting cases; the Pippard limit (non-local) when the coherence length $\xi \gg \lambda$, London limit (local) when $\lambda \gg \xi$. The second condition is easier to satisfy when working with thin specimen near the transition temperature.

Two types of dependence have been investigated, the size dependence and the temperature dependence.

THE SIZE DEPENDENCE:

According to London theory the critical magnetic field of a thin film of the thickness d is given by,

$$H_c = H_{cb}\left[1 - \frac{2\lambda_L}{d}\tanh\frac{d}{2\lambda_L}\right]^{-1/2} \qquad 3.6$$

where H_{cb} is the critical field for the bulk material, λ_L is London penetration depth and H_c is the critical field for the film. In the above

expression, the variation of magnetic field inside a film of thickness d is assumed to be,

$$\frac{H(x)}{H(0)} = \frac{\cosh x/\lambda_L}{\cosh d/2\lambda_L} \qquad 3.7$$

Ittner (1960), assuming the field variation to be according to the calculations of Schrieffer (1957)

$$\frac{H(x)}{H_0} = \frac{4}{d} \sum_{n=0}^{\infty} \frac{k_n \sin k_n x}{k_n^2 + K(k_n)} \qquad 3.8$$

where $k_n = \frac{(2n+1)\pi}{d}$ and $K_{(k)}$ is given by

$$K(k) = -\frac{4\pi \vec{J}(k)}{c\,\vec{A}(k)}, \quad \vec{J} \text{ and } \vec{A}$$

being the current density and vector potential respectively, shows that the equation (3.6) represents the correct behaviour if λ_L is replaced by λ_ϵ where λ_ϵ is found to vary with film thickness and purity.

The penetration depth has been found to vary with thickness in the experiments of Lutes (1957), Schawlow (1958) and Glover and Tinkham (1956, 1957). All microscopic theories predict variation of λ with thickness and mean free path. Ittner calculated the value of λ_ϵ/d by substituting his data on critical fields in tin films in equation 3.6 He found that if the mean free path and film thickness was greater than ξ, the penetration depth did not vary appreciably. In case either mean free path or film thickness was less than ξ, the penetration depth increased significantly with thickness. In his experiment the variation of $\lambda_\epsilon(T)/\lambda_\epsilon(0)$ as a function of $\left[1-(\frac{T}{T_c})^4\right]^{-1/2}$ is found to be different from the prediction on the basis of B C S theory but is in agreement with the experiment of Schawlaw and Devlin. Toxen (1961) on his measurements with indium films found the variation of λ with thickness in agreement with Ittner's results.

Toxen (1962) obtained expressions for the critical fields of thin films. By making use of G - L theory he finds a relationship between critical field and magnetic susceptibility in the weak field limit. Then by combining this with Schrieffer's (1957) calculation of weak field susceptibility in terms of non-local parameters, he obtains expressions for the critical fields in terms of non-local parameters. His results can be stated as follows:

(i) Assuming specular reflection at the film surfaces - (whereas a is half thickness),

$$\frac{H_c}{H_{cb}} \simeq 2.01\left[\left(\xi_0 \lambda_L^2\right)/a^3\right]^{1/2} \qquad 3.9$$

(ii) For random scattering -

$$\frac{H_c}{H_{cb}} \simeq 2.31\left(\xi_0 \lambda_L^2/a^3\right)^{1/2} \qquad 3.10$$

A comparison of these equations shows that the non-local calculation is not sensitive to the type of reflection assumed. Toxen's model is in agreement with his experimental data on indium films.

TEMPERATURE DEPENDENCE OF THE CRITICAL FIELDS

Ginzburg (1958) on the basis of G - L theory found that near T_c the critical field is given by the following expression: (equation 1.28)

$$H_c = \frac{\sqrt{6}\ \lambda_{00}\sqrt{T_c}}{d}\left|\frac{d H_{cb}}{dT}\right|(\Delta T)^{1/2}$$

when λ_{00} is the penetration depth at $0^{\circ}K$. Both the thickness dependence and temperature dependence have been experimentally verified by Ginzburg and Shalnikov (1960).

Douglass and Blumberg (1962) calculated the critical fields in the London limit. Near T_c, the critical field is given by

$$H_c(T) = 1510\,[\lambda(0,d)/d](\Delta t)^{1/2}(1+\epsilon\Delta t) \qquad 3.11$$

where ϵ is a number independent of film thickness but depends upon the form of expression assumed for the free energy in the superconducting state. For Ginzburg - Landau form (1950), $\epsilon = 0.31$ and for Bardeen (1954) $\epsilon = -0.19$. They also find the penetration depth to be size dependent.

Bardeen (1962) calculated the critical field near T_c by minimising free energy and calculating the equilibrium value of Δ_k, the energy gap parameter. His expression for H_c is given by,

$$H_c^2 = \frac{4k\Delta T\Delta_{k_1}}{a\,\Delta_{k0}} \qquad 3.12$$

where Δ_{k0} is the energy gap at $0^\circ K$, $\Delta T = T_c - T$ and $a = \frac{g_L d^2}{\lambda^2 H_0^2}$

$2d$, film thickness g is a dimensionless geometrical factor depending upon the shape of the sample and the type of scattering assumed.

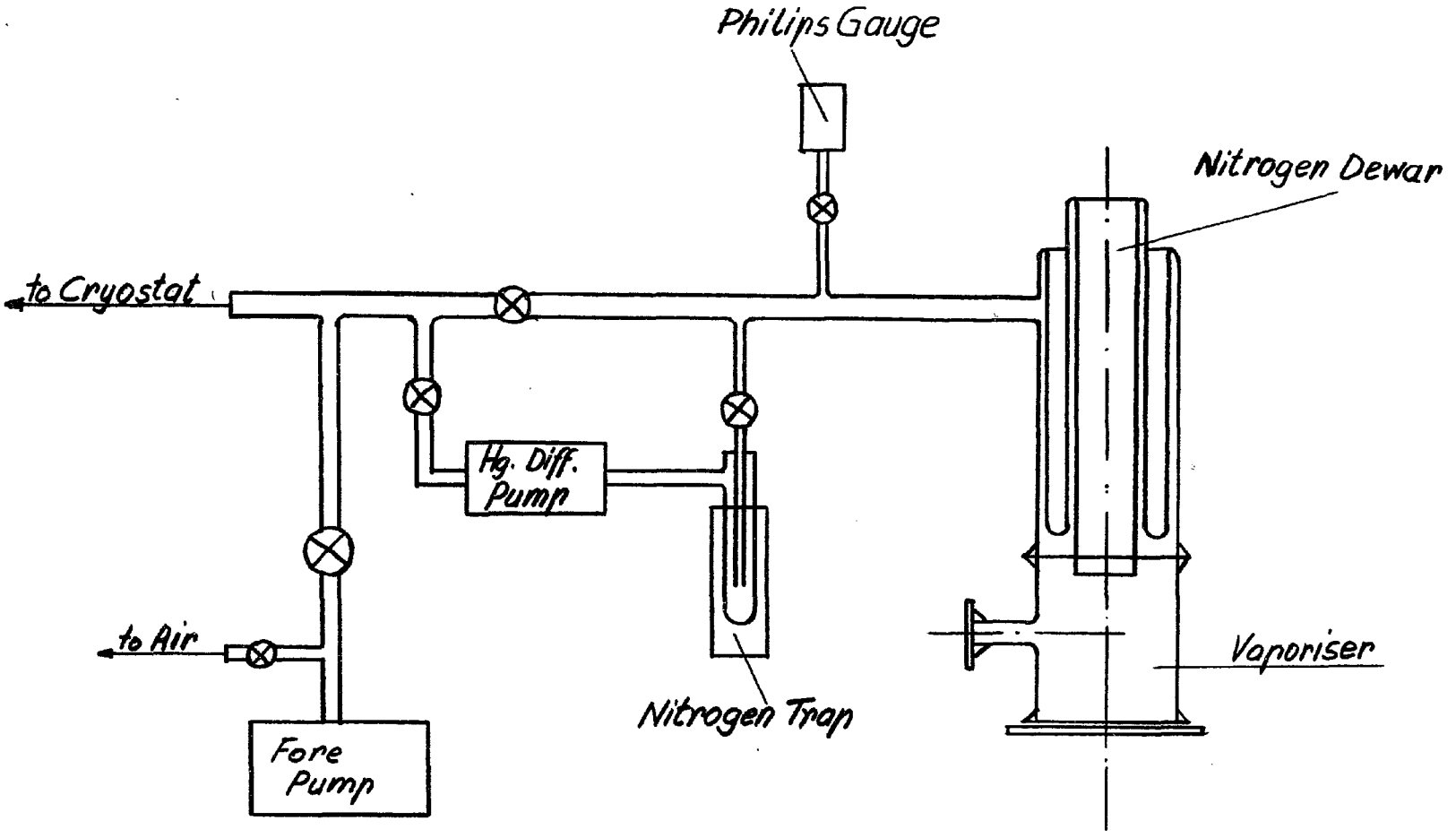

FIG. 4.1

Vacuum System for Vaporiser

CHAPTER IV

SPECIMEN PREPARATION AND MOUNTING

Most of the work done on superconductivity in thin films has been done on films deposited on flat substrates. Such films though easier to make suffer from the disadvantage of having sloping edges, which if not removed may lead to misleading results. Besides even for films with edges trimmed the problem of finding the distribution of current is a difficult one. In order to escape these difficulties, it was decided to deposit films on cylindrical rods. In the design of the apparatus the following requirements were kept in view.

(i) Ability to produce vacuums of the order of 10^{-6} mm or better.

(ii) Provision for cooling the substrate to liquid nitrogen temperatures.

(iii) Arrangement for rotating the specimen at suitable speeds during deposition to ensure uniformity of the deposit.

(iv) Provision of high current leads for rapidly vaporising the metal to be deposited.

(v) A suitable shield for protecting the substrate when deposition is not desired, as in the initial outgassing.

The vacuum system as shown in the figure4.1consists of the following parts.

(1) An oil diffusion pump, backed by a mechanical pump, capable of producing vacuum of the order of 10^{-7} mm.of Hg. The first nitrogen trap is provided to trap any oil vapours escaping into the vaporisation chamber.

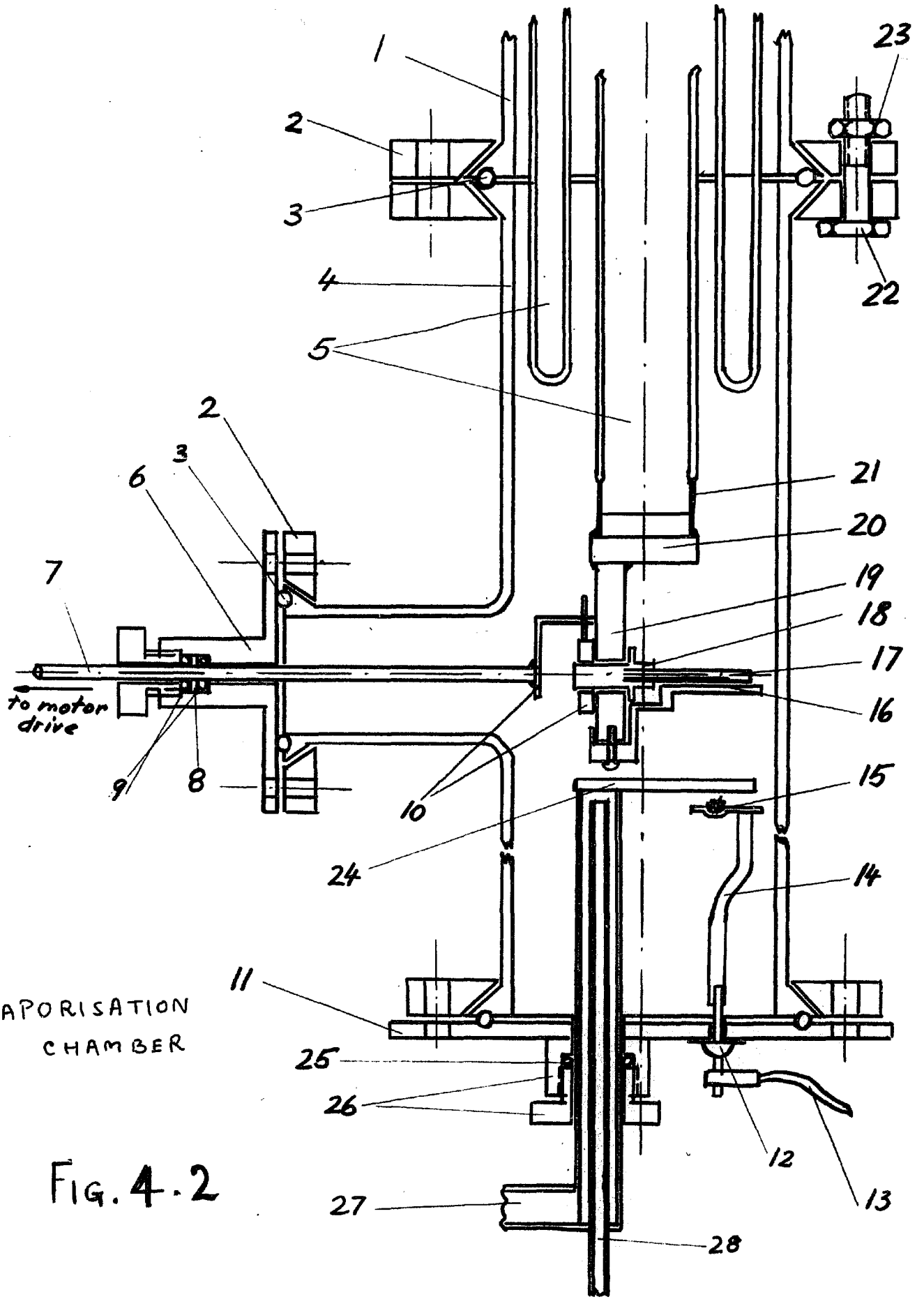

VAPORISATION CHAMBER

FIG. 4.2

1. Nitrogen dewar
2. Aluminium flange
3. O-ring
4. Evaporation bell jar
5. Nitrogen dewars
6. O-ring seal flange
7. Drive shaft
8. Spacer
9. O-rings
10. Drive clutch
11. Brass plate
12. Heavy duty kovar seals
13. Cable
14. Electrical lead and boat support
15. Boat
16. Shield
17. Specimen
18. Specimen holder
19. Brass bar
20. Copper flange
21. Kovar glass seal
22. Bolt
23. Nut
24. Water cooled shield
25. O-ring
26. O-ring seal
27. Water outlet
28. Water inlet

A Philip's vacuum gauge was used for measuring the vacuum. On the high side of the vacuum the pumping resistance was kept small by using larger size glass tubes and stop cocks. Apiezon N type grease was used at the stop cocks. Kel-F O-rings and gaskets supplied by Vinylloyd Company, Los Angeles, used in the vaporisation chamber and driving assembly helped in obtaining better vacuum. Thus vacuum of the order of 10^{-7} mm. was not difficult to attain.

(2) The second liquid nitrogen trap is for maintaining the substrate at liquid nitrogen temperature. It is closed at the bottom by soldering a copper block to the kovar piece at the end of the trap. In order to secure a leak free joint, a special type of stainless steel solder, Eutec Rod 157, manufactured by the Electric Welding Co. of Canada, was used. On cooling, copper contracts more than kovar, hence the copper piece was made to fit the outside of the Kovar piece. The thick copper block provided good thermal capacity and conductivity. Attached to this block was another block of brass and a mask for obtaining films at the ends.

(3) The vaporisation chamber shown in the figure 4.2 was a cylindrical Corning glass pipe 30 cm. long and 11 cm. in diameter. The top end of this was tied to the lower part of the system carrying the second nitrogen trap and the bottom end was closed with a brass disc by using standard seals. Instead of using the conventional O-rings, Kel-F O-rings were used. The brass disc carried two heavy current leads through the kovar seals capable of carrying 50 amperes of current. It also carried a movable shield through an O-ring seal. The position of the shield could be adjusted from outside.

The vaporisation chamber also had a side tube for the drive shaft for rotating the substrate. The drive shaft consisted of a stainless steel rod passing through a double O-ring seal. The outer end of the shaft

was connected to a d.c. motor whose speed could be varied by adjusting the current through the motor. The end inside the chamber had an L shaped piece joined to it to rotate the specimen by a clutch drive. Earlier, instead of using the mechanical drive, a magnetic drive was tried. This consisted of a magnet attached to the central axis of the gear box inside the vacuum and made to rotate by a powerful magnetron magnet mounted on an electric motor outside. This drive was not found satisfactory as the bar magnet moved in jerks instead of moving uniformly.

In the earlier stages of the project, the films were deposited on glass rods. Seven carefully cleaned glass rods were mounted in a vertical array. All the rods could be rotated simultaneously by employing a gear box having seven pinions which had holes for inserting brass plugs to which the rods were attached by nail varnish. In order to estimate the film thickness, a deposit was collected on a glass plate which was weighed and the thickness of films on the rods was estimated by assuming the validity of the inverse square law. For vaporising indium and tin, conical baskets of tungsten wire were made and painted with alumina in water. After drying, these were baked in vacuum to expell absorbed gases. A good portion of the charge was vaporised before allowing deposition on the substrates. A water cooled shield made this possible. However, films thinner than 0.2 μ were not found to be conducting.

A systematic search was made to look for the cause for lack of continuity in the films. An examination under high powered microscope revealed the formation of agglomerates. This could have arisen due to a number of reasons. A search was carried out investigating the following possibilities.

(i) Inadequate cleanliness of the surface of the substrate.

(ii) Formation of agglomerates due to non-normal incidence of the vapour beam.

(iii) Temperature rise due to poor thermal contact with the nitrogen cooled metal blocks.

(i) It was suspected that nail varnish due to its high vapour pressure might form a thin film on the substrate. Substitution of glyptal in place of nail varnish did not improve matters. Next it was tried to hold the substrates by mechanical grip. Several schemes of making chucks which would grip the substrate were tried but the substrate broke in many cases. Finally the most practical way found was to drill a hole in the brass holder perpendicular to the substrate, tap it and hold the substrate in place by a screw. On account of the small size of the rods (0.2 mm in diameter) a small size (no 00 - 90) of the screw was used. A tiny pellet of indium was placed between the screw and the glass rod before tightening the screw. This arrangement was found to be satisfactory for holding the substrate but the continuity in the films was still lacking. Greater precautions were taken for cleaning the substrate. These included using double distilled water and degreasing the rods in chlorethane vapour bath. The substrate and the holder were handled with clean tweezers. The rods were dipped in a bath of pure propyl-alcohol and mounted in the vacuum system to leave a protective film of propyl-alcohol which was removed by ion bombardment in vacuum by Tesla coil. But still the films were discontinuous.

(ii) It has been shown by Holland (1953) that the atoms coming at oblique angles of incidence lead to the development of a coarse texture, because the condensation is confined to the peaks of the bigger grains. It was

decided to design a slit adjustable in width which would stop oblique incidence. The size of the substrates was also increased to 3 mm. In order that the film be uniform in thickness along the length it was necessary that the rotation of the substrate be free from any movement perpendicular to the axis of rotation. This was achieved by constraining the free end of the rod to move in a circular slot. These changes still left the films no better.

(iii) The third possibility, that formation of agglomerates might be the result of a temperature rise of the substrate, was investigated next. The evaporation was done in bursts of one second each. Different kinds of glass rods and quartz rods were tried but without any effect. The alumina painted tungsten boat was abandoned and replaced by tungsten and tantalum boats. This needed more current and the leads which hitherto had been of brass were made of stainless steel rods so that they could withstand higher temperature, at the same time providing a low heat leakage to the kovar seals. Thicker kovar seals for carrying currents of 50 amperes were used. A heavy duty transformer which could deliver currents up to 75 amperes was used to supply power to the boats. This enabled higher rates of deposition. Finally when all these changes proved to be fruitless, it was decided to try sapphire as substrate which, as is well known, has a high thermal conductivity. The films deposited on sapphire rods were found to be conducting. The flame polished sapphire rods of different sizes have been supplied by Adolf Meller & Co., Providence, R.I.

In most cases the vacuum before the start of deposition was of the order of 10^{-7} mm of mercury. During vaporisation it rose to about 6×10^{-6} mm but was never worse than 10^{-5} mm. Before the sapphire rods were cooled

to liquid nitrogen temperatures, the charge, indium or tin, was heated to get rid of absorbed gases. The spherical drop left after heating looked clean and free from any oxide. During this preliminary heating, the shield was interposed between the boat and the substrate to protect the latter from any volatile impurities or gases. The indium or tin used was 99.999% pure and was obtained from the Consolidated Mining and Smelting Company, Trail, B.C.

The film deposition took place in 30 to 150 seconds, the time depending upon the film thickness. The speed of rotation was kept at 3 revolutions per second. The charge was vaporised to completion. For a number of specimens the sapphire rods were weighed before and after the deposition and the film thickness was calculated from the dimensions of the substrate and the mass of the deposit. The ratio of the mass of metal vaporised to that collected on the substrate was found to be constant. The weighings were done with the help of a micro balance kept in an air conditioned room and mounted on shock proof supports. The weighing accuracy with the micro balance was $\pm$ 2 μgrams and the minimum mass of the deposit for the thinnest film was 67 μgms. Thus the determination of mass deposited by weighing the mass evaporated from the molybdenum boats, provided dependable results.

Before breaking the vacuum, liquid nitrogen in the trap was driven off by using compressed air and the system was allowed to return to room temperature. In order to make thicker deposits at the end, the specimen, after weighing, was mounted back in the vacuum system and a shield was inserted to allow deposition only at the ends.

After the fabrication of the film was complete, the specimen was

Old Specimen Holder

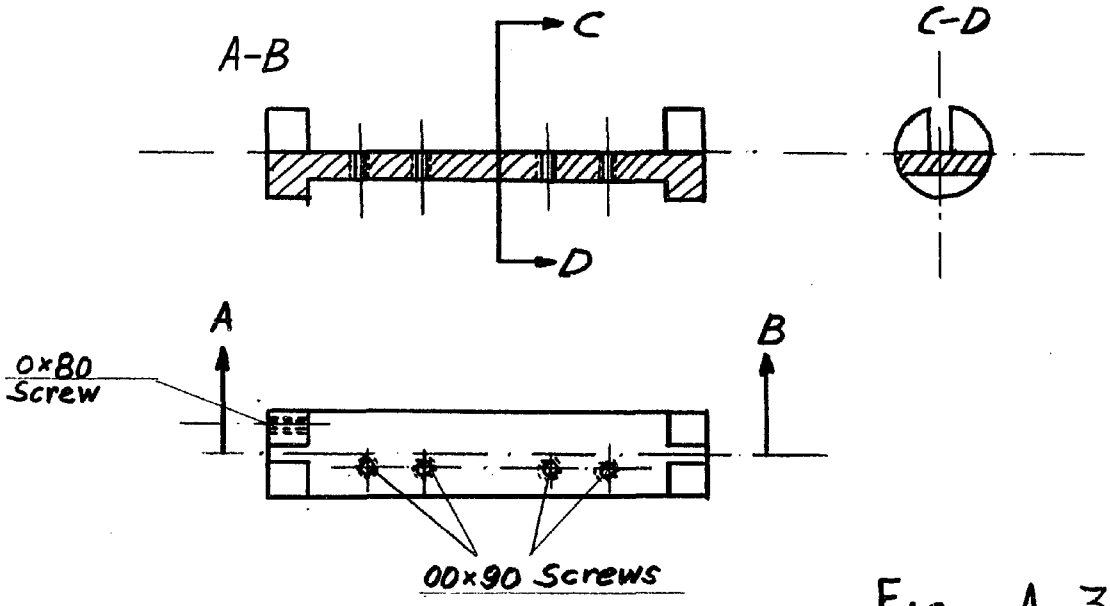

FIG. 4.3 a

New Specimen Holder

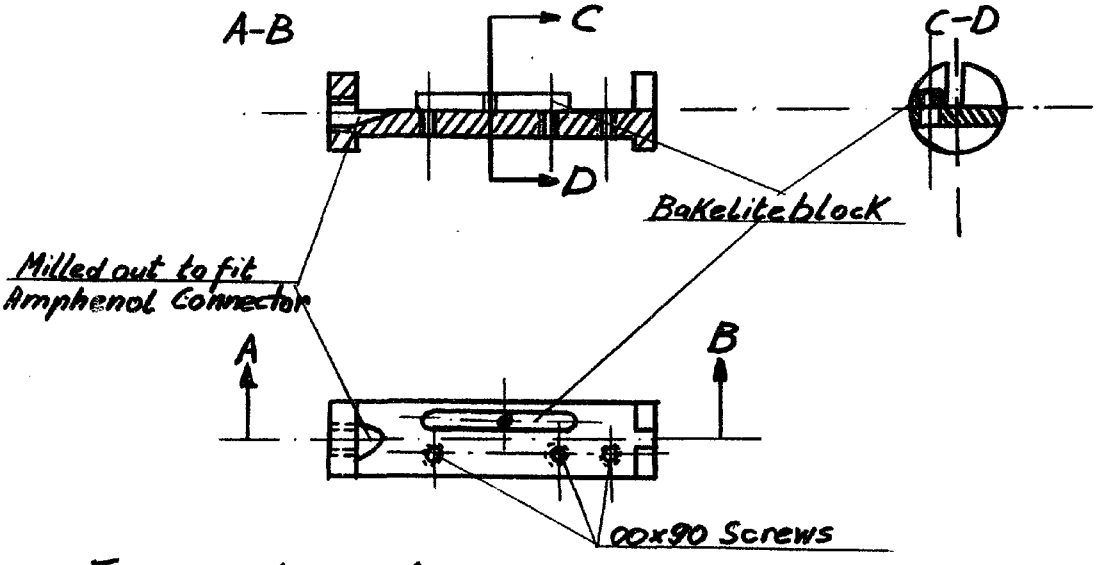

FIG. 4.3 b

Scale: 1×1

mounted on a specimen holder. The details of the specimen holders are shown in figure 4.3 a, b. Figure 4.3a is the earlier design used for work with pulses of long rise time of $\sim$ 1 μs. Essentially the specimen holder consisted of a rod of bakelite milled in the middle as shown in the figure to accommodate the specimen on four no. 30 copper wire hooks which served as the current and potential leads. To one end of the bakelite rod was screwed a circular disc of brass which served as one current lead. After the specimen was mounted as described below, the holder was slid into a coaxial copper tube having a circular brass disc soldered to one end. The coaxial mounting was used to protect the specimen from the magnetic fields of the currents in the return lead when the critical currents were being measured. A couple of holes were drilled into the brass plates to maintain a circulation of liquid helium. The thin copper hooks, supported by brass screws through bakelite, were used to provide strain free mounting. In earlier mountings when the specimen was laid along the grooves in copper cups which were used as current and potential leads, the specimen was bent considerably when dipped in liquid nitrogen. The copper hook mounting proved quite satisfactory and was also adopted in the modified design to be described below.

The modification in the specimen holder was necessary to enable the use of fast rising pulses, having a rise time of 7 nano seconds. In the previous holder the current and potential leads from the specimen were some distance apart. A fast rising current pulse passing through the specimen produces magnetic flux as shown in the fig. 4.4a. This magnetic flux gives rise to a back e.m.f. Due to the inductance common to the current and voltage circuits, the back e.m.f. has the same direction in the voltage circuit as well. Let the specimen be approximated by a combination of R

and L in series where R is the resistance of the specimen and L, the self-inductance of the section of the specimen between the first potential contact and the short circuit, as shown in the figure. This approximation is justified, as the end of the specimen holder is a short circuit and we are considering only a small section of the line. For a 3 cm. long section the inductance L is $\sim 0.02\,\mu H$ and for a pulse of a rise time of 7 nano seconds $V_L \simeq 3$ volts per ampere of current pulse. At helium temperatures, in a state when the specimen is being switched from the superconducting to the normal state R may be ~ 0.01 ohm. Thus the inductive voltage may be larger than the resistance one by two orders of magnitude.

Two modifications in the specimen holder were introduced, one was to use Amphenol type 27-10, 50 Ω subminax connectors, these being screwed to the brass plate, and the second was to compensate the inductive pulse by introducing a loop in the voltage leads, wound so as to produce a pulse equal and opposite to the one being compensated. In fact, by winding the loop in the opposite sense, it was possible to enhance the inductive pick up. The exact compensation could be achieved by suitably choosing the number of turns in the loop and adjusting their position relative to the specimen, a change in either could lead to under or over compensation. The holder thus modified is shown in the fig. 4.3 b.

The above modification did not prove satisfactory because the introduction of the inductance in the form of the loops in the potential circuit slowed the rise of the potential pulse. Thus the current and the potential pulse shapes differed from each other.

The next attempt was to reduce the magnitude of the inductive pulse by bringing the potential lead very close and parallel to the specimen so

Equivalent Circuits for Specimen in Holder

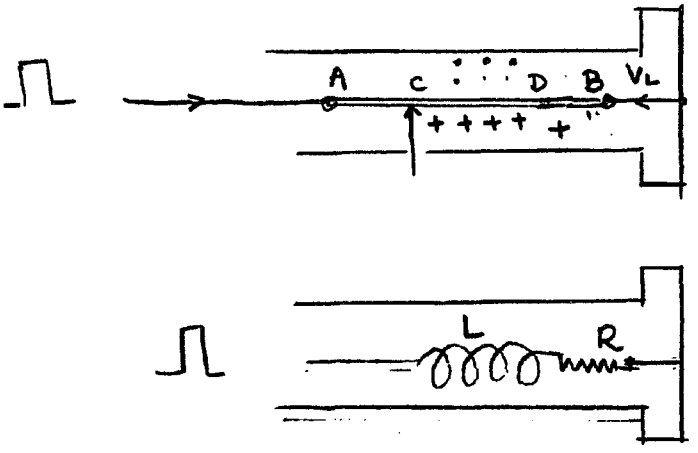

A - B Specimen
C - D Potential Contacts

Fig. 4.4a

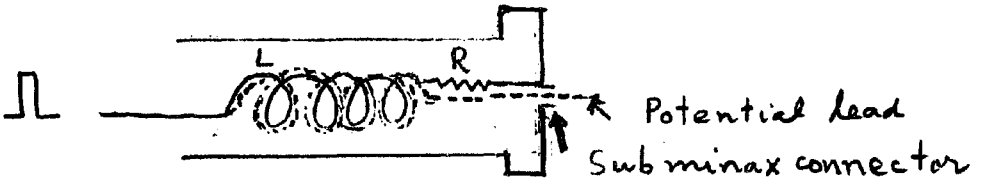

Fig 4.4b

that on the passage of the current pulse through the specimen, the current and the potential leads enclosed the same flux, thereby eliminating the inductive voltage considerably. This arrangement is shown in the fig. 4.4 b. To bring the potential lead very close to the specimen a rectangular block of bakelite was screwed to the holder and the potential lead was glued to it by nail varnish. One end of the potential lead was soldered to the central pin of the subminax connector and the other end, just extending beyond the rectangular block was made into a hook to support the specimen. A # 30 copper wire soldered to the outer lead of the subminax connector had another hook to support the specimen and served as a current lead. It was decided to use only one potential lead in view of the very stringent requirement of minimising the area between the potential lead and the specimen.

The current and voltage leads were attached to the specimen by using silver print. Other methods of attaching leads, like the use of Wood's metal and wetted thin gold leaf were also tried but did not prove very reliable. It was suspected that the contact resistance at the current leads when attached with silver print might lead to the production of heat when the current pulse was passed through the specimen. To avoid this, the current leads were joined to the specimen by using indium metal which was heated by a small soldering iron and was carefully applied on the thick contact film. This operation was done very carefully and quickly to avoid any damage to the thinner part of the film. The potential lead was still connected by using silver print.

Tin films prepared at liquid nitrogen temperatures showed quite broad transitions unlike the indium films for which the transition was reasonably sharp. In fact the transitions in tin films showed a marked

plateau and were as broad as 250 milli degrees. The existence of a plateau flanked by two regions where the change in the resistance was gradual was a common feature of the most tin films deposited at liquid nitrogen temperature, the substrate used being sapphire. This will be discussed in more detail in the Chapter VI.

CHAPTER V

EXPERIMENTAL SETUP AND PROCEDURE

This chapter has been divided into the following subsections:

1. Cryogenic apparatus;
   - (i) Cryostat,
   - (ii) Temperature regulation and measurement,
   - (iii) Leads inside the cryostat.
2. Apparatus for producing pulses.
3. Measurement of critical currents.
4. Magnetic field coil and compensation of earth's field.
5. Experimental procedure.

1. CRYOGENIC APPARATUS

The cryostat used for the experiment consisted of a helium dewar surrounded by liquid nitrogen dewar. The helium dewar was one metre long and the upper 65 cm. had an inner diameter of 6.0 cm, the remaining part having an inner diameter of 4 cm. This type of dewar was chosen for convenience of the alignment of the sample in the magnetic field as will be described later.

The helium dewar was provided with a tap for evacuation at the beginning of each run to remove any helium gas which had leaked into the inner space. The nitrogen dewar was sealed once and for all. The brass cap at the top to which the helium dewar was fastened had several tubes

going down into the cryostat to enable pumping on the helium for lowering the temperature, to measure vapour pressure, connection to the recovery line and for providing leads into the cryostat for the measurements.

The temperature of the helium bath was lowered by pumping on it with a Kinney pump. Due to the poor conductivity of helium I, the temperature at various places in the bath could be quite different. A heater having a resistance of 600 ohms, wound from advance wire # 40 was placed inside the bottom of helium dewar and a current of 10 m.a. was kept flowing to stir the bath. The pressure was stabilised by using a cartesian diver type of pressure stabiliser. A small oil manometer having little inertia indicated the stability of the vapour pressure of helium. The temperature stabilisation was checked by a carbon resistance thermometer. The carbon resistance used was an Ohmite 22 Ω 1 Watt resistance which was ground till the resistance at room temperature was 40 ohms. This was done for two reasons, one to ensure good thermal contact with helium by removing all insulation and second to produce reasonable variation with temperature in the range of temperatures desired. The resistance was measured by a Leed and Northrup wheatstone bridge to which e.m.f. was supplied by a 1.5 volt dry cell with a resistance of 10,000 ohms in series. A small current through the resistance was used to cause little variation in the temperature of the resistance. A Honeywell Electronic Galvanometer was used as a null indicator. The resistance thermometer was used to monitor the constancy of the temperature. The temperature was measured by noting the vapour pressure of helium with the help of a mercury manometer which was read by a cathetometer. For calculation of the temperatures, the 1958 vapour pressure scale was used. The corrections were applied for the change in the density of mercury. The hydrostatic correction was also applied.

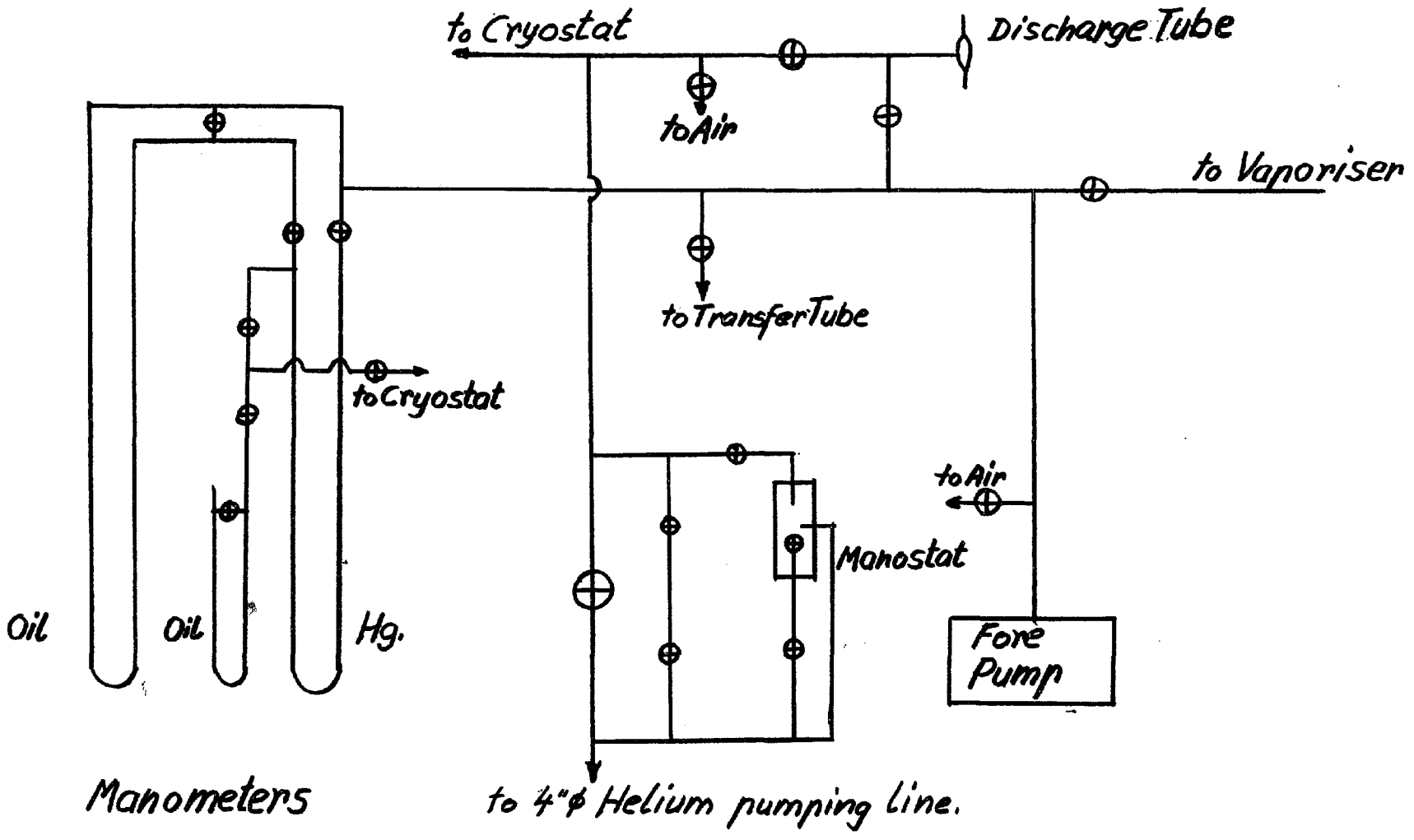

Fig. 5.1 Vacuum System for Cryostat.

Observations were taken after ensuring that the oil manometer and the null indicator showed constant readings. (See fig. 5.1 for vacuum system.)

The electrical leads up to the top of the cryostat were coaxial cables RG-58-C/U. Kovar seals were used for getting the leads into the cryostat. For current leads, insulated advance wire # 24 and for potential leads wire # 32 were used. Copper leads of size required for the coaxial cable are found to be unsuitable due to their high thermal conductivity resulting in the rapid loss of helium. With pulses of slower rise time, two specimens were under observation in one helium run. Thus three current leads and four potential leads were provided. This arrangement was adequate for slower pulses. With the pulses having a rise time of 7 nano seconds, it was necessary to use coaxial lines having a characteristic impedance of about 50 ohms. RG-58-C/U cable was used up to the top of the cryostat. Thicker Kovar seals with tapering outer copper connector were used to let the leads into the cryostat. This arrangement was adopted to match the characteristic impedance to minimise the reflections. Inside the cryostat the potential and the current leads were concentric stainless steel tubes of 0.95 cm. and 0.30 cm. diameter. These tubes were separated by teflon spacers. At the end of the concentric tubes serving as potential leads, an amphenol subminax connector no. 27 - 8 was soldered. From there onwards the lead was amphenol R.F. cable No. 421 - 105 in which the iron wire inner conductor was replaced by copper wire of the same diameter in order that the applied magnetic field may not be perturbed. At each end of this cable 27-7 type amphenol subminax connectors were crimped by means of a special crimping tool. In order to minimise the reflection due to impedance mismatch at the bottom of the specimen holder, a 50 ohm resistance, non-inductively wound on a flat piece of mica, was used. The wire used for this resistance

was of nichrome, .002 inch diameter, having a resistance of 73.0 ohms per foot. The change in its resistance from room temperature to the helium temperature was less than 10%. This resistance was housed inside a german silver tube to the ends of which subminax connectors 27 - 7 were soldered. The concentric tubes serving as current leads terminated in a brass tube, which was soldered to the outer one. The inner conductor was connected to a 50 ohm resistance. The brass tube had a slot at the bottom to facilitate soldering of the central lead from the specimen holder to the 50 ohm resistance. The outer copper tube of the specimen holder was screwed to the brass tube first and then the central lead of the specimen was soldered to the 50 ohm resistance. Care was taken to avoid any excessive heat during soldering so that the specimen may not be damaged. With the fast pulses, only one specimen could be used in one run.

2. THE PRODUCTION OF CURRENT PULSES

The first attempt to generate the pulses was to employ a mechanical, spring loaded switch, which produced pulses of 10 millisecond duration. The heating of the specimen, soon after the transition took place was found to be excessive, resulting in the burning of the specimen. The next attempt, therefore, was to produce pulses of shorter duration. A condenser charged and discharged by a switch proved unsatisfactory due to high frequency oscillations resulting from the machanical bouncing of the switch. The following three different types of pulses were used for observing the current transitions:

(i) Rutherford Pulser,

(ii) Thyratron Pulser,

(iii) The Discharge Line type Pulser.

(i) Rutherford Pulser - B7B was a commercial unit which could supply 50 volts and had an internal impedance of 50 ohms. This pulser was mainly used for supplying low currents which were a little difficult to obtain with the thyratron pulser. This unit could produce square pulses of rise times ranging from 30 nano seconds to one microsecond. The pulse duration and pulse repetition rate could also be varied within wide limits. For repetition rates below 20 pulses per second, external drive was used. The external drive consisted of a Krohn-Hite ultra low frequency oscillator model 400 - C, which drove a relay used for triggering. Thus quite low repetition rates were obtained. It was found that the repetition rates, as high as 200 P.P.S. did not effect the transitions for the pulse magnitudes used here.

(ii) Thyratron Pulser - This pulser produced single shot pulses of current magnitudes up to 15 amperes. The rise time of the pulses could also be varied within wide limits. The circuit diagram of this pulser is shown in figure 5.2. The first tube in the circuit is Xenon filled 2 D 21 thyratron. This is used to produce a firing pulse for 3 C 45 hydrogen filled thyratron. Pressing the push button switch causes the 0.02 μF condenser to discharge a pulse which fired the 3 C 45. The plate voltage to the 2 D 21 was supplied by a Dressen - Barnes Model 32 - 101 regulated power supply. The high voltage required for 3 C 45 was supplied by Technical Measurement Corporation model HV - 4 A power supply capable of giving an output voltage ranging from 500 volts to 1600 volts. The rise time of the pulse was controlled by the inductance in the plate circuit of the 3 C 45. This also heavily damped high frequency plasma oscillations occuring in the thyratron during firing. Two variable resistances, 100 ohms and 1000 ohms were used to control the current amplitudes. For controlling higher current ampli-

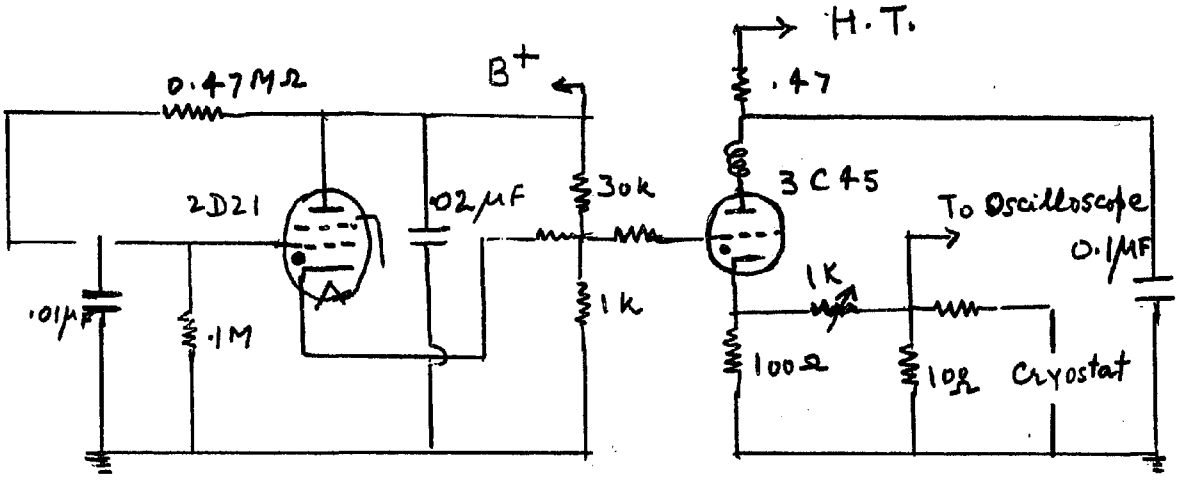

Fig. 5.2 Thyratron Pulser

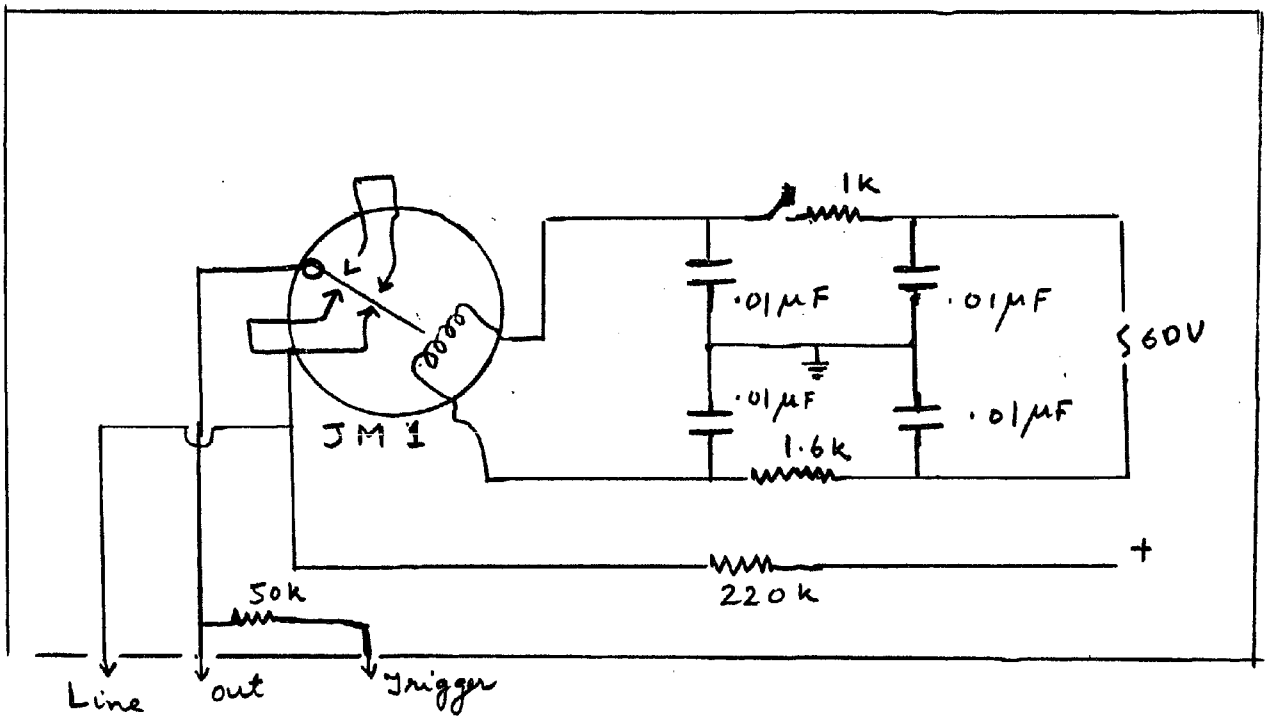

Fig. 5.3 Discharge Line Pulser

tudes, the high tension power supply voltage was varied. The thyratron pulser provided most of the current pulses in measuring critical currents. The speed of the rise time was however limited by the presence of high frequency plasma oscillations and the inductance associated with the condenser.

(iii) The Discharge Line Type Pulser - This pulser was used for producing fast rising pulses of rise time 7 nano seconds and duration 80 nano seconds. The circuit diagram with the component values is given in figure 5.3. In principle, it consists of an open ended transmission line being charged to a d.c. potential through a high resistance. The line is discharged through a switch into a load resistance equal to the characteristic impedance of the line. The length of the open ended transmission line governs the duration of the pulse. The switching device used in the pulser was a Potter and Brumfield J M 1 mercury relay. Essentially the relay consists of two sets of platinum contacts, a single movable armature and a small reservoir of mercury hermetically sealed under high pressure of hydrogen. When the coil is energised, the normally closed contacts are open and on de-energising, the armature reed returns the contacts to the closed position. The mercury pool provides fresh contact during each switching operation by capillary action. The contacts in this switch are rated at 500 volts and 5 amperes, not to exceed 250 volt-ampere. The charging leak resistance of 220 K ohms was kept close to the end of the line to avoid any stray capacitance which might modify the reflection coefficient at the open end. The charging time constant which is the product of the leak resistance and total capacity of the line was chosen to be long enough to avoid any partial recharging in case of contact bounces but short enough to permit full charging during off part of the

cycle. The leads to the output terminals, which were B N C connectors, were kept as short as possible and were properly shielded. An additional output was provided for use in the external triggering. The 0.01 μF condensers shown in the circuit served to filter high frequencies from the power supply voltage. The rise time of the pulses generated was 3 nano seconds. During the rise, a low amplitude high frequency jitter was present. This was removed by connecting a 100 $\mu\mu$F condenser across the output. The resulting rise time was 7 nano seconds.

3. THE MEASUREMENT OF THE CRITICAL CURRENTS

Since the current transitions were broad the critical current was defined to be the one needed to restore 1/2 of the resistance in the normal state. In case of the measurements with pulses of longer rise times, the current pulse was gradually increased and the potential differences across the specimen were observed by using Tetronix 545 Model oscilloscope employing D type differential plug in unit which had voltage sensitivity of 1 m.v. per cm. with a band width of 0.3 mcs. To measure the currents through the specimen, potential differences across a known resistance in the current circuit were observed on another Tetronix 545 A model oscilloscope. From the knowledge of the voltages and currents, resistances were calculated and the critical current, the current corresponding to 1/2 the resistance in the normal state, was found. This was done at each temperature.

The measurement of critical currents with fast rising pulses proved to be a little more difficult. As mentioned earlier, reflections arising from impedance mismatch were minimised by taking care that the line was matched at all the points where joints were used either to carry leads into the cryostat or to connect different sizes of transmission lines.

Whenever the two sizes differed, tapering joints were used for connection. Any large reflections could be seen as echoes and the position of the mismatch could be calculated by noting the position of the hump on the voltage pulse. Since the rise time of the Tetronix oscilloscope model 545 A was not fast enough, a Tetronix model 661 sampling oscilloscope was used. This oscilloscope has a rise time of 0.35 nano second. The external trigger to the oscilloscope was provided by the discharge line pulser. The residual mutual inductance of the specimen made it difficult to observe the resistive voltage in the first 30 nano seconds. To overcome this difficulty, a compensating pulse, identical in shape and magnitude to the inductive part of the voltage pulse was generated as described below. For affecting the compensation, the temperature of the helium bath was lowered below T_c and a current pulse much less than the critical value, was passed through the specimen. The resulting voltage pulse was an inductive pulse. The compensating pulse was applied to the second input of the oscilloscope, inverted inside the oscilloscope and subtracted so as to make the voltage pulse zero everywhere. For generating the compensating pulse, a T was connected to the output of the pulser. One end of the T carried the main pulse to the specimen, while the other end was connected through two attenuators, one fixed and the other a variable Hewlett Packard V H F type 355 A, to a differentiating network. The fixed attenuator consisted of a T, with a resistance of 4000 ohms in the series arm and 50 ohms in the parallel arm, chosen for impedance matching. Carbon type resistances were used to keep the inductance to a minimum. This network was enclosed inside a brass tube, the two ends of which carried B N C type connectors. The differentiator was a variable trimmer condenser housed inside a brass tube having Amphenol SO - 239 and PL - 259 connectors at the ends. A slot in the brass tube

EXPERIMENTAL ARRANGEMENT
for CRITICAL FIELD MEASUREMENT

Specimen

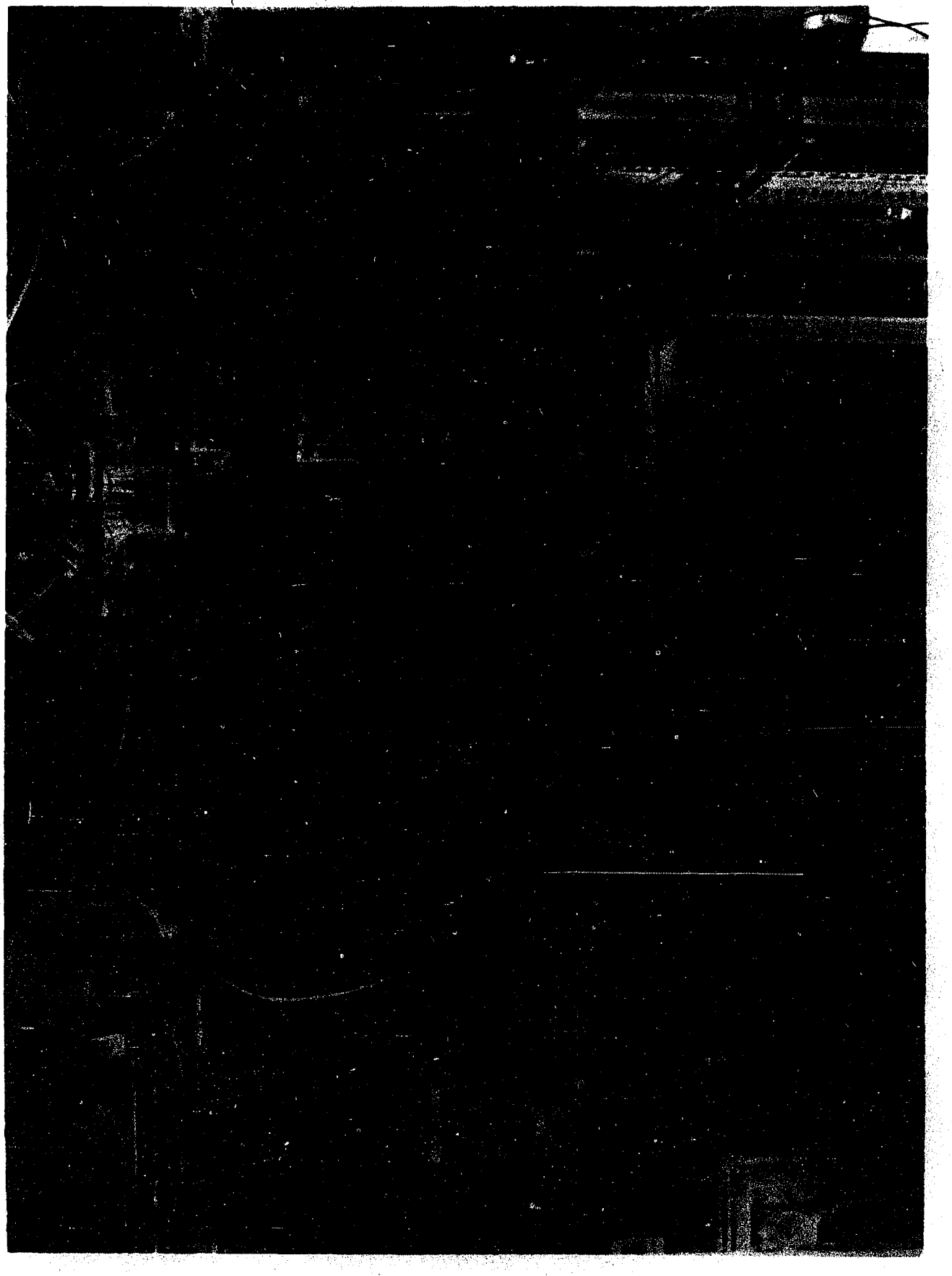

made it possible to adjust the condenser to alter the wave shape of the compensating pulse, its magnitude being controlled by the Hewlett Packard variable attenuator. A suitable length of delay cable was inserted in this circuit to make the compensating pulse coincide with the inductive pulse coming from the specimen. Once the compensation was effected, it was found to be good throughout the experiment. The current pulse was measured by reading the output of the power supply used for supplying d.c. voltage to the discharge line pulser. A Hewlett Packard model 410 B vacuum tube voltmeter was used for this purpose. The voltage pulses were phptographed by using a Du Mont model 264 oscilloscope record camera. The current was varied by varying the d.c. voltage to the pulser. For each temperature a graph between the resistance and current was plotted and the critical currents were found by finding the current giving rise to 1/2 the resistance in the normal state.

4. THE PRODUCTION OF MAGNETIC FIELDS

A coil 24 cm. long and 18 cm. in diameter was used for the production of the magnetic fields needed for observing the transitions in the magnetic field. The coil produced fields up to 700 oersteds without being cooled, the field per ampere of current being 35.4 oersteds. For producing higher magnetic fields up to 3500 oersteds, the coil had to be cooled in liquid nitrogen. The coil was carried on a portable aluminium frame as shown in the photograph. It was mounted between two aluminium plates, having the same size of holes as the coil by three brass rods, 0.5 inch thick. The inclination of the coil could be adjusted by altering the length of the supporting brass rods with a screw motion. This assembly was suspended from two aluminium rails and could travel on roller bearings. In order to provide for travel in a perpendicular direction, two brass bars of

rectangular cross section fitted with roller bearings were screwed to the top of aluminium railing; these roller bearings could travel on another set of aluminium railings. Thus the coil was capable of being adjusted in all possible directions. Such arrangement was necessary to align the specimen parallel to the magnetic field. In view of the fact that the specimen was mounted on flexible copper hooks alignment could only be completed at the helium temperatures. The use of narrow tail dewars coupled with the provided adjustability of the coil made alignment quite accurate and convenient. The alignment was made by maximising the magnetic field for restoring the resistance in the specimen. In order to make cooling with liquid nitrogen possible, the coil was placed in a cylindrical brass box which was placed inside a rectangular wooden box screwed to the top aluminium plate carrying the coil. The space between the brass box and the wooden box was filled with styrofoam to reduce the loss of liquid nitrogen. The wooden box served another purpose; it was used as a frame for winding three pairs of coils for compensating earth's field. In the above construction, iron was avoided as far as possible.

5. THE EXPERIMENTAL PROCEDURE

After the transfer of the liquid helium in the cryostat, the resistance of the specimen was determined by passing currents of 0.5 to 2.0 m.a. and reading the voltage across the specimen by a Hewlett Packard model 425 A micro volt ammeter. Next the coil assembly was placed around the dewars and the position of the coil adjusted so that the centre of the specimen coincided with the centre of the coil. The temperature of the helium bath was lowered by pumping on it, a current of 10 m.a. running in the heater to keep the helium bath stirred. As soon as the resistance of the specimen became nearly half of its value in the normal state, the

currents through the degaussing coils were adjusted to minimise the resistance. These currents were maintained throughout the run. The currents needed for the cancellation of the horizontal components of earth's field were more sensitive to adjustment. In actual practice the currents in the three pairs of the coils were predetermined at room temperature by observing the oscillations of a suspended bar magnet for horizontal degaussing and by using a dip needle for degaussing the vertical component. The currents determined by the two methods were found to be consistent. These currents were determined once and for all for all the runs.

The next step was to observe the superconductive transition in zero field. The bath temperature was raised and was again lowered in small steps, every time stabilising the temperature and noting the resistance of the specimen. This was continued until the specimen was completely superconducting. A plot of the resistance versus temperature was used for finding the value of transition temperature. The temperature was lowered by a few millidegrees and the current and the magnetic field transitions were observed. To observe the current transitions, the current pulse was increased in small steps and every time the voltage pulse was either visually observed or photographically recorded. In the case of fast pulses the procedure for compensation of the inductive voltage was undergone prior to observing current transitions and the compensating pulse so determined was applied. The current pulse increase was continued until the normal resistance was restored. From this data, the value of the critical current was determined. To observe transition in the magnetic field, the specimen was first aligned parallel to the magnetic field, by adjusting the position and inclination of the coil, thereby maximising the magnetic field. The adjustment was found very sensitive to the inclination of the coil. Even

half a turn of the screw, which amounted to a change of about 10' in the inclination was enough to produce a detectable change in the resistance.

CHAPTER VI

EXPERIMENTAL RESULTS AND THEIR DISCUSSION

The parameters determined experimentally for the films of various thickness are:

(1) Film thickness,

(2) Film resistivity at room temperature and helium temperature,

(3) Transition temperature and the transition width,

(4) Critical currents as a function of temperature,

(5) Critical magnetic fields as a function of temperature.

(1) Measurement of the Film Thickness:

A very accurate determination of the film thickness is a quite difficult task. A wide variety of methods have been used for thickness determination. These are:

(i) Multiple beam interferometric technique,

(ii) Method of X-ray absorption,

(iii) Radio active tracer technique,

(iv) Radio frequency method,

(v) Measurement of electrical conductivity,

(vi) Direct weighing.

The last method is the one most frequently used and in cases where the weight of the deposit is sufficiently large to be weighed accurately it can give an accuracy comparable to any of the other methods listed above.

With films deposited on sapphire rods of 1.5 mm. in diameter, the weight of the thinnest deposit collected was 67 μ gms., the accuracy of the micro-balance used was $\pm$ 2 μ gms. In all cases it was customary to take a known amount of charge and evaporate it to the completion. The ratio of the weight of the charge to the weight of the deposit bore a nearly constant ratio, the departure not exceeding 12%. This was verified for all the films on 1.5 mm. diameter rods. For the films deposited on the thin rods of 0.4 mm. in diameter, the deposit was not weighed and the thickness was estimated from the knowledge of the weight of the charge used. It may be remarked that this method of the thickness determination can only provide a measure of the surface density of the deposit, in view of the fact that the density of the metal in bulk may differ from its density in the form of a film.

The film thickness was also calculated by resistance measurement. Following Toxen (1961) the thickness d is given by:

$$d = \frac{\rho^{b}_{rt} L}{2\pi r (R_r - R_H)} \qquad 6.1$$

where ρ^{b}_{r} is the resistivity in bulk at room temperature, L the film length, r the radius of the substrate, R_r the resistance at the room temperature and R_H the resistance at 4.2° K. The resistance calculated this way was found to be lower than estimated by the mass determination, the departure generally lying between 10 to 20%. This departure may have been caused partly due to the uncertainty in the knowledge of the effective film length. In view of this the determination of the film thickness by weighing will be taken to be more reliable.

(2) Film Resistivity at Room Temperature and Helium Temperature:

According to the free electron theory of metals the product of resistivity and mean free path is given by

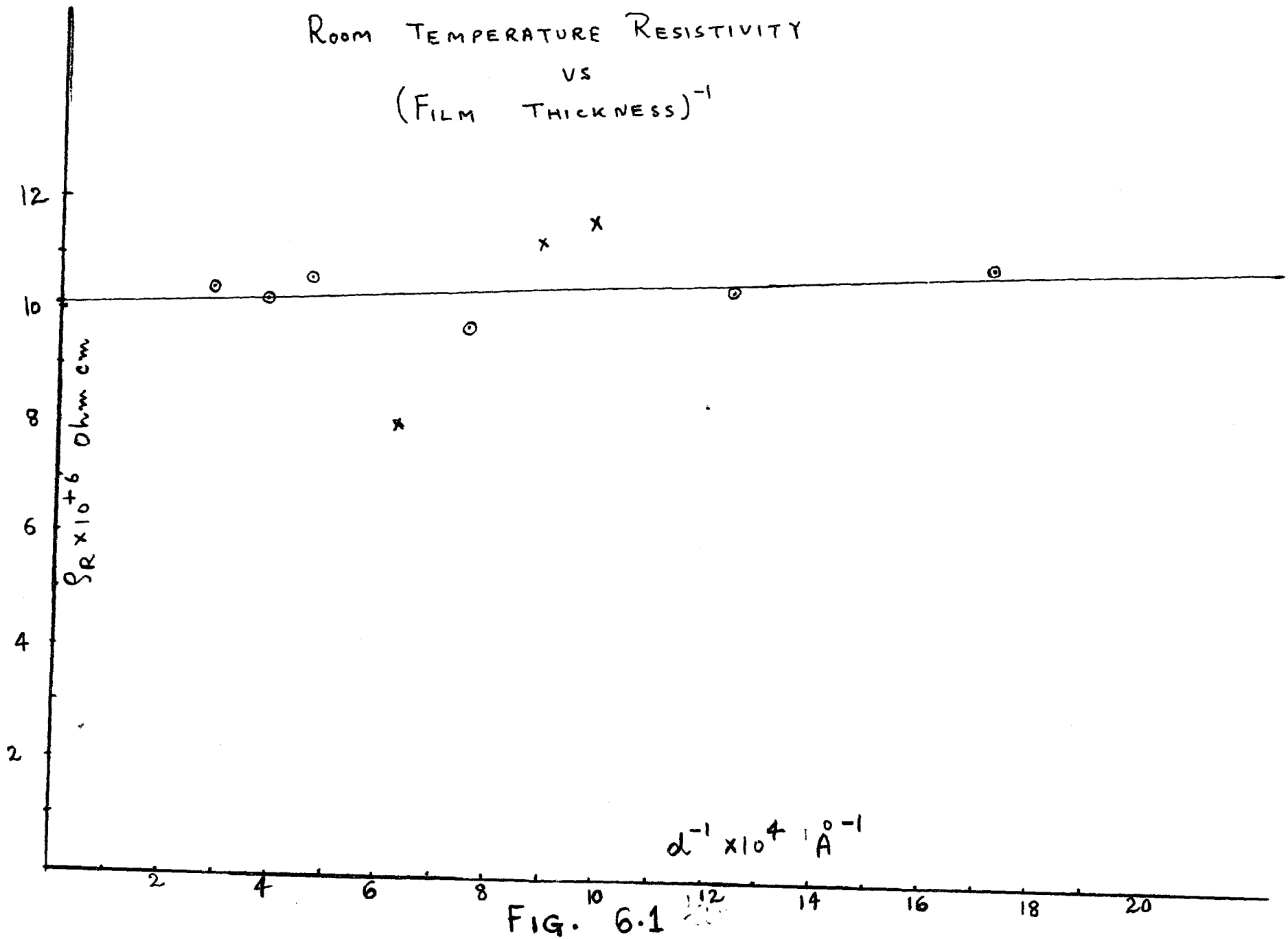
Room Temperature Resistivity
vs
(Film Thickness)$^{-1}$
12
10
8
6
4
2
$\rho_R \times 10^{+6}$ ohm cm
2
4
6
8
10
12
14
16
18
20
$d^{-1} \times 10^4$ Å^{-1}

Fig. 6.1

$(\rho_H d)^{-1}$ versus $\log d$ (d, film thickness, ρ_H film resistivity at He temperature)

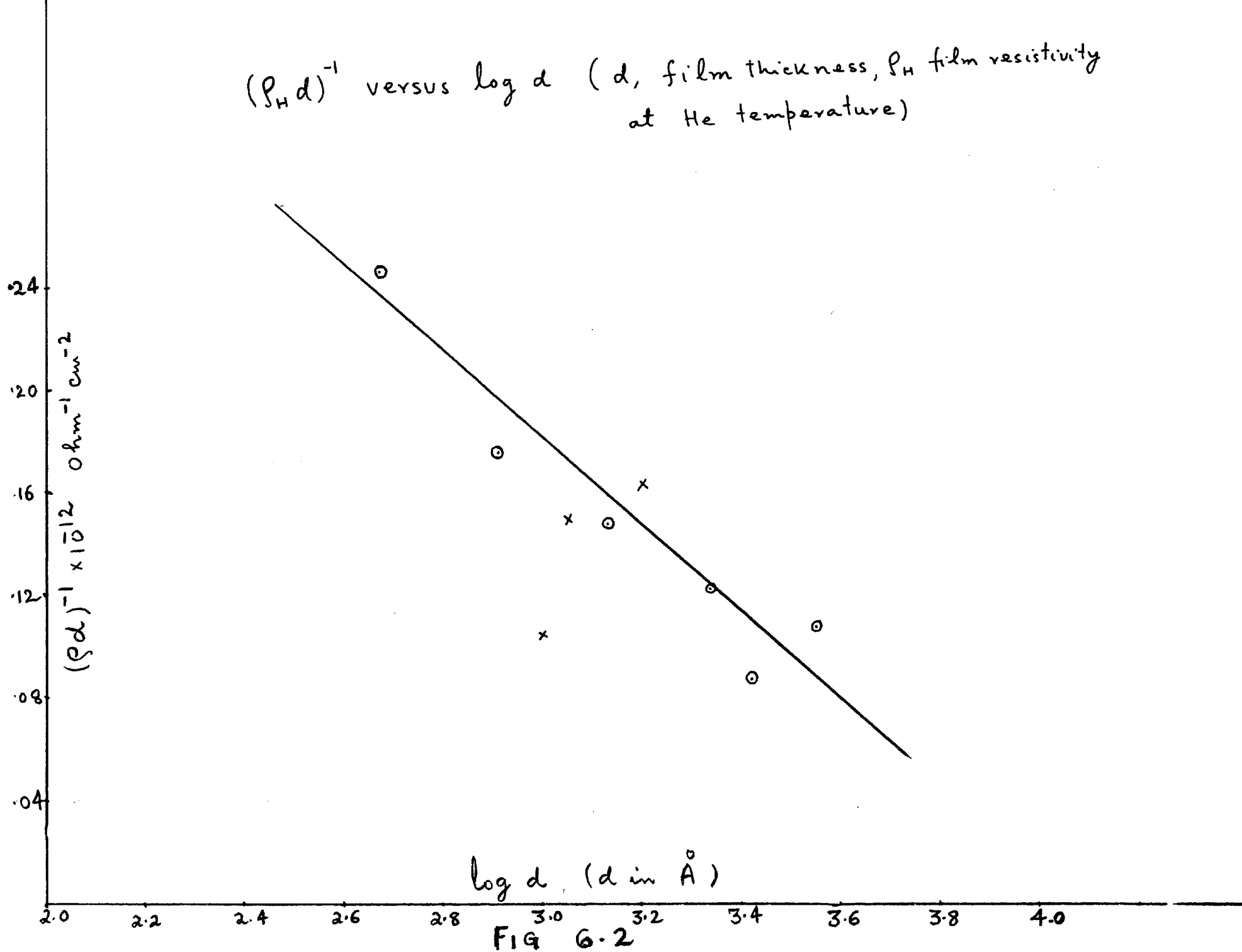

FIG 6·2

$$\rho^b \, l^b = \frac{m^* v}{n e^2}, \qquad 6.2$$

where n is the number of conduction electrons per cm^3., v is the Fermi velocity, m^* the effective electron mass, e the electron charge, ρ^b and l^b are the bulk resistivity and the bulk mean free path respectively. If we assume that the number of conduction electrons remains constant with temperature, $\rho^b \, l^b$ is constant and independent of temperature. Equation 6.2 gives the dependence of resistivity on mean free path. In case of thin films, the mean free path is limited by the boundary. Fuch's expressions (1938) for two limiting cases are given by equations 3.1 and 3.2.

At room temperature, the bulk mean free path for indium $\sim$100 A° and for the film thickness under investigation $\frac{d}{l^b} \gg 1$ and therefore equation 3.2 is applicable. In the figure 6.1 ρ has been plotted versus d^{-1}. The slope and the intercept of the straight line give l^b_{273} and ρ^b_{273}. The values so determined are, l^b_{273} = 119 A°, ρ^b_{273} = 10.07 x 10^{-6} ohm cm. $\rho^b_{273} \, l^b_{273}$ = 1.2 x 10^{-11} ohm cm^2 In view of the fact that the effective length of the film was not known very accurately, there is some scatter on the graph. The points shown by circles are for the films for which the effective length was determined carefully with a microscope. The straight line fit is only for such films. At helium temperature, $l^b_{4.2} \gg$ d and the equation 3.1 holds. The figure 6.2 shows a plot of $(\rho \, d)^{-1}$ versus log d and from the slope and the intercept we get, $\rho^b_{4.2}$ = 0.129 x 10^{-6} ohm cm., $l^b_{4.2}$ = 7940 A° and $l^b_{4.2} \, \rho^b_{4.2}$ = 1.028 x 10^{-11} ohm $cm.^2$. Thus ρl is found to be practically constant and independent of temperature.

It is possible to estimate the coherence length ξ_0 from the knowledge of $\rho^b \, l^b$ as follows. According to the B C S theory, ξ_0 is given by,

$$\xi_0 = \frac{\hbar v}{\pi \Delta_k(0)} \qquad 6.3$$

where v is the Fermi velocity, $\Delta_K(0)$ is the energy gap at 0° K. Also the effective electron mass m^* is given by,

$$m^* = \frac{1}{2} \frac{h}{v} \left(\frac{3n}{\pi}\right)^{1/3} \qquad 6.4$$

According to Keesom and Perlman (1956), we have

$$m^* = 7.3 \left(n V_m^3 / n_a\right)^{-1/3} m\gamma \qquad 6.5$$

where V_m is the molar volume, m the electronic mass, n_a is the number of atoms per unit volume and γ the electronic specific heat in units of milli-joules / mole degree^2. Combining equations 6.2, 6.3, 6.4 and 6.5 we obtain,

$$\xi_0 = \frac{1.68 \times 10^{-2} V_m h^3}{m c^2 N^{1/3} \Delta_K(0) \gamma \rho_1} \qquad 6.6$$

where N is Avogadro's number. If we substitute the various quantities for indium as quoted by Toxen (1961), we have

$$\xi_{0} = 258 \times 10^{-10} / \rho_1 \qquad 6.7$$

Substituting for ρ_1 in this equation, we can calculate ξ_{0}.

The various estimates are given below in table I.

TABLE I

	ξ_0	ρ_1
* Dheer (1959)	4300 Å	0.6×10^{-11} ohm cm.^{2}
Davies (1960)	4400	
* Roberts	2900	0.89×10^{-11} "
Toxen (1961)	2600	0.98×10^{-11} "
Toxen (1962)	2600 ± 400 Å	2.0×10^{-11} "
This work (Room Temperature)	2150 ± 900	1.2×10^{-11} " ± 0.42
(Helium Temperature)	2500 ± 550	1.028×10^{-11} " ± 0.23

* See Toxen (1961) for references.

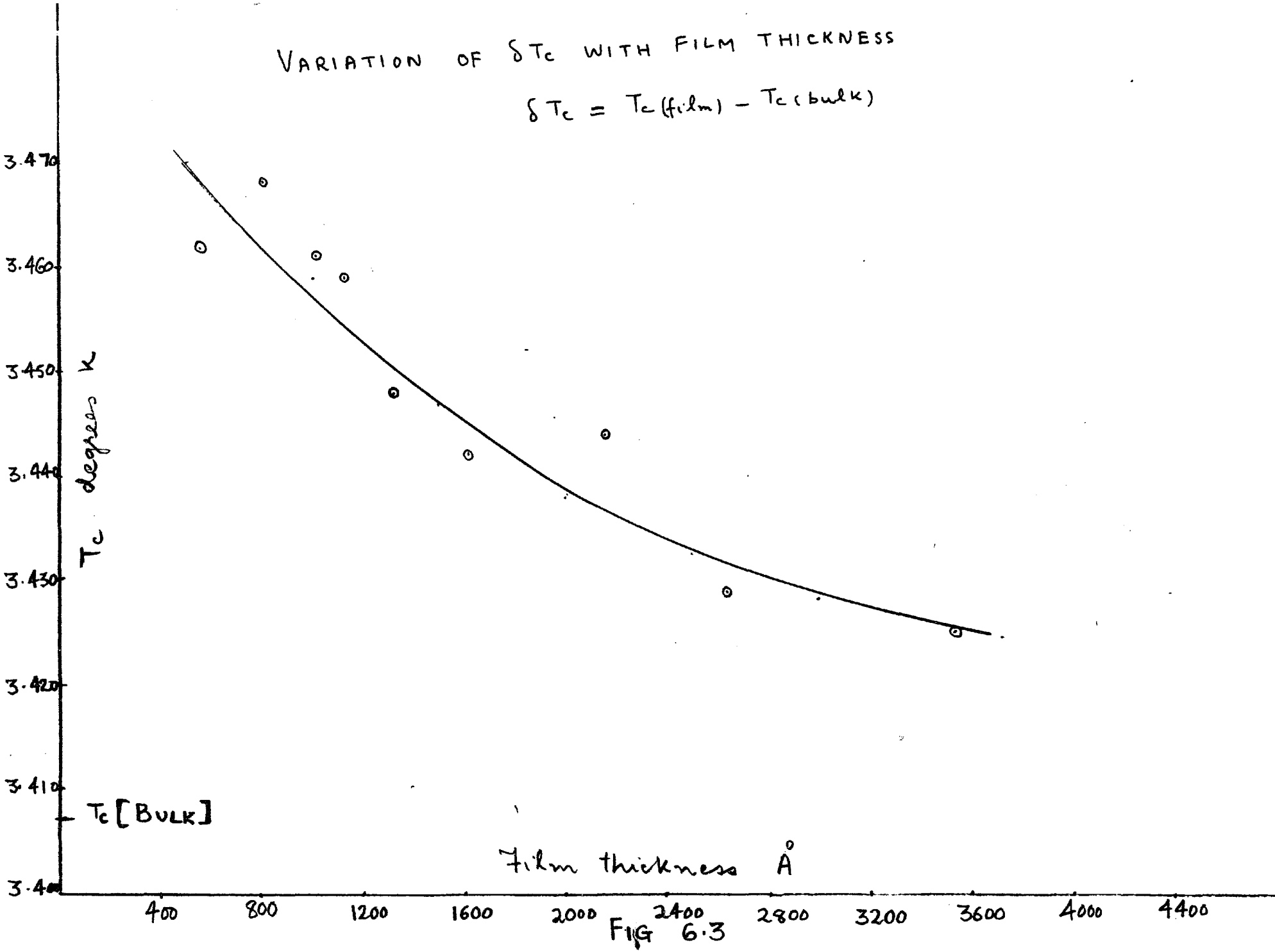
VARIATION OF δTc WITH FILM THICKNESS
δTc = Tc(film) − Tc(bulk)
3.470
3.460
3.450
3.440
3.430
3.420
3.410
3.400
Tc degrees K
Tc [BULK]
400
800
1200
1600
2000
2400
2800
3200
3600
4000
4400
Film thickness Å

FIG 6.3

The data of Dheer and Roberts are based on the measurements of high frequency surface impedance and Davies also used data on surface impedance to estimate ξ_0. Toxen's estimates are based on the resistivity measurements and critical magnetic field measurements.

(3) Transition Temperature and the Transition Width:

As mentioned in Chapter III, the transition temperature for thin films departs from its value in the bulk material. Toxen (1961) found that for the indium films deposited on vitreous silica substrate, the relationship between T_c and d is given by,

$$\delta T_c = \frac{52}{d} - \frac{750}{d^2}$$

where δT_c is the difference in the T_c for the film and bulk material and d is the film thickness in angstrom units. In fig. 6.3 is shown a plot of δT_c versus d from the present work and the data is found to fit the equation,

$$\delta T_c = \frac{73.4}{d} - \frac{21300}{d^2} \qquad 6.8$$

The fact that T_c for the films is higher than T_c for the bulk material indicates that the films are under tensile stress which of course is to be expected because the coefficient of expansion for indium is greater than that for sapphire.

The transition width, defined to be the temperature interval between 10% and 90% of the resistance in the normal state, lies between 3 and 8 milli-degrees for the indium films. There is no systematic variation of the transition width with film thickness.

For tin films the transition picture was quite different. For the films deposited at the liquid nitrogen temperature, the transitions were quite broad and were characterised by a marked plateau. However, the films

ELECTRON MICROGRAMS OF FILMS

Figure 6.4 a 1400 Å Tin film (liquid N_2 temp.) X 5000

Figure 6.4 b Tin film (room temp.) X 5000

Figure 6.4 c Indium film (liquid N_2 temp.) X 5000

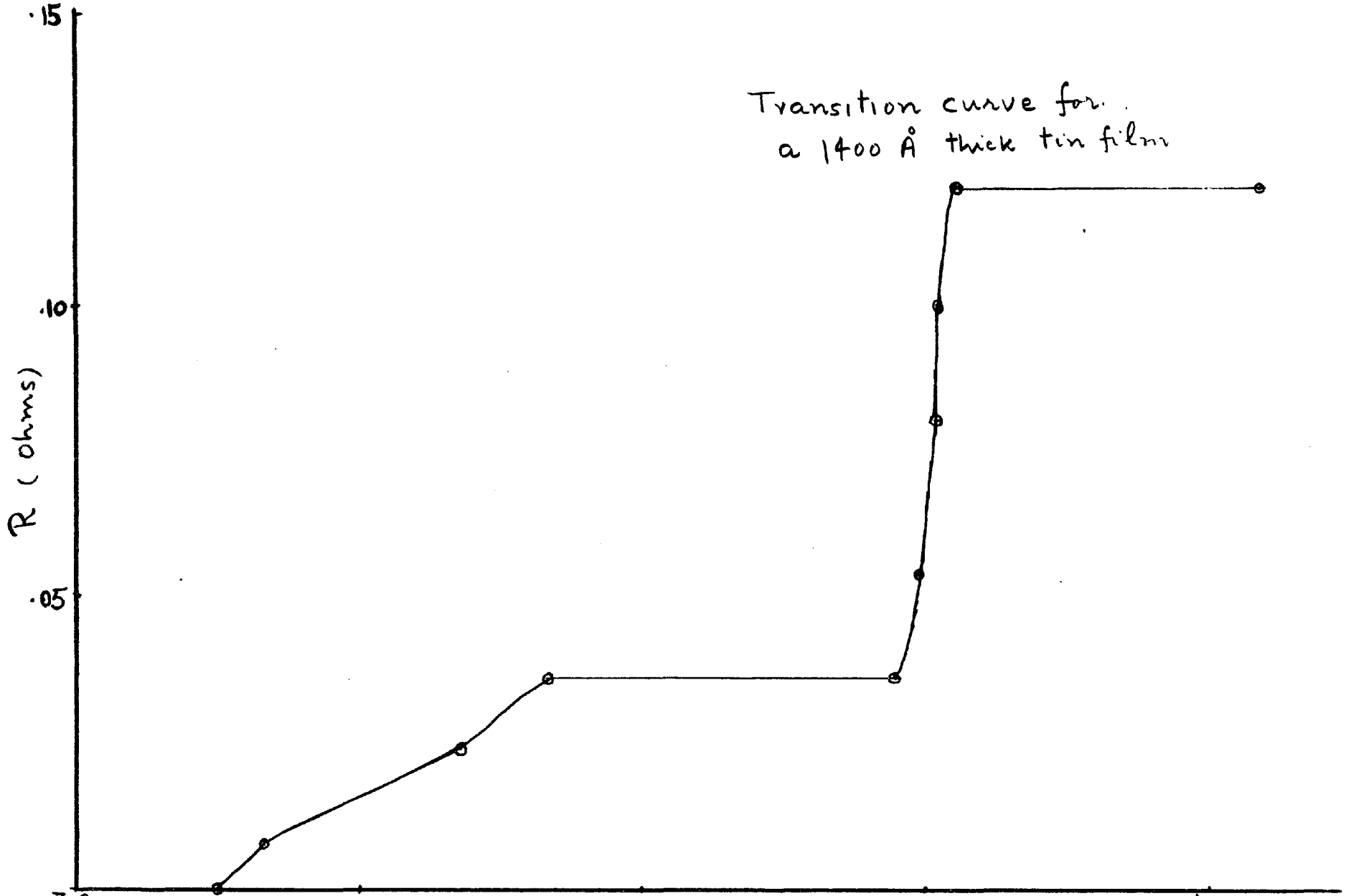
Transition curve for
a 1400 Å thick tin film
.15
.10
.05
R (ohms)
3.600
3.700
3.800
3.900
4.000
T °K

FIG. 6.5

deposited at room temperature showed narrow transitions but films thinner than 900 Å, lacked conductivity. The transition temperature for these films differed from the bulk value considerably. For the two films 946 Å and 3250 Å thick T_c was 3.907° K and 3.862° K respectively as compared to the value 3.728° K for bulk tin. Tin films were photographed with an electron microscope. Fig. 6.4a gives electron micrograph for a 1400 Å thick film deposited at the liquid nitrogen temperature, the transition curve for which is given in fig. 6.5. The structure shows some evidence of twinning. Figure 6.4b gives the electron micrograph for the tin film deposited at the room temperature. This shows a smooth structure. Figure 6.4c shows an electron micrograph of an indium film, 5000 Å in thickness, deposited on glass substrate in the earlier stages, when the films less than 2000 Å thickness were found to be lacking in conductivity. This film shows very coarse structure, perhaps due to the formation of agglomerations.

4. Critical Currents:

The indium films investigated lie in the range from 580 Å to 3540 Å in thickness. The dependence of critical currents on temperature is governed by the ratio $\frac{\psi_o K^d}{\lambda_o}$ as mentioned in the first chapter (equations 1.29 and 1.30). The penetration depth depends upon both the film thickness and the temperature, this will be discussed later in this chapter. The table II below gives the theoretical and the experimental values of λ_o, at various temperatures. The second column gives the theoretical values for the bulk material calculated by taking λ_{oo} = 640 Å (Lock 1951) and assuming $\lambda_o = \lambda_{oo}/\left[1-\left(\frac{T}{T_c}\right)^4\right]^{1/2}$. The third, fourth and fifth columns are the experimental values determined from our work and are taken from figure 6.13 for three films whose thicknesses are given at the top of the column.

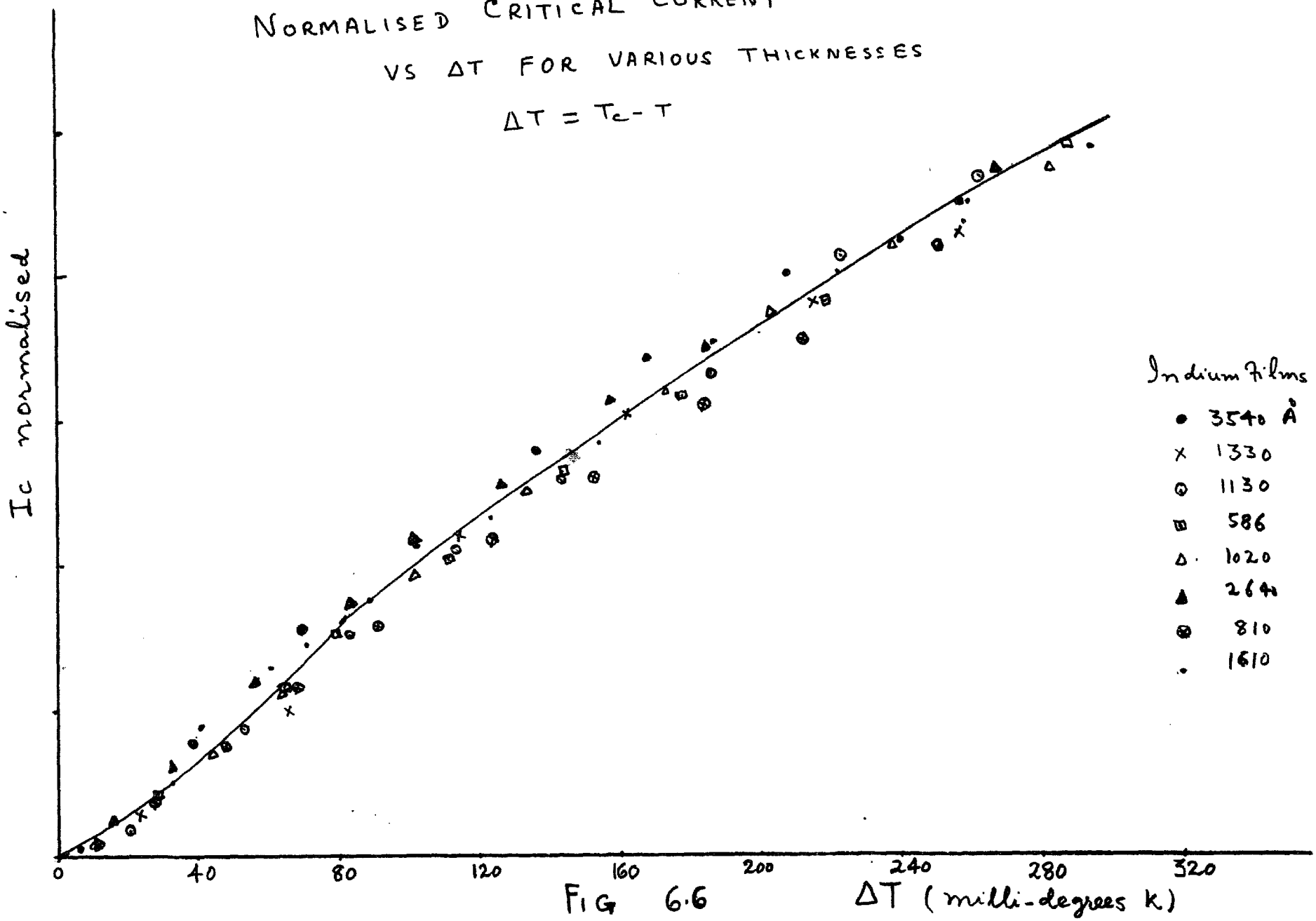
NORMALISED CRITICAL CURRENT
VS ΔT FOR VARIOUS THICKNESSES
ΔT = Tc - T
Ic normalised
Indium films
3540 Å
1330
1130
586
1020
264
810
1610
0
40
80
120
160
200
240
280
320
ΔT (milli-degrees K)

FIG 6.6

TABLE II

ΔT °K	Bulk	3540 Å	2640 Å	580 Å
.050	2690 Å	3600	4700	6100
.100	1790	2400	3575	4575
.200	1375	1650	2550	3500
.300	1088	1325	2050	2960

Thus the condition $\frac{\gamma_{ok} d}{\lambda_o} < 1$ is satisfied by all the films, except the one 3540 Å thick, for the region $\Delta T \leqslant 0.150^{\circ}$ K. If we assume the critical current I_c being given by $I_c \propto (\Delta T)^n$, then for the case $\frac{\gamma_{ok} d}{\lambda_o} < 1$, n = 1.5, for $\frac{\gamma_{ok} d}{\lambda_o} > 1$, n = 1.12.

The measurement of critical currents presents difficulties for two main reasons, firstly due to extremely high speed of the transition and secondly due to very low thermal capacity of the film and the consequent rise in the film temperature. The above reasons become specially important when the current transitions are broad. Both direct current and pulses have been used for critical current measurements. The results will be discussed separately.

Pulse Measurements

In the present work, two types of pulses were used. For most of the films deposited on 1.5 mm. diameter sapphire substrates, either the Rutherford pulser or thyratron pulser was used as described in Chapter V. The thyratron pulses, which were used for most of the data had a rise time of 1.2 micro second and decay time of 2.5 micro second. These were single shot pulses. The critical currents, obtained by measuring the current needed to restore half the resistance in the normal state, were normalised to the value ΔT = 0.3° K and have been plotted in fig. 6.6. For the first region, ΔT = 0.08° K,

$n = 1.27$ and subsequently for $0.08^{\circ}K \leqslant \Delta T \leqslant 0.30^{\circ}$ K, $n = 0.85$. These curves were fitted by the method of least squares with the help of Fortran 1620 IBM computer. It may be noted that the value of n found by minimising the residuals in log $I_c \Delta T$ was found to be = 1.41, as compared to $n = 1.27$. found by minimising those for I_c and ΔT. These values may be compared with those of Alekseevski and Mikheeva who for the pulses of 0.1 second duration find $n = 0.6$ and for the pulses of rise time 250 micro second find $n = 1$. In view of the fact that the transition could occur within the rise time of the pulse, it was felt that the departure from the theoretical value of $n = 1.5$ could be due to Joule heating. In fact with the pulses of increasing magnitude it was possible to see the evidence for the Joule heating after a certain resistance was restored in the film. The voltage pulse shape consisted of an initial rise followed by a further rise with change of slope. The latter was due to Joule heating. In fact in the earlier rise too, in view of the fast speed of transition it is conceivable that some heating might have occurred.

The fast pulses used to investigate the current transition free from Joule heating, had a rise time of 7 nano seconds. The specimen was a film of indium 585 $\mathring{A}$ thick coated on a sapphire rod of 0.4 mm. diameter. The ends where current leads were attached had a heavy coat of indium, and the current contacts were made with indium metal as described in Chapter IV. The thick indium coating, though advantageous from the point of view of Joule heating had one disadvantage. The transition temperature for the thicker part is lower than that for the thinner part. Hence if the thin film is to be driven normal by current pulses, in the immediate neighbourhood of the transition temperature for thin film, the thicker part might be driven normal earlier, leading to the production of Joule heating in the thicker part of the film.

OSCILLOGRAMS OF CURRENT INDUCED TRANSITION

X axis 1 small div = 1 m.s.

Y axis " " = [illegible] V

A " " = 1 m.v.

B " " = 2 m.v.

C " " = 4 m.v.

$T = 3.413^{\circ} K$

Figure 6.7 a

X - axis 1 small div = 1 m.s.

Y - axis

A " " = 10 m.v.

B " " = 20 m.v

C " " = 40 m.v.

$T = 1.488^{\circ} K$

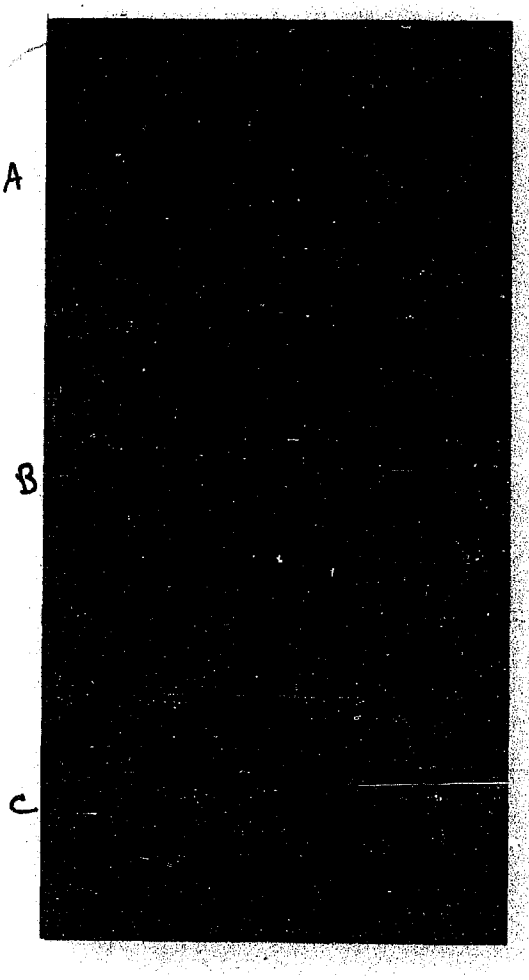

Figure 6.7 b

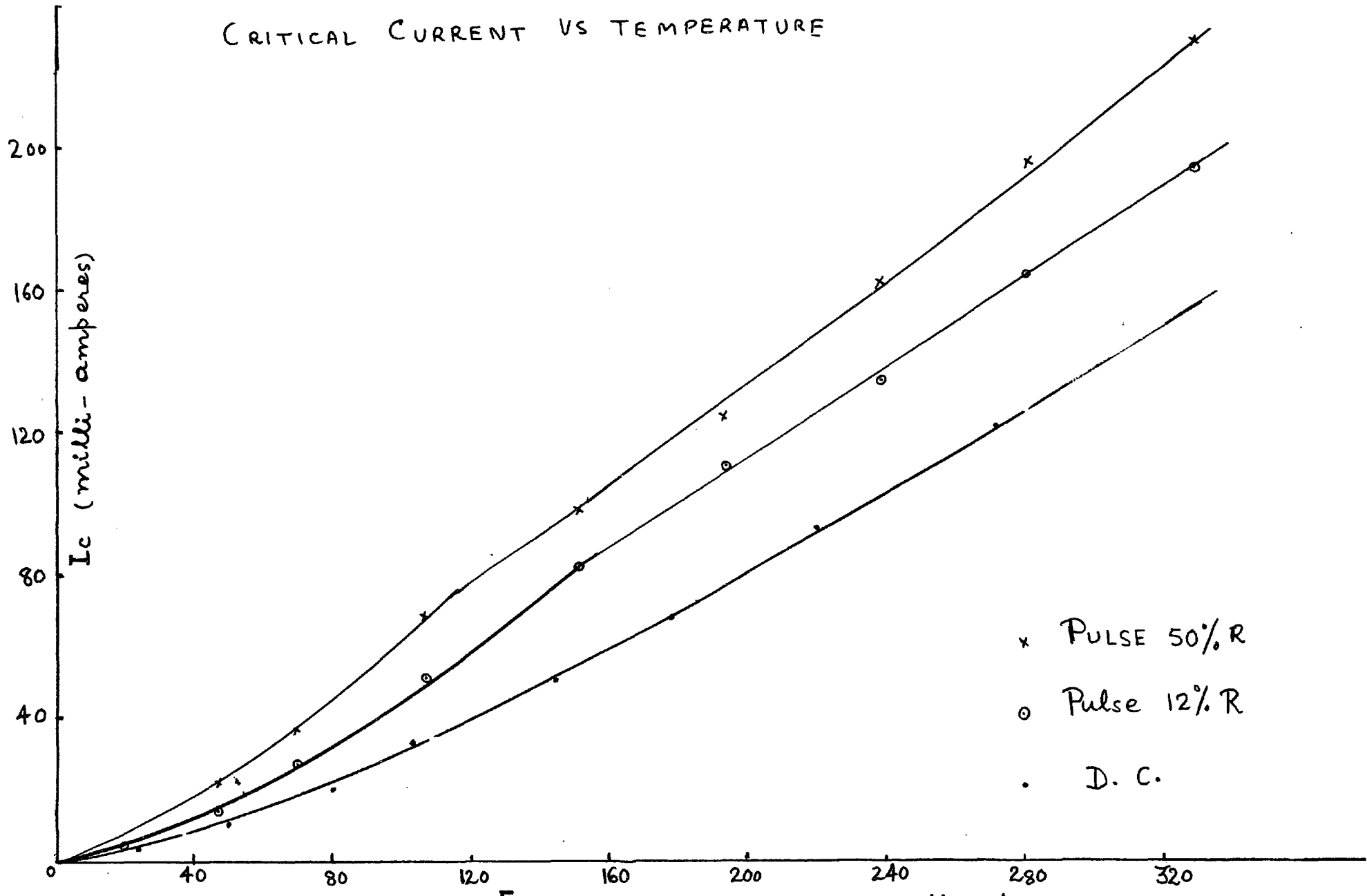
CRITICAL CURRENT VS TEMPERATURE
200
160
120
80
40
0
Ic (milli-amperes)
40
80
120
160
200
240
280
320
ΔT (milli-degrees K)
× PULSE 50% R
o Pulse 12% R
. D. C.

FIG. 6.8

One way out of this was to have the ends coated with a metal having higher T_c. Lead and tin were tried but the contacts did not prove very reliable. However, if the indium film is made quite thick, as was actually done, the residual resistance of the thick part will be very small and the heat developed will be negligible. That this is so was shown by the transitions in the temperature region close to T_c. The voltage pulse shapes for $\Delta T = 0.049^\circ$ K are shown in figure 6.7a. The transitions here appear to be isothermal. At lower temperatures the nature of transition changes and as the current is increased, heating of the film becomes evident as shown in the fig. 6.7b where each small division represents one nano second. The voltages read for calculation of the appearance of resistance are the ones after 20 nano seconds of the start of the current pulse. This time interval was chosen because in the normal state the voltage pulse rises in $\simeq 12$ nano seconds as can be seen from figure 6.7a. The critical currents (corresponding to 0.5 R) determined by using fast pulses are plotted as a function of ΔT in figure 6.8. This curve has two regions, in the first region from $0 \leqslant \Delta T \leqslant 0.115^\circ$ K, n = 1.41 and for the second region 0.115° K $\leqslant \Delta T \leqslant 0.300^\circ$ K, n = 1.06.

To examine whether the transitions observed are isothermal at the instant of observation, currents corresponding to 12%, 25%, 50%, 75% and 90% of the resistance in the normal state were determined graphically. In case some heating had occurred, the value of n should be less for the currents corresponding to the appearance of larger fraction of the resistance. This is found to be so, the values of n for the appearance of 12%, 25%, 50%, 75% and 90% of the resistance in the normal state are $1.46^{\pm.02}$, $1.45^{\pm.04}$, $1.41^{\pm.01}$, $1.40^{\pm.09}$ and $1.22^{\pm.06}$ respectively in the region $0 \leqslant \Delta T \leqslant 0.110^\circ$ K. In figure 6.8 is also shown a plot of critical current for the restoration of 12% resistance. For

this curve, as is clear from the figure the first region extends up to $\approx 0.150^{\circ}$ K as against the corresponding value of 0.115° K for restoring 50% resistance. This indicates that the critical currents observed for restoring 50% resistance were influenced by heating.

The second region where n = 1.06 commences at $\Delta T = 0.150^{\circ}$ K for 12% R and at $\Delta T = 0.115^{\circ}$ K for 50% R. The penetration depth for the magnetic fields from the table II for a film of 580 Å thickness is 2960 Å at $\Delta T = 0.3^{\circ}$ K. Hence $\frac{\gamma_{0}\kappa d}{\lambda_{\delta}} < 1$ and one would expect theoretically n = 1.5 for all the temperatures in the range $0 \leqslant \Delta T \leqslant 0.300^{\circ}$ K. The early commencement of the second region could be due to increasing effect of the Joule heating even for the critical currents corresponding to the appearance of 12% R. This might be the case in view of the fact that the transitions are extremely fast.

Transition Times and Transition Delays

There appears to be some confusion in the literature in the use of the expressions, transition times and transition delay. Below is given a brief summary of the various attempts made to measure transition times or transition delays or a combination of both.

1. Woodford and Feucht (1958): Transitions induced by magnetic field took place within a nano second. This inference was drawn from their observation that the conversion effeciency of their superconducting superheterodyne mixer remained unimpaired up to a frequency of about 1000 MC/sec.

2. Broom and Rhoderick (1959): For tin films, they find no delay within the resolution time of their oscilloscope (15 nano seconds.) for the current induced transitions.

3. Schmidlin et al (1960 a): They define the transition time as the time delay between the current and voltage traces at half amplitudes, corrected for the time required for the signal to make a return trip from the specimen. Their transition times depend upon the current magnitude and perhaps the substrate. The transition times ranged from 2 nano seconds to 2 micro seconds.

4. Kolchin et al (1961): They define transition time to be the interval between the instants of achieving half maximum by the current in the specimen and the voltage across it. The transition time varied with current amplitudes and was found to be less than 5 nano seconds for large currents.

5. Abraham (1960): He found the speed of transition from the superconducting to the normal state to be less than 0.15 nano second. The measurement was made on a tin film less than 100 $\mathring{A}$ thick which in the normal state had the resistance equal to the characteristic impedance of the transmission line. If a fast rising square-wave d.c. pulse is passed through the film, the superconducting film would reflect the pulse with change in sign, cutting short the pulse viewed on the oscilloscope. When the pulse amplitude exceeds the critical value thereby driving the film normal with the resultant loss of reflection, the viewed pulse rose back to its original value as soon as the transition was completed.

In our work, the technique used for measuring the transition delay and the transition times is quite simple as described below. If the voltage pulse is photographed when the specimen is above T_c, the start of the rise on it could be regarded as the reference point for counting the transition delay. In the superconducting state, after the compensation for the inductive pulse was made, the voltage pulse did not begin until after a delay

of about 7 nano seconds. This delay was found to be independent of the current amplitude. For example in the figure 6.7a, the first small pip at the left marks the instant where the voltage pulse would have commenced rising in the normal state. The time delay in this photograph is ~ 6 nano seconds.

The voltage pulse in the normal state had the same rise time whether it was a voltage pulse from the specimen at a temperature below T_c or above T_c. Thus the transition time was so small that it could not be measured. The apparent delay followed by avalanche like transition suggests some sort of co-operative mechanism bringing about instantaneous decay of the Cooper pairs.

The large dependence of transition time on current amplitudes in the work of Schmidlin et al. and Kolchin et al. seems to have been caused by the transition being heavily influenced by the Joule heating. In fact for their measurements Schmidlin et al. used pulses of much larger rise times. Also in their measurements on a tin film of 1200 Å thickness, n seems to be less than unity even close to T_c. This appears to suggest that transitions observed by them were highly influenced by heating. Thus the dependence of transition times as observed by them does not appear to be surprising.

Thermal Effects

As mentioned earlier, the transitions at lower temperatures are marked by generation of Joule heat as is evident from the figure 6.7b. By calculating the resistance corresponding to two instants, one say 20 nano seconds after the initiation of the pulse and the other 40 nano seconds after, it is possible to get an approximate estimate of the temperature rise, provided the following assumptions are made.

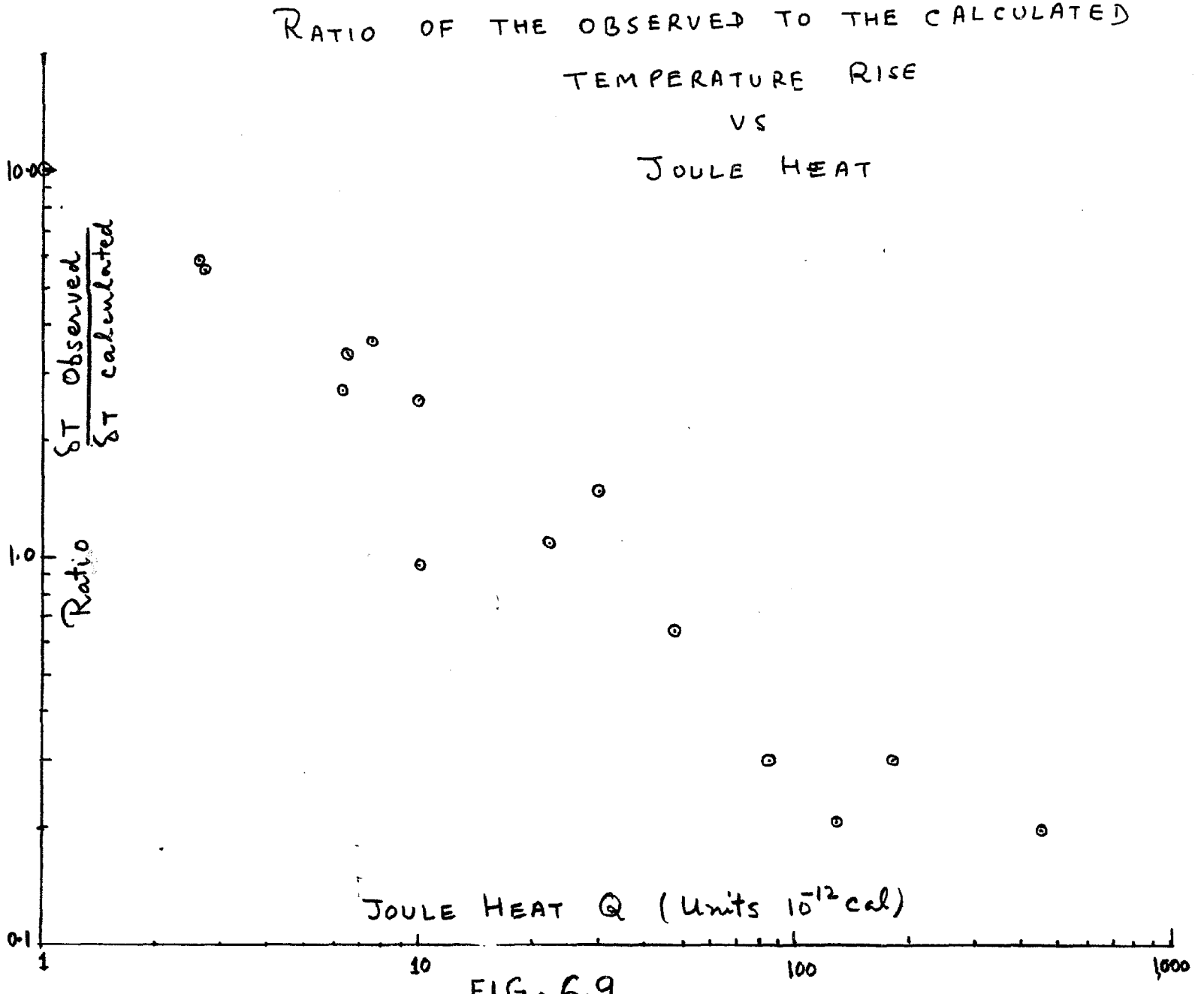
RATIO OF THE OBSERVED TO THE CALCULATED
TEMPERATURE RISE
VS
JOULE HEAT
10.0
1.0
0.1
Ratio
δT observed / δT calculated
1
10
100
1,000
JOULE HEAT Q (Units 10^{-12} cal)

FIG. 6.9

(i) At the first instant, the appearance of resistance is a consequence of the transition, unaffected by Joule heating. This is not rigorously true if we imagine the transition to be very fast.

(ii) During the interval of 20 nano seconds between the first and the second instants, the entire Joule heat heats up the film and the substrate or helium does not participate in the heat dissipation. This seems to be a fair assumption as despite the high thermal conductivity of sapphire, the heat transfer to the sapphire rod is governed by the Kapitza boundary resistance between the film and the substrate. If one makes use of the data by Little (1959), it can be shown that the heat communicated to sapphire rod during the 20 nano second interval is negligible. The heat transfer to helium bath is known to be a relatively slow process.

The temperature rise in the film can be estimated by constructing curves of resistance versus temperature with I = constant from the resistance versus current characteristics for T = constant. From the knowledge of δR, the change in the resistance between the two instants, the change in the temperature is calculated from the R - T characteristics for that particular current. This δT may be called the observed temperature rise.

Another way of estimating the temperature rise is by calculating the energy dissipated, and knowing the thermal capacity of the film the temperature rise is found out. This may be called the calculated temperature rise. In this calculation it is assumed that the entire thin film (not counting the thicker part of the film) is heated uniformly.

Comparison of δT observed and calculated reveals some interesting points. (See figure 6.9.) For low values of the currents, δT observed is found to be greater than δT calculated, in general the ratio goes on

diminishing from a value 10 for $Q = 10^{-12}$ cal. to a value $\simeq 1$ for $Q = 22.5 \times 10^{-12}$ cal. For increasing currents the decrease continues and for $Q = 450 \times 10^{-12}$ cal, ratio = 0.2. Higher value of the ratio could be interpreted by assuming, that for smaller power input, the temperature rise occurs only at the resistive parts of the film and if the velocity of propagation of the thermal waves is small, the effective thermal capacity of the film is smaller than the calculated value. For larger energy dissipation, the ratio decreases for two reasons, firstly the resistance appears at more points and secondly due to the increased velocities of thermal propagation, not only the entire thin film but also the thicker film at the ends acts as a heat sink. This explanation seems to amount to a qualitative evidence for the existence of thermal wave fronts, moving with great speeds.

From the above description it appears that the current pulses rising with great speed would, at least in principle, enable the study of transition without the accompanying thermal effects. This, however, is not correct due to the fact that the surface impedance, at the high frequencies introduces additional power losses and will tend to set a limit to the speed for the rise of the current pulse.

The surface resistance becomes perceptible when the photon energies of the high frequency component of the pulse become comparable or exceed the energy gap at that temperature. In view of the dependence of the energy gap on temperature, for the temperature region close to T_c, these frequencies are $\sim 10^{10}$ c/s. The highest frequencies used in this work are lower than the above.

Kolchin et al (1961) find that with faster rising pulses, the critical current decreases, this being interpreted by them as heating due to eddy

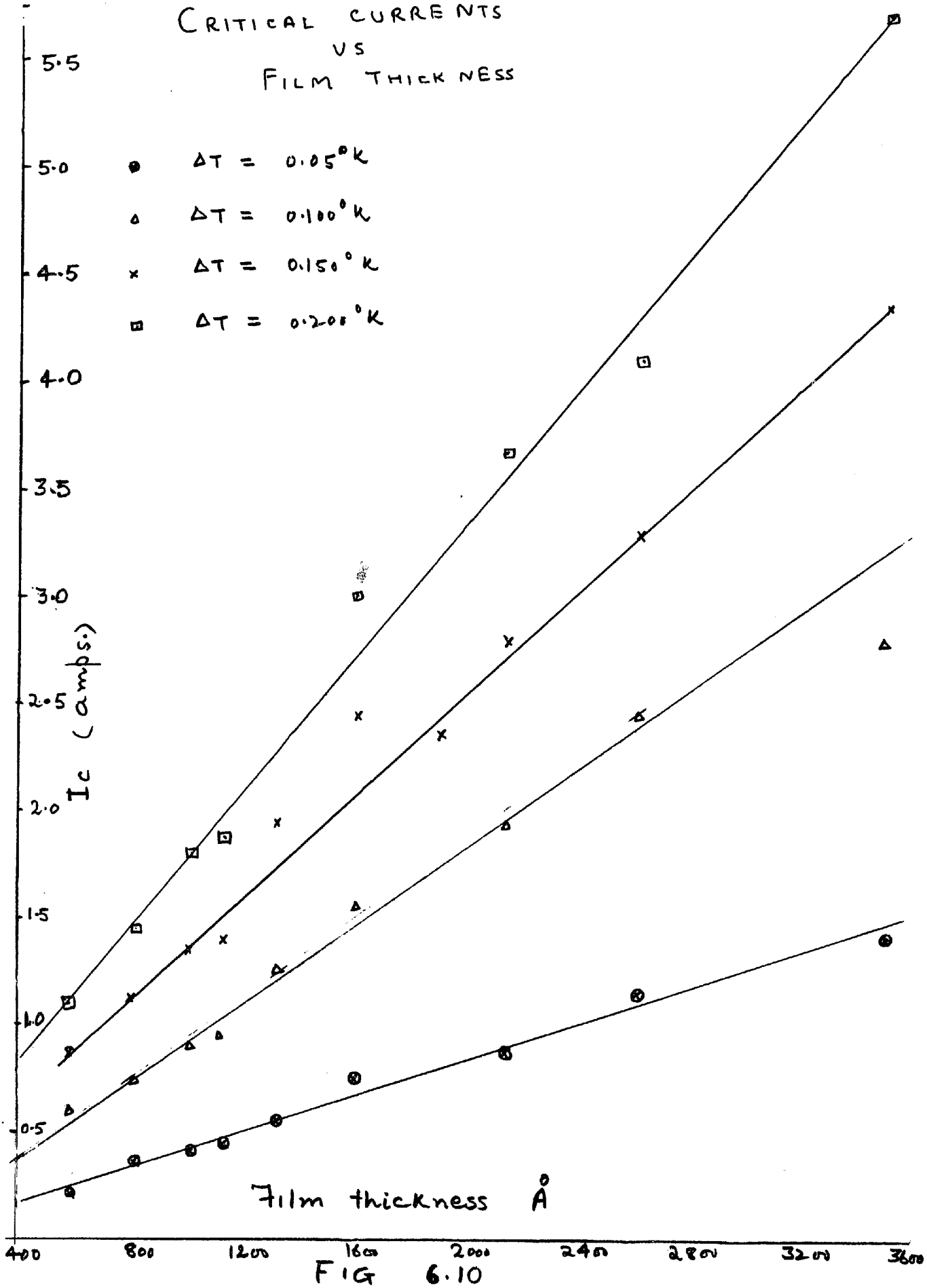
CRITICAL CURRENTS
VS
FILM THICKNESS
ΔT = 0.05°K
ΔT = 0.100°K
ΔT = 0.150°K
ΔT = 0.200°K
Ic (amps.)
5.5
5.0
4.5
4.0
3.5
3.0
2.5
2.0
1.5
1.0
0.5
Film thickness Å
400
800
1200
1600
2000
2400
2800
3200
3600

FIG 6.10

currents and amounts to an argument for not using fast rising pulses for observing isothermal transitions. In the present work, no direct evidence for eddy current heating could be obtained.

D. C. Transitions

Ginzburg and Shalnikov (1960) measured the critical currents for their tin films using direct currents and found that for the temperature range $\Delta T \approx .4^{\circ}$ K, $I_c \propto (\Delta T)^{1.5}$. The critical currents using d.c., measured in our work for the 585 Å thick indium film, are shown in figure 6.8. With d.c., the transitions occur very snappily, but show hysteresis for increasing and decreasing currents. Hysteresis for d.c. transitions was also observed by Bremer and Newhouse (1959). The hysteresis was absent in the pulse transitions. A comparison of the critical currents obtained by using pulses and direct currents (figure 6.8) shows that the d.c. values are lower indicating that these transitions belong to the thinner parts of the film. For d.c. values n = 1.31 in the temperature range $\Delta T = 0.300^{\circ}$ K.

Dependence of Critical Currents on Film Thickness

According to equation 1.29, $I_c \propto d$. The critical currents for indium films have been plotted as a function of film thickness in figure 6.10 for various values of ΔT. The dependence is seen to be linear in agreement with the theory.

Critical Currents for Tin Films

For two tin films 946 Å and 3250 Å in thickness, the critical currents were determined by using the pulses from the thyratron pulser. The $I_c - \Delta T$ plot was similar to the one for indium films, for the region $0 \leq \Delta T \leq .060^{\circ}$K, $n \simeq 1.3$ and for the second region $n \simeq 0.9$.

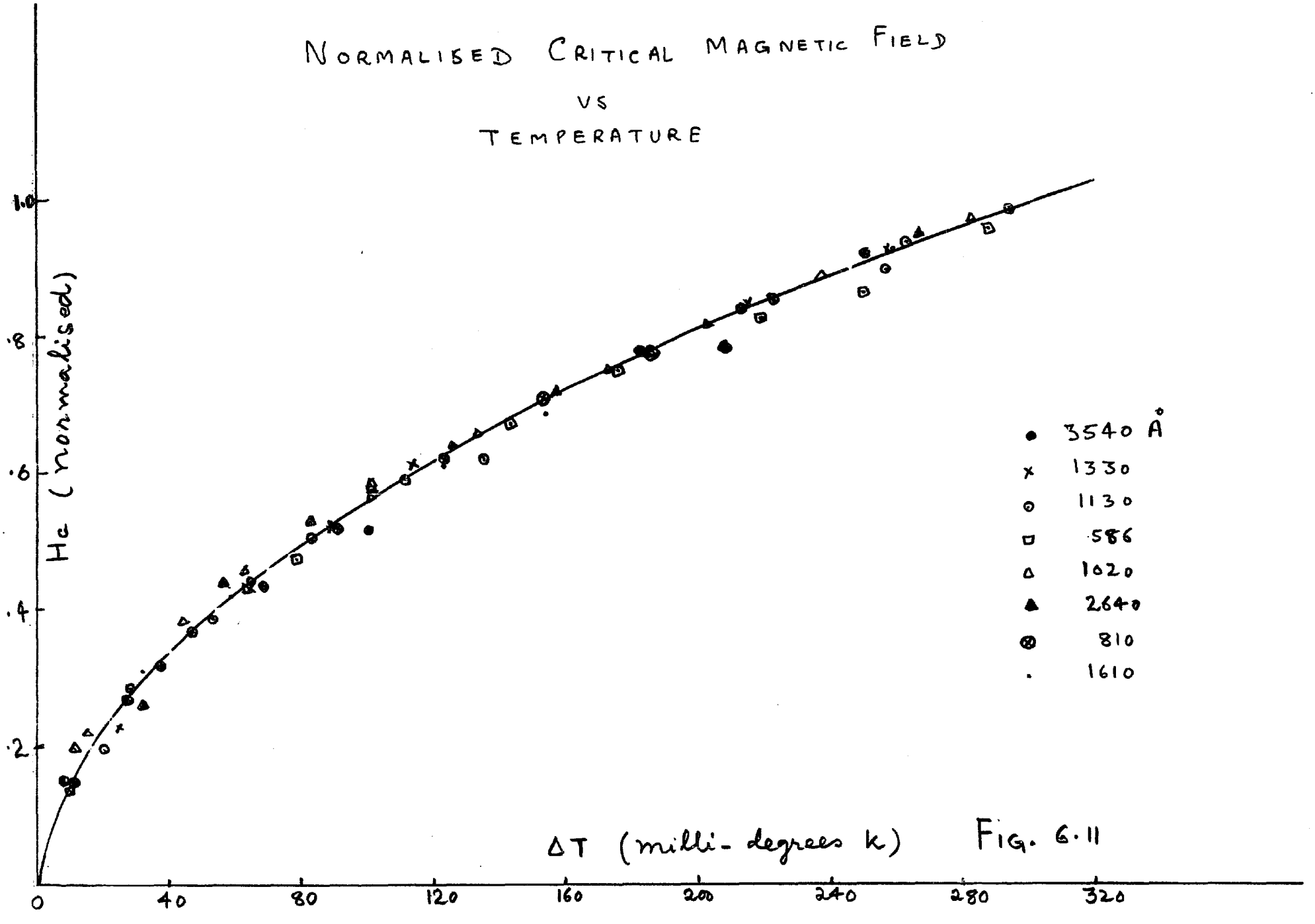
NORMALISED CRITICAL MAGNETIC FIELD
VS
TEMPERATURE
Hc (normalised)
1.0
.8
.6
.4
.2
0
40
80
120
160
200
240
280
320
ΔT (milli-degrees k)
3540 Å
1330
1130
586
1020
2640
810
1610

FIG. 6.11

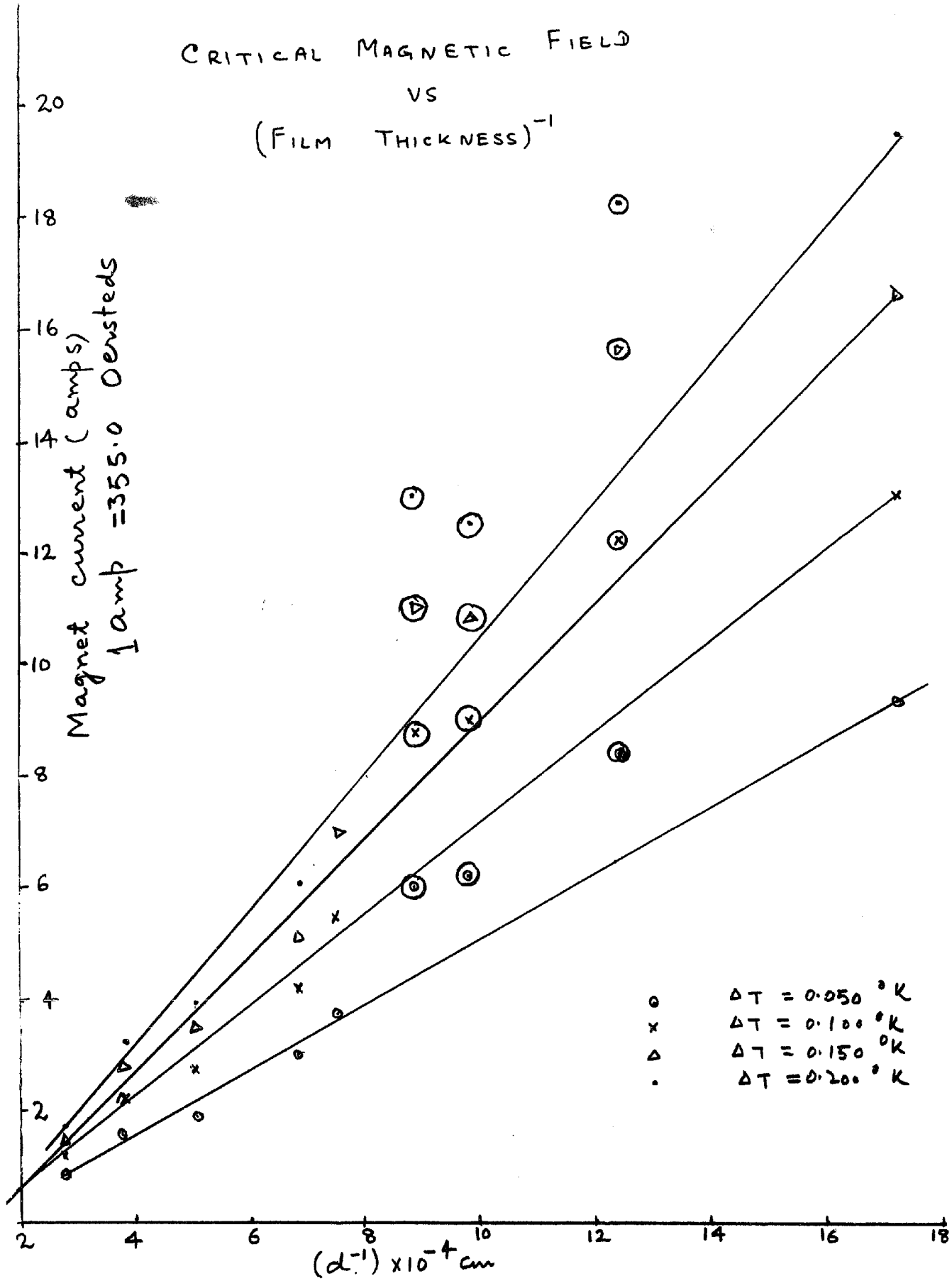
CRITICAL MAGNETIC FIELD
VS
(FILM THICKNESS)$^{-1}$
Magnet current (amps)
1 amp = 355.0 Oersteds
20
18
16
14
12
10
8
6
4
2
2
4
6
8
10
12
14
16
18
$(d^{-1}) \times 10^{-4}$ cm
$\Delta T = 0.050$ °K
$\Delta T = 0.100$ °K
$\Delta T = 0.150$ °K
$\Delta T = 0.200$ °K

Fig. 6.12

Effective Penetration Depth

Indium Films vs Y

Film thickness

$$Y = \left[1 - \left(\frac{T}{T_c}\right)^4\right]^{-1/2}$$

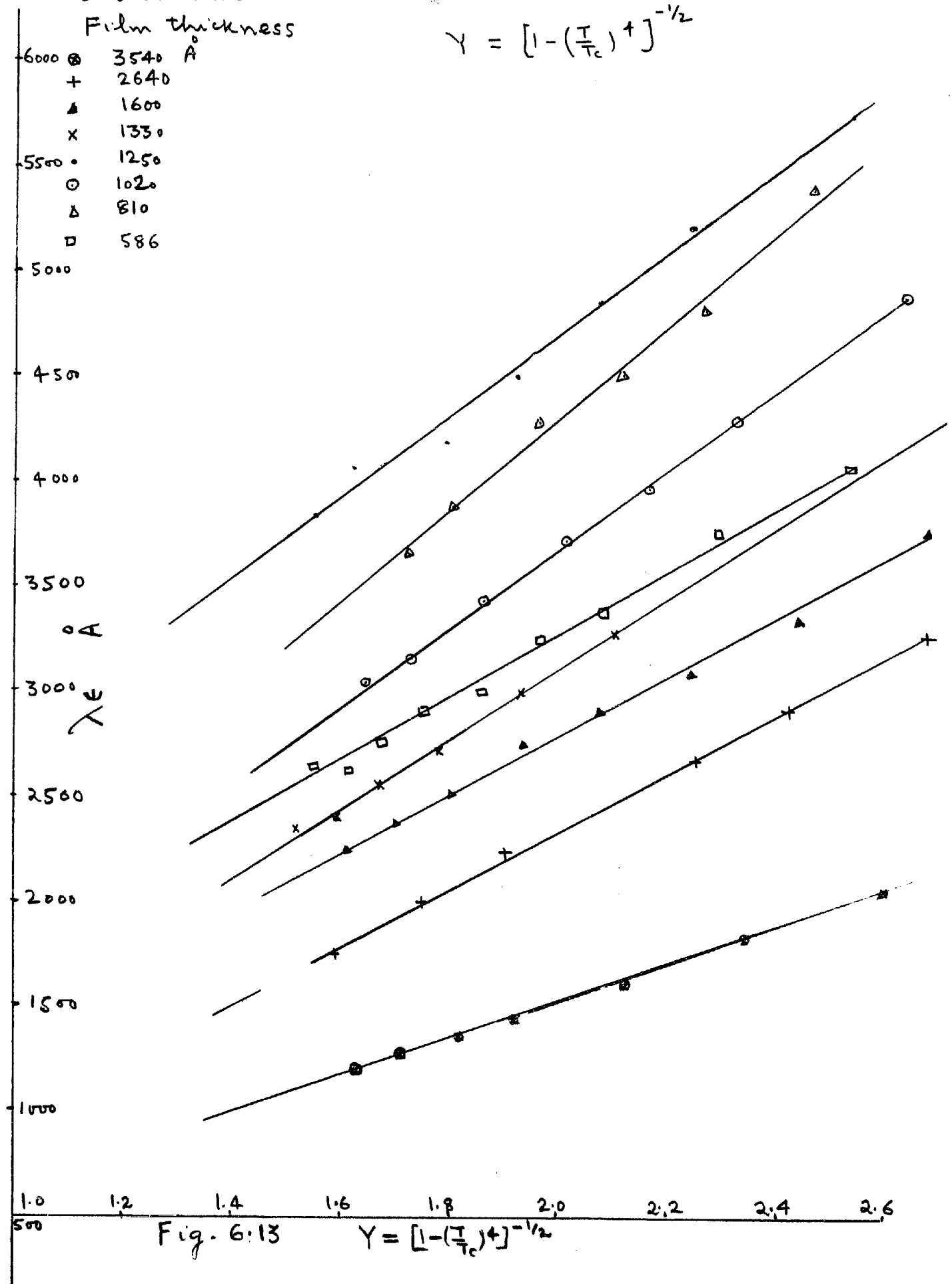

Fig. 6.13

Effective Penetration Depth vs Y

$$Y = \left[1-\left(\frac{T}{T_c}\right)^4\right]^{-1/2}$$

TIN FILMS

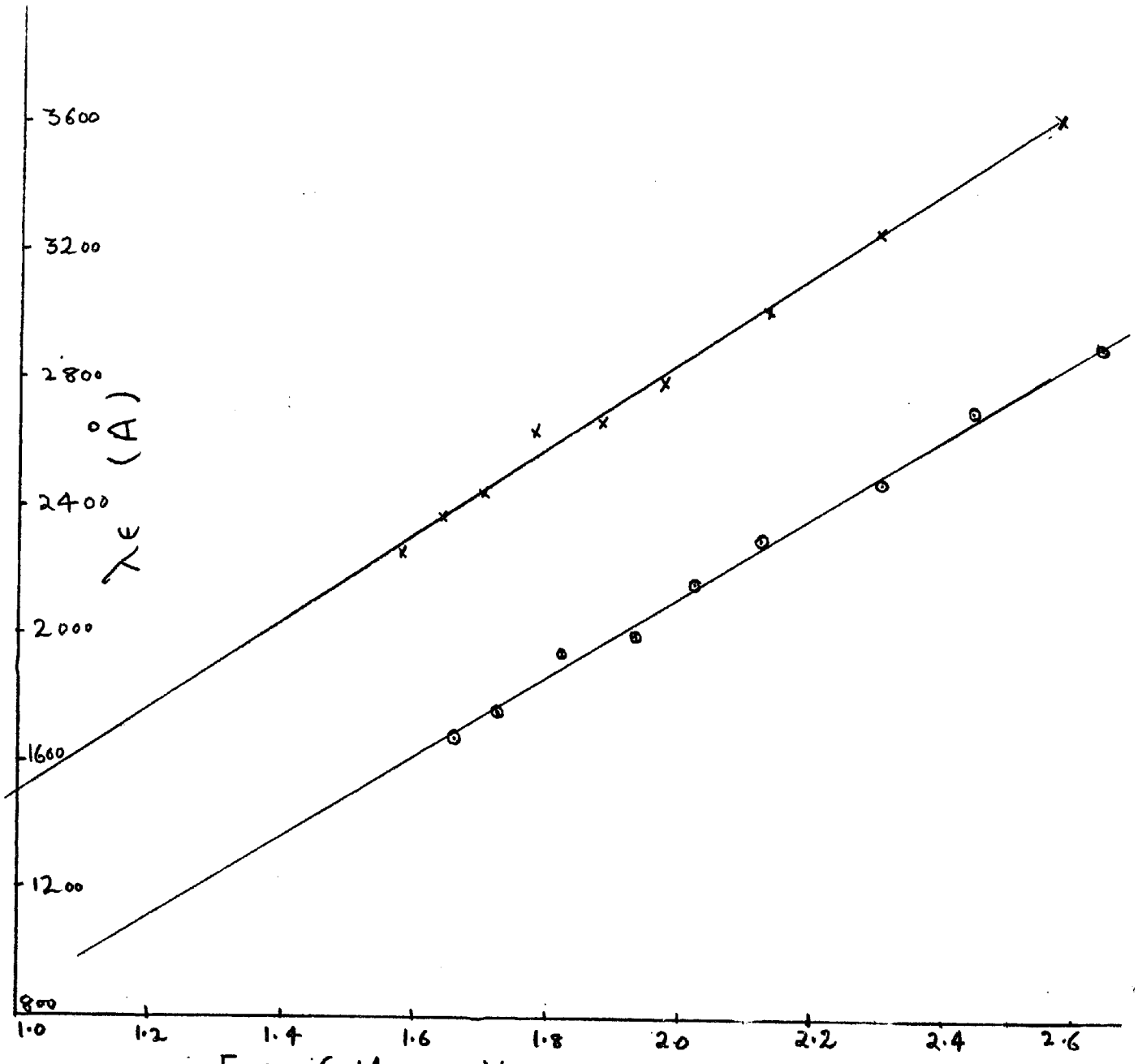

FIG 6.14

5. Critical Magnetic Fields:

According to equation 1.28, $H_c \propto (\Delta T)^{1/2}$. For various indium films, the critical fields are plotted as a function of ΔT as shown in figure 6.11, H_c were normalised to the value corresponding to $\Delta T = .300^\circ$ K. An equation $H_c = A\ (\Delta T)^n$ was fitted to the data with the help of IBM Fortran 1620 computer and the best fit is obtained for $n = 0.50$. Thus the dependence of the critical fields on temperature is in agreement with the theory. For tin films, this dependence is also verified.

In figure 6.12, the critical magnetic fields have been plotted as a function of $\frac{1}{d}$, for various values of ΔT. The points indicated with large circles do not fit the linear dependence. For these films, T_c was higher than for the others in the same thickness range. These same films also show abnormal behaviour in the variation of λ with y, where $y = \frac{1}{\left[1-(\frac{T}{T_c})^4\right]^{1/2}}$ as will be discussed in the following section.

Dependence of λ on Film Thickness and Mean Free Path.

Following Ittner, the effective penetration depth λ_ϵ has been calculated by solving equation 3.6, for both indium and tin films. λ_ϵ has been plotted as a function of y, in figure 6.13 for the indium films and in figure 6.14 for tin films. In the temperature range of $\Delta T \simeq 0.4^\circ$ K, all the points lie on straight lines. These straight lines have been extrapolated to get $\lambda_\epsilon(0)$ corresponding to $y = 1$. In general $\lambda_\epsilon(0)$ is found to increase with diminishing thickness. It is obvious from figure 6.13 that for three films 810 Å, 1020 Å and 1250 Å in thickness, the penetration depths are unusually high, but these are also the films which show abnormal behaviour in H_c versus $\frac{1}{d}$ plot. Calculation of the bulk mean free path from the resistivity data also shows that for these films the mean free path is

RATIO OF CRITICAL FIELD H_c TO $(1-t)^{1/2}$ VS TEMPERATURE

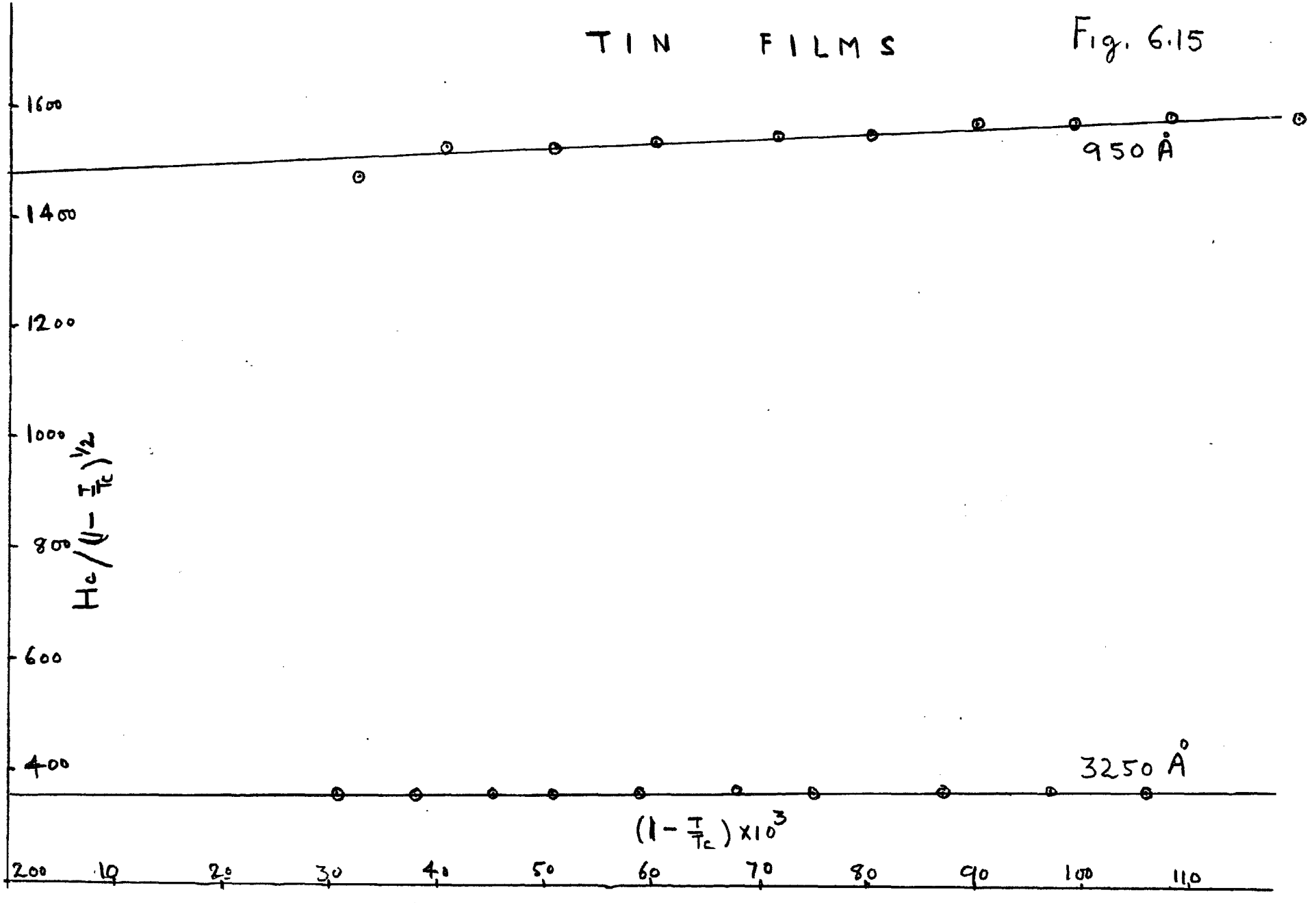

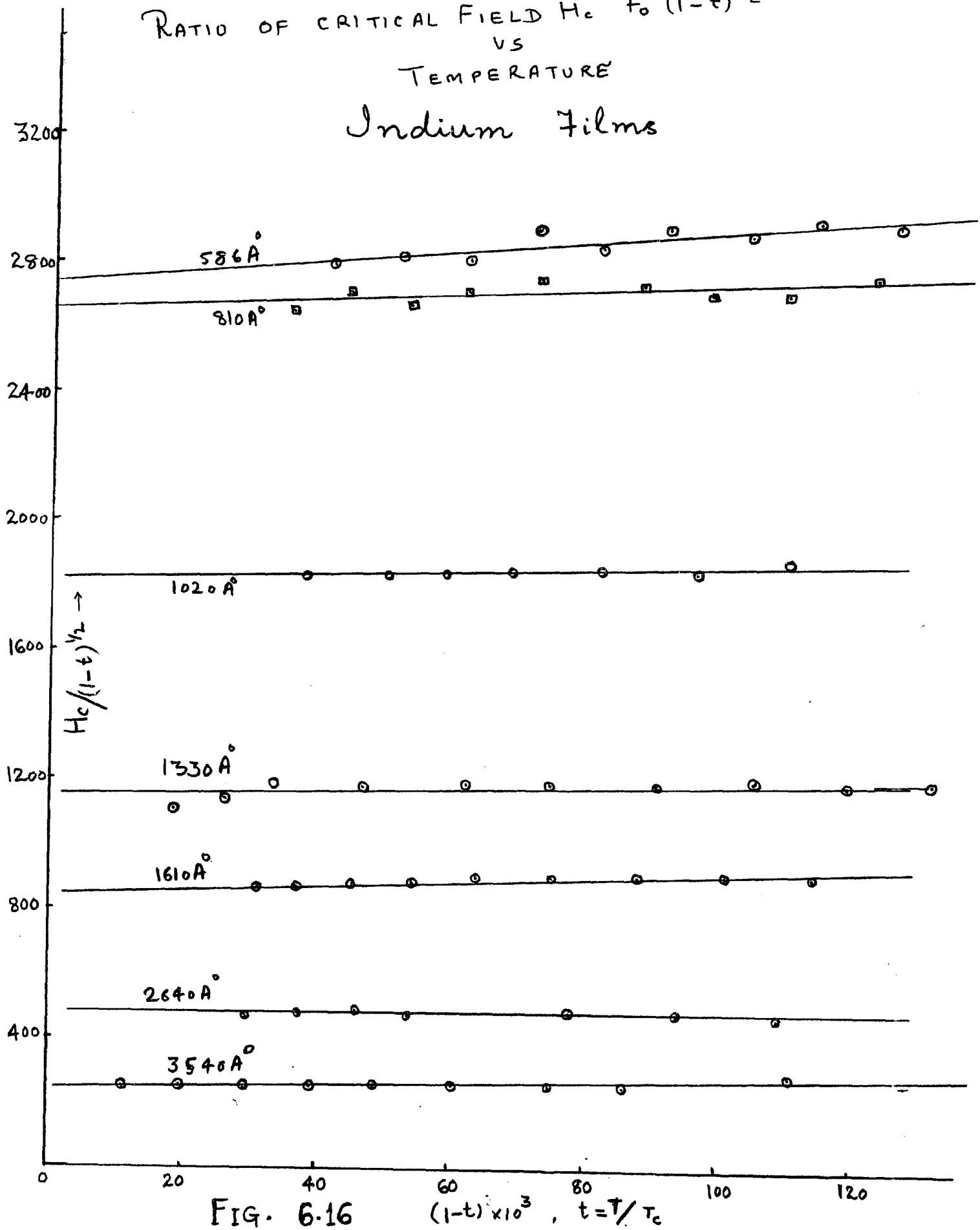
RATIO OF CRITICAL FIELD Hc to (1-t)^1/2
VS
TEMPERATURE
Indium Films
3200
2800
2400
2000
1600
1200
800
400
586 A°
810 A°
1020 A°
1330 A°
1610 A°
2640 A°
3540 A°
Hc/(1-t)^1/2 →
0
20
40
60
80
100
120
(1-t) x10^3 , t = T/Tc

FIG. 6.16

smaller than expected and consequently the increase in the penetration depth could be due to both the thickness and mean free path effects.

Strictly speaking, one is not justified to extrapolate the straight line to get $\lambda_\epsilon(0)$. As pointed out by Miller (1959) when the theoretical values of $\lambda(T)$ are plotted as a function of y, a straight line fit is obtained which bends below $y \simeq 1.5$, the difference between the slope for large y and the intercept at y = 1 being of the order 10%.

There is yet another way of calculating the penetration depth. For tin films, the critical magnetic field is given by equation 3.11. In figure 6.15, $H_c(T) / (\Delta t)^{1/2}$ has been plotted as a function of $\Delta t/T_c$ from this the value of $\lambda(o,d)$ and ϵ has been calculated as given in the table III. These values for ϵ favour the Ginzburg - Landau expression for free energies as referred to in Chapter III.

The equation corresponding to 3.11 for indium films is not available because the expression for $\lambda(T, d)$ in which the temperature and thickness dependence were factorable could not be found in the literature. However, let us assume that $H_c(T)$ for indium is given by an expression of the form

$$H_c(T) = b \frac{\lambda(o,d)}{d} (\Delta t)^{1/2} (1 + \epsilon \Delta t) \qquad 6.9$$

where b is an unknown constant. For 3540 Å thick film the value of $\lambda(o,d)$ (i.e. λ_ϵ) as found by extrapolating to y = 1 in figure 6.13 is 650 Å. Substituting this value in equation 6.9, b can be calculated and this value has been used for the calculation of $\lambda(o,d)$ for other films from the curves of figure 6.16. These values of $\lambda(o,d)$ together with λ_ϵ, as calculated from figure 6.13 are given in the table III.

TABLE III

Indium Films

Film Thickness	$\lambda(0,d)$	λ_ϵ	ϵ
3540 Å	650Å	650 Å	1.65 ± .0.16
1330	1157	1350	0.46 ± 0.16
586	1230	1750	0.57 ± 0.13
1020	1377	1750	
2640	960	945	- .04 ± 0.12
810	1636	2175	0.28 ± 0.13
1610	1046	1375	0.68 ± 0.14

Tin Films

910	990	1500	0.63 ± 0.09
3250	760	860	0.44 ± 0.10

CHAPTER VII

SUMMARY AND CONCLUSIONS

Most of the results presented in the last Chapter are for indium films in the thickness range of 580 Å to 3540 Å. Due to difficulties encountered in preparing thin films of tin, only two tin films 910 Å and 3250 Å thick have been investigated.

The measurement of resistivity at room temperature and helium temperature enabled the calculation of ρ_1 and ξ_0 and these results have been listed in Table I along with the results of other workers. Our estimates are in fair agreement with the other values.

The transition width for indium films, as measured by resistance measurements, was found to lie between 3 and 8 milli-degrees. The transition temperature was found to increase with decreasing film thickness.

For a 585 Å thick indium film, the critical currents were measured by using pulses of a rise time of 7 nano seconds, the transitions being observed with the help of Tektronix type 661 sampling oscilloscope having a rise time of 0.35 nano seconds.* These measurements gave $n = 1.46$ for $0 \leqslant \Delta T \leqslant 0.150^\circ$ K and $n = 1.02$ for 0.150° K $\leqslant \Delta T \leqslant 0.300^\circ$ K. The Ginzburg-Landau theory predicts $n = 1.5$ for the entire region under observation i.e. $0 \leqslant \Delta T \leqslant 0.300^\circ$ K for a film of this thickness. The smaller value of n in the second region may be a consequence of the increasing Joule heating. For most films of both indium and tin, $n = 1.27$ for the region $0 \leqslant T \leqslant 0.08^\circ$ K,

and $n \simeq 0.87$ for the region $0.08^{\circ}\ K \leq \Delta T \leq 0.300^{\circ}\ K$ when the measurements were made using pulses of a rise time of 1.2 micro seconds. The d.c. measurements on the 585 Å thick film give a value $n = 1.31$ in the region $0 \leq \Delta T \leq 0.300^{\circ}\ K$ but the d.c. critical currents are found to be lower than the pulse values suggesting that in the d.c. measurements only the weak parts of the film are being investigated. Thus the results of Ginzburg and Shalnikov in which they find $n = 1.5$ for the region $0 \leq \Delta T \leq 0.4^{\circ}\ K$ do not seem to be surprising. The d.c. transitions in our work were marked by hysteresis unlike the transitions with the current pulses.

According to the G - L theory $I_c \propto d$. In our work this is found to be correct. If in equation 1.29 we substitute for λ_∞ the value found by us with the magnetic field measurements, our critical currents are found to be lower than the ones predicted by the G - L theory.

Our measurements with fast rising pulses seem to indicate a transition delay of about 7 nano seconds practically independent of the current amplitude. This is followed by a very fast transition from the superconducting to the normal state. The dependence of the transition times on the current amplitudes, as reported by Schmidlin et al. and Kolchin et al, seems to have been highly influenced by the Joule heating and therefore their transition times do not seem correct. On analysing the thermal rise in the resistance of the specimen, there seems to be some evidence for the thermal propagation of thermal wave fronts as reported by Bremer and Newhouse ~~but the velocities of propagation observed in our work seem to be quite high in agreement with the work of Broom and Rhoderick and Cherry and Gittleman.~~

The temperature dependence of the critical magnetic field is in

complete agreement with the behaviour predicted by the equation 1.28; and so is the dependence of field on film thickness. The critical field data has been used for calculating the effective penetration depth and it has been found that the penetration depth increases with decrease in both the film thickness and the mean free path. These results are in qualitative agreement with the theoretical and experimental findings of other workers. In order to separate the mean free path and thickness effects quantitatively it would be necessary to fabricate all the specimens under strictly identical conditions, possibly in one single operation.

*These measurements are the first ones to be made by combining the use of a compensated geometry with fast rising current pulses. (Bardeen 1962)

BIBLIOGRAPHY

General References:

I. Shoenberg, D., Superconductivity, Cambridge University Press, 1952.

II. London, F., Superfluids, Vol. I, New York, Wiley, 1950.

III. Bardeen, J. and Schrieffer, J.R., Recent developments in Superconductivity, Progress in Low Temp. Physics, Vol. III, C.J. Gorter, ed.; Interscience.

IV. Schafroth, M.R., Solid State Physics, 10, eds. Seitz and Turnbull, Academic Press. (1960)

V. Bardeen, J., Handbuch der Physik, Vol. XV, S. Flugge, ed.; Berlin, Springer, 1956.

VI. Holland, L., Vacuum Deposition of Thin Films, 1956, Chapman and Hall, Lond.

VII. Structure and Properties of Thin Films, Proc. Inter. Conf. ed. Neugebauer, Newkirk and Vermilyea, 1959, J. Wiley, N.Y.

Individual References:

Abraham, D. (1960) Solid State Electronics 1, 340.

Abrikosov, A.A. (1957) Soviet Physics JETP, 5, 1174.

Alekseevskii, N.E. and Mikheeva, M.N. (1957) Soviet Physics JETP, 4, 810.

Alekseevskii, N.E. and Mikheeva, M.N. (1960) Soviet Physics JETP, 11, 212.

Aziz, A.A. and Baird, D.C. (1959) Can. Jour. Phy. 37, 937.

Bardeen, J. (1954) Phys. Rev. 94, 554.

Bardeen, J. (1962) Rev. Mod. Phys. 34, 667.

Bardeen, J. (1962 a) IBM Jour. Res. and Dev. 6, 3.

Bardeen, J., Cooper, L.N. and Schrieffer, J.R. (1957) Phys. Rev. 108, 1175.

Bardeen, J. and Pines, D. (1955) Phys. Rev. 99, 1140.

Behrndt, M.E., Blumberg, R.H., and Giedd, G.R. (1960) IBM Jour. Res. and Dev. 4, 184.

Biondi, M.A., and Garfunkel, M.P. (1959) Phys. Rev. 116, 853.

Bogoliubov, N.N. (1958) Nuovo cimento 7, 794.

Bohm, D. and Pines, D. (1953) Phys. Rev. 92, 609.

Bremer, J.W., and Newhouse, V.L. (1958) Phys. Rev. Lett 1, 282.

Bremer, J.W., and Newhouse, V.L. (1959) Structure and Properties of Thin Films Edited by Neugebauer, Newkirk and Vermilyea, John Wiley & Sons.

Broom, R.F. and Rhoderick, E.H. (1959) Phys. Rev. 116, 344.

Broom, R.F. and Rhoderick, E.H. (1960) Brit. Jour. App. Phys. 11, 292.

Cherry, W.H. and Gittleman, J.I. (1960) Solid State Electronics 1, 287.

Cooper, L.N. (1956) Phys. Rev. 104, 1189.

Davies, E.A. (1960) Proc. Roy. Soc. A 255, 407.

DeHaas, W.J. and Voogd, J. (1931) Leiden Comm., 214 c.

DeLano, R.B.Jr. (1960) Solid State Electronics 1, 381.

Douglass, D.H., and Blumberg, R.H. (1962) Phys. Rev. 127, 2038.

Evans, D.M., and Wilman, H. (1952) Acta cryst., Camb., 5, 731.

Faber, T.E. (1952) Proc. Roy. Soc. A 214, 392.

Faber, T.E. (1957) Proc. Roy. Soc. A, 241, 531.

Frank, F.C. and Van der Merwe, J.H. (1949) Proc. Roy. Soc. 200, 125.

Frohlich, H. (1950) Phys. Rev. 79, 845.

Frohlich, H., Pelzer, H. and Zienau, S. (1950) Phil. Mag. 41, 221.

Fuchs, K. (1938) Proc. Camb. Phil. Soc. 34, 100.

Geballe, Matthias, Hull, and Corenzwit (1961) Phys. Rev. Lett. 6, 275.

Ginzburg, V.L. (1956) Soviet Physics JETP, 3, 621.

Ginzburg, V.L. (1956) Soviet Physics Doklady 1, 541.

Ginzburg, V.L. (1958) Dok. Akad. Nauk 118, 464.

Ginzburg, V.L., and Landau, L.D. (1950) JETP, U.S.S.R. 20, 1064.

Ginzburg, N.I. and Shalnikov, A.I. (1960) Soviet Physics JETP, 10, 285.

Glover, R.E., III (1958) Proc. V Inter. Conf. Low Temp. Phys. p. 330.

Glover, R.E., and Tinkham, M. (1956) Phys. Rev. 104, 844.

Glover, R.E., and Tinkham, M. (1957) Phys. Rev. 108, 243.

Goodman, B.B. (1962) IBM Jour. Res. and Dev. 6, 63.

Gorter, C.J. and Casimir (1934) Physica 1, 306.

Gor'kov, L.P. (1959) Soviet Physics JETP, 9, 1364.

Ittner, W.B. (1960) Phys. Rev. 119, 1591.

Jennings, L.D., and Swenson, C.A. (1958) Phys. Rev. 112, 31.

Kahan, DeLano, Brennenmann, Tsui (1960) IBM Jour. Res. and Dev. 4, 173.

Keesom, W.H., and Kok, J.A. (1932) Commn. Phys. Lab. Uni. Leiden, no. 230 e.

Keesom, W.H., and Kok, J.A. (1934) IBID no. 232 a.

Keesom, P.H., and Perlman, N., Encycl. of Phys. (Springer - Verlag, Berlin, 1956) Vol. XIV.

Kohchin, Mikhailov, Reinov, Rumyantseva, Smirnov and Totubalin (1961) Soviet Physics JETP, 13, 1083.

Landau, L.D. and Lifshitz, E.M. (1958) Statistical Physics, p. 434, Pergamon Press,

Levinstein, H.J. (1949) Jour. Appl. Phys. 20, 306.

Little, W.A. (1959) Canad. Jour. Phys. 37, 334.

Lock, J.M. (1951) Proc. Roy. Soc. A 208, 391.

London, H. and London, F. (1935) Proc. Roy. Soc. A 149, 71.

London, H. and London, F. (1935) Physica 2, 341.

Lutes, O.S. (1957) Phys. Rev. 105, 1451.

Matthias, B.T. (1957) Prog. Low Temp. Phys. Vol. 2, edited by C.J. Gorter.

Matthias, B.T., Geballe, T.H., Compton, V.B. (1963) Rev. Mod. Phys. 35, 1.

Maxwell, E. (1950) Phys. Rev., 78, 477.

Meissner, W. and Ochsenfeld, R. (1933) Naturwissenschaften, 21, 787.

Miller, P. (1959) Phys. Rev. 113, 1209.

Morse, Olsen and Gavenda (1959) Phys. Rev. Lett. 4, 193.

Nambu, Y. and Jona-Lasimo, G. (1961) Phys. Rev. 122, 345.

Onnes, H.K. (1911) Comm. Phys. Lab. Univ. Leiden, Nos. 119, 120, 122.

Pippard, A.B. (1953) Proc. Roy. Soc. A 216, 547.

Pines, D. (1958) Phys. Rev. 109, 280.

Reynolds, Serin, Wright, and Nesbitt (1950) Phys. Rev. 78, 487.

Rhodin, T.N. (1949) Disc. Faraday Soc. 5, 215.

Rogers, K.T. (1960) Thesis; University of Illinois.

Shalnikov, A.I. (1940) Jour. Exp. Theor. Phys. U.S.S.R. (Russian) 10, 630.

Shalnikov, A.I. (1945) J. Phys. U.S.S.R. 9, 202.

Schawlow, A.L. Phys. Rev. 109, 1856, (1958)

Schmidlin, F.W. and Crittenden, E.C. (1958) Proc. Vth Inter. Conf. Low Temp. Phys. (1958).

Schmidlin, F.W., Learn, A.J., Crittenden, E.C., Jr. and Cooper, J.N. (1960). Solid State Electronics 1, 323.

Schrieffer, J.R. (1957) Phys. Rev. 106, 47.

Shoenberg, D. (1939) Nature, Lond. 143, 434.

Silsbee, F.B. (1916) J. Wash. Acad. Sci. 6, 597.

Smallman, C.R., Slade, A.E., and Cohen, J.L. (1960) Proc. I.R.E. Sept., 1562.

Sommerhalder, R., Jaggi, R. (1960) Helv. Phys. Acta 33, 1.

Sondheimer, E.H. (1952) Advances in Phys. 1, 1.

Toxen, A.M. (1961) Phys. Rev. 123, 442.

Toxen, A.M. (1962) Phys. Rev. 127, 382.

Woodford, J.B., and Feucht, D.L. (1958) Proc. Inst. Radio Engrs. 46, 1871.

Yosida (1958) Phys. Rev. 111, 1255.